EXHIBIT A

Impaired S cr tion of Very Low Density Lipoprotein–Triglycerides by Apolipoprotein E–deficient Mous Hepatocyt s

Folkert Kuipers,* Miek C. Jong,§ Yuguang Lin,* Miranda van Eck,¶ Rick Havinga,* Vincent Bloks,* Henkjan J. Verkade,* Marten H. Hofker,** Han Moshage,‡ Theo J.C. van Berkel,¶ Roel J. Vonk,* and Louis M. Havekes§‖

*Laboratory of Nutrition and Metabolism, and ‡Division of Gastroenterology and Hepatology, Groningen Institute for Drug Studies, Academic Hospital Groningen, 9713 GZ Groningen; §TNO Prevention and Health, Gaubius Laboratory, 2301 CE Leiden; ‖Department of Cardiology, and Department of Internal Medicine, University Hospital Leiden, 2300 RC Leiden; ¶Division of Biopharmaceutics, Sylvius Laboratories, and **MGC - Department of Human Genetics, University of Leiden, 2300 RA Leiden, The Netherlands

Abstract

To explore mechanisms underlying triglyceride (TG) accumulation in livers of chow-fed apo E–deficient mice (Kuipers, F., J.M. van Ree, M.H. Hofker, H. Wolters, G. In't Veld, R.J. Vonk, H.M.G. Princen, and L.M. Havekes. 1996. *Hepatology.* 24:241–247), we investigated the effects of apo E deficiency on secretion of VLDL-associated TG (*a*) in vivo in mice, (*b*) in isolated perfused mouse livers, and (*c*) in cultured mouse hepatocytes. (*a*) Hepatic VLDL-TG production rate in vivo, determined after Triton WR1339 injection, was reduced by 46% in apo E–deficient mice compared with controls. To eliminate the possibility that impaired VLDL secretion is caused by aspecific changes in hepatic function due to hypercholesterolemia, VLDL-TG production rates were also measured in apo E–deficient mice after transplantation of wild-type mouse bone marrow. Bone marrow–transplanted apo E–deficient mice, which do not express apo E in hepatocytes, showed normalized plasma cholesterol levels, but VLDL-TG production was reduced by 59%. (*b*) VLDL-TG production by isolated perfused livers from apo E–deficient mice was 50% lower than production by livers from control mice. Lipid composition of nascent VLDL particles isolated from the perfusate was similar for both groups. (*c*) Mass VLDL-TG secretion by cultured apo E–deficient hepatocytes was reduced by 23% compared with control values in serum-free medium, and by 61% in the presence of oleate in medium (0.75 mM) to stimulate lipogenesis. Electron microscopic evaluation revealed a smaller average size for VLDL particles produced by apo E–deficient cells compared with control cells in the presence of oleate (38 and 49 nm, respectively). In short-term labeling studies, apo E–deficient and control cells showed a similar time-dependent accumulation of [^{3}H]TG formed from [^{3}H]glycerol, yet secretion of newly synthesized VLDL-associated [^{3}H]TG by apo E–deficient cells was reduced by 60 and 73% in the absence and presence of oleate, respectively. We conclude that apo E, in addition to its role in lipoprotein clearance, has a physiological function in the VLDL assembly–secretion cascade. (*J. Clin. Invest.* 1997. 100:2915–2922.) Key words: transgenic mice • lipoproteins • liver • cholesterol • apolipoprotein B

Introduction

Apolipoprotein E (apo E) is an important protein constituent of triglyceride (TG)[1]-rich chylomicrons and VLDL. apo E functions as a ligand in the receptor-mediated uptake of these lipoproteins by the liver (1) and may modulate their lipoprotein lipase–mediated processing (2, 3). It has also been suggested that apo E plays a role in the secretion–recapture process (4, 5). In this process, internalization of circulating lipoproteins is facilitated through binding of the particles to heparan sulfate proteoglycans and subsequent enrichment with apo E in the hepatic sinusoidal space of Disse. Furthermore, recent in vitro studies have indicated that apo E may serve a function in intracellular metabolism and distribution of endocytosed lipids in macrophages and hepatoma cells (6, 7).

The generation of apo E–deficient mice has established directly the importance of apo E in control of plasma cholesterol levels (8, 9). apo E–deficient mice show markedly elevated plasma cholesterol levels when fed a normal chow diet, due to accumulation of VLDL/LDL-sized particles in their circulation (10–12). These particles contain predominantly apo B48 and are relatively enriched in cholesterol and cholesterol ester and depleted in TG (10–12). As recently reviewed by Plump and Breslow (8), these particles are mainly remnants of intestinal chylomicrons.

Data in the literature suggest that apo E may also have a function in the assembly and/or secretion of VLDL by the liver. Studies by Strobl et al. (13) showed that stimulation of hepatic VLDL production in rats by feeding them sucrose-rich diets enhances apo E synthesis and secretion by promoting transcription of the apo E gene. Hamilton et al. (14) demonstrated that apo E is present in nascent VLDL particles within putatively forming Golgi secretory vesicles of rat hepatocytes. Studies by Fazio et al. (15) showed that most of the apo E secreted by human hepatoma cells (HepG2) becomes associated with large TG-containing lipoproteins when lipogenesis and TG secretion are stimulated, whereas the total amount of apo E synthesized and secreted is not affected. More recently,

Part of this work has been presented at the 69th Scientific Sessions of the American Heart Association in New Orleans, LA in November 1996, and in abstract form (1996. *Circulation.* 94:I–519).

Address correspondence to Dr. F. Kuipers, Groningen Institute for Drug Studies, Department of Pediatrics, Academic Hospital Groningen, Hanzeplein 1, 9713 GZ Groningen, The Netherlands. Phone: 31-50-363-2669; FAX: 31-50-361-1746; E-mail: f. kuipers@med.rug.nl

Received for publication 16 June 1997 and accepted in revised form 1 October 1997.

J. Clin. Invest.

0021-9738/97/12/2915/08 $2.00
Volume 100, Number 11, December 1997, 2915–2922
http://www.jci.org

1. *Abbreviations used in this paper:* LDH, lactate dehydrogenase; LFC, low fat/low cholesterol; TG, triglyceride.

Fazio and Yao (16) reported that the association between apo E and TG-rich lipoproteins in HepG2 and rat hepatoma cells (McA-RH7777) takes place intracellularly rather than extracellularly, after their secretion into the medium. Finally, recent studies by our group demonstrated that apo E–deficient mice accumulate large amounts of TG in their livers (17). Therefore, altogether, scattered evidence is available to suggest that apo E has a function in VLDL assembly and/or secretion.

In this paper, we investigated the effects of apo E deficiency on VLDL-TG synthesis and secretion in vivo as well as in vitro, using apo E–deficient mice, perfused apo E–deficient mouse livers, and isolated apo E–deficient hepatocytes. These studies demonstrate unequivocally that VLDL-TG production is severely impaired in the absence of apo E, whereas TG synthesis in apo E–deficient hepatocytes is not affected. In addition, impaired VLDL-TG production is also observed in apo E–deficient mice in which plasma cholesterol levels have been normalized by transplantation of wild-type bone marrow. These data lead us to conclude that apo E has a modulating role in the VLDL secretion cascade, representing a novel physiological function of this ubiquitous apolipoprotein.

Methods

Animals. apo E–deficient mice were generated as described previously (12). apo E–deficient and control (C57BL/6J) mice were housed in a light- and temperature-controlled environment and had free access to water and food.

To induce bone marrow aplasia, apo E–deficient and control mice (age 5–6 wk) were exposed to a single dose of 13 Gy (0.28 Gy/min, 200 kV, 4 mA) x-ray total body irradiation using an Andrex Smart 225 (Andrex Radiation Products A/S, Copenhagen, Denmark) with a 4-mm aluminum filter, 1 d before transplantation. Bone marrow cell suspensions were isolated by flushing the femurs and tibias from control mice with PBS. Single-cell suspensions were prepared by passing the cells through a 30-μm nylon gauze. Irradiated apo E–deficient and control recipients received 1.5×10^7 bone marrow cells by intravenous injection into the tail vein. Mice used for bone marrow transplantation experiments were housed in sterilized filter-top cages and fed sterilized chow (SRM-A; Hope Farms BV, Woerden, The Netherlands) containing 5.7% fat (wt/wt). Drinking water was supplied with antibiotics (83 mg/liter ciprofloxacin and 67 mg/liter polymyxin B sulphate) and 6.5 g/liter glucose.

For liver perfusion studies, female apo E–deficient and control mice were used that were fed a low fat/low cholesterol (LFC) semisynthetic diet, composed essentially according to Nishina et al. (18) (Hope Farms BV). The LFC diet contained 50.5% sucrose, 12.2% corn starch, 5% corn oil, and 5% cellulose, by weight, and was fed to the mice for a period of 3 wk.

Male apo E–deficient and control mice were used for cell isolations. These mice were fed a normal chow diet (RMH-B; Hope Farms BV) containing 6.2% fat and ~ 0.01% cholesterol by weight.

Experimental protocols were approved by the Ethics Committee for Animal Experiments of the University of Groningen.

Serum lipid and lipoprotein analysis. Levels of total plasma cholesterol and TG were measured, with or without free glycerol, using commercially available enzymatic kits (236691 and 701904; Boehringer Mannheim GmbH, Mannheim, Germany, and 337-B; Sigma Chemical Co., St. Louis, MO, respectively). The phospholipid content of nascent VLDL particles secreted from the perfused mouse liver was determined using an analytical kit (Wako Chemicals GmbH., Neuss, Germany). Total cholesterol and free cholesterol contents in nascent VLDL fractions were measured fluorometrically (excitation: 325 nm; emission: 415 nm) in a phosphate buffer (pH = 7.4) using cholesterol oxidase and peroxidase (Boehringer Mannheim GmbH), 0.5% Triton X-100 (Merck, Darmstadt, Germany), 20 mM cholic acid, and 4 mg/dl para-hydroxy-phenyl-acetic acid (Sigma Chemical Co.). Before measurements, total cholesterol was extracted using KOH/ethanol/hexane, and free cholesterol using ethanol/hexane. Esterified cholesterol was calculated as the difference between total and unesterified cholesterol.

Protein concentrations in VLDL fractions were measured according to Lowry et al. (19) using BSA (Sigma Chemical Co.) as standard.

In vivo hepatic VLDL-TG production using Triton WR1339. Untreated and bone marrow–transplanted mice were injected intravenously with 500 mg of Triton WR1339 (Sigma Chemical Co.) per kg body wt as a 15-g/dl solution in 0.9% NaCl after an overnight fast. Previous studies have shown that plasma VLDL clearance is virtually completely inhibited under these conditions (20). Blood samples (50 μl) were taken at 0, 1, 2, 3, and 4 h after Triton WR1339 injection, and plasma TG was measured enzymatically as described above. Plasma TG concentrations were related to the body mass of the animals, and the hepatic TG production rate was calculated from the slope of the curve and expressed as micromoles per hour per kilogram body weight.

Liver perfusion experiments. Experiments were always begun between 10 and 11 a.m. Fed mice were anesthetized by intraperitoneal injection of 0.5 ml/kg Hypnorm (Janssen-Cilag Pharmaceutica BV, Tilburg, The Netherlands) and 12.5 mg/kg midazolam (Roche Netherlands BV, Mijdrecht, The Netherlands). After cannulation of the portal vein with an Abbocath-T cannula (26 G × 19 mm; Abbott Laboratories, Kent, UK), livers were isolated and perfused (1.5 ml/min) in a recycling fashion. The liver and the perfusate were maintained at 37°C throughout the experiment. The recirculating perfusate (20–30 ml) was an RPMI buffer (RPMI 1640 medium; ICN Biomedicals, Inc., Costa Mesa, CA), pH 7.5, containing 1 mM vitamin C, 5 mM glutathione, and 2.5% (wt/wt) BSA. Oleate was added as a BSA-complex to the perfusate to reach a concentration of 1 mM in all experiments. The perfusate was gassed with 95% O_2/5% CO_2. All the perfused livers were functionally viable by gross appearance after a 3-h perfusion period. At termination of the experiment, livers were perfused with blue dye (Polysciences Inc., Warington, PA) to assess grade of perfusion, cleansed of all extrahepatic nonperfused tissue, and weighed.

Before isolation of nascent VLDL, the 20–30 ml of perfusate was concentrated to 10 ml (Centriprep 30; Amicon, Inc., Danvers, MA). Nascent VLDL fractions ($d < 1.006$ g/ml) were isolated by ultracentrifugation at 40,000 rpm in a swingout rotor (model SW-40; Beckman Instruments International S.A., Geneva, Switzerland) for 18 h at 5°C. Each VLDL sample was dialyzed extensively against PBS overnight at 4°C. The lipid composition of the nascent VLDL particles was analyzed as described above.

Preparation and culture of mouse hepatocytes. Hepatocytes were isolated from mouse livers as described previously by Klaunig et al. (21). Briefly, the portal vein was cannulated with a 22-gauge plastic cannula. First, the liver was perfused with calcium-free HBSS containing glucose (10 mM) and Hepes (10 mM), pregassed with 95% O_2/5% CO_2, and adjusted to pH 7.42, at a flow rate of 4 ml/min. Subsequently, the liver was perfused with a collagenase solution (20 mg collagenase [Sigma Chemical Co.]/200 ml calcium-containing [5 mM] HBSS) for ~ 10–15 min until swelling of the liver was observed. Hepatocytes were then gently released from the surrounding capsule. Isolated hepatocytes were washed three times with Williams' E medium (Life Technologies Ltd., Paisley, UK) containing 5% (wt/wt) BSA. Hepatocytes were isolated with similar yields from livers of control and apo E–deficient mice, with average values of $\sim 6 \times 10^7$ cells/liver. The viability of hepatocytes was assessed by trypan blue (final concentration 0.2%) exclusion immediately after isolation, and varied between 65 and 80% of the total amount of cells isolated. No differences were observed in this respect between cells isolated from apo E–deficient and control mice. Cells were plated in 35-mm 6-well plastic dishes (Costar Corp., Cambridge, MA), precoated with collagen (Serva Feinbiochemica, Heidelberg, Germany), at a density of

1.0×10^6 viable cells/well in 2 ml culture medium. After a 2-h adherence period, nonviable cells were removed from the cultures by careful washing. The culture medium consisted of Williams' E medium supplemented with 10% FCS (Bio Withaker, Verviers, Belgium), 100 μg/ml of penicillin and streptomycin (Life Technologies Ltd.), 4 mU/ml insulin, and 0.02 μg/ml dexamethasone (both from Novo Nordisk Pharma BV, Amsterdam, The Netherlands) as described previously by Princen et al. (22). Cells were incubated at 37°C in an atmosphere of 95% air/5% CO_2 and rapidly formed monolayers.

The total synthesis and secretion of proteins by cultured hepatocytes was determined by [^{3}H]leucine incorporation into TCA-precipitable proteins. For this purpose, [^{3}H]leucine (2 μCi/ml per well; Amersham International, Little Chalfont, UK) was added to the medium 3 h before termination of cell incubation. Both the protein synthesis and the secretion of newly synthesized protein were similar in overnight cultured hepatocytes isolated from apo E–deficient and control mice.

Lactate dehydrogenase (LDH) activity in media and cells was determined as reported previously (23). No differences were observed in LDH leakage from hepatocytes isolated from apo E–deficient or control mice. In all cases, > 95% of the LDH activity was found intracellularly.

Experimental protocols for cultured hepatocytes. After an overnight culture, FCS-containing medium was removed from the wells, and cells were washed twice with FCS/hormone-free medium. Cells were incubated subsequently with FCS/hormone-free medium (1 ml/well, pH 7.4) containing 0.25 mM BSA only, or BSA–oleate complex (0.75 mM oleate/0.25 mM BSA) at 37°C for either 4 or 24 h. In all experiments, oleate was used to stimulate hepatocytic lipogenesis. Medium containing BSA–oleate complexes was freshly prepared on the day of each experiment.

To determine the glycerolipid synthesis and secretion rates, [^{3}H]glycerol (4.4 μCi, 25 μM final concentration; Amersham International) or [^{3}H]oleate (2 μCi, in 10 μl ethanol; Amersham International) was added to each well according to different experimental protocols (see figure citations in Results). All incubations were performed in triplicate and terminated by placing the culture plates on ice. Media were collected and centrifuged at 10,000 rpm for 2 min to remove suspended cells. Cells were washed three times with cold PBS and harvested using a rubber policeman in 2 ml PBS. Samples were frozen at −20°C before analysis.

Cholesterol synthesis by cultured cells was estimated by measuring [^{14}C]acetate (Amersham International) incorporation into sterols. Previous studies have indicated that this method yields relative values for cellular lipid synthesis similar to those obtained with [^{3}H]water in cultured hepatocytes (24).

Assessment of cellular and VLDL lipid content. Nascent VLDL particles ($d < 1.006$ g/ml) were isolated from the medium by ultracentrifugation at 41,000 rpm in a TST 41.14 rotor (Kontron Instruments, Milan, Italy) for 24 h at 4°C. The radiolabeled lipids from VLDL and cells were extracted with chloroform/methanol (1:2, vol/vol). Before lipid extractions, cells were first thawed and resuspended by passing through 26 G (0.45 × 25 mm) needles five times. Radiolabeled cellular TG, free cholesterol, cholesterol ester, and phospholipids were separated by TLC on silica gel 60 plates (Merck) with hexane/diethylether/acetic acid (80:20:1, vol/vol/vol) as resolving solution. Before TLC analysis, tripalmitin (Sigma Chemical Co.) in chloroform was added to each sample as a carrier for TG determination. After iodine staining of the silica gel plates, the spots containing the lipids of interest were scraped into vials and assayed for radioactivity by scintillation counting.

In another set of experiments, TG content of VLDL and cells was measured using a commercially available kit from Boehringer Mannheim GmbH as described above. Free cholesterol and cholesterol ester contents were determined according to the methods developed by Gamble et al. (25). Phospholipids were determined by measuring the phosphorus content of lipid extracts after perchloric acid treatment (26).

Electron microscopy. VLDL fractions were prepared for electron microscopy analysis within 1 h after their isolation by ultracentrifugation. The particles were allowed to adhere to hydrophilic carbon films and were immersed in 2% potassium phosphotungstate (pH 7.4) as a negative stain. Electron micrographs were obtained in a transmission electron microscope (model EM208; Philips Electron Optics, Eindhoven, The Netherlands). Size distribution of VLDL particles was determined using Quantimet 520+ software (Leica Cambridge Ltd., Cambridge, UK).

Western blotting of apo B. VLDL particles were isolated from the media by ultracentrifugation as described above and adsorbed to hydrated colloidal fumed silica (Cab-O-Sil, particle size 0.011 μm; Sigma Chemical Co.) as reported previously (27). The VLDL apo B and apo E contents were analyzed by immunoblotting as described by Lin et al. (28) using rabbit anti–rat apo B serum showing cross-reactivity with murine apo B (a kind gift of Roger A. Davis, San Diego State University, San Diego, CA) and rabbit anti–mouse apo E serum (kindly provided by Pieter H.E. Groot, SmithKline Beecham Pharmaceuticals, The Frythe, Welwyn, UK).

Results

In vivo VLDL-TG production rate in apo E–deficient mice: effect of bone marrow transplantation. The effect of apo E deficiency on the in vivo VLDL-TG production rate was determined by injecting apo E–deficient and control mice with Triton WR1339. Table I shows that the hepatic TG production rate was reduced in apo E–deficient mice compared with controls (61.1±3.6 vs. 112.6±19.4 μmol TG/h/kg, respectively). To verify whether this effect is attributable to the lack of apo E within the hepatocytes, and not to aspecific changes in liver function due to the hypercholesterolemia associated with apo E deficiency, wild-type mouse bone marrow cells expressing apo E were transplanted into apo E–deficient mice. In these mice, bone marrow–derived macrophages are the only sources of apo E, i.e., there is no expression of apo E in hepatocytes.

Table I. Plasma Lipid Levels and In Vivo VLDL-TG Production Rates in apo E–deficient and Control Mice: Effects of Bone Marrow Transplantation

Mice	*n*	TC	TG	PR
		mmol/liter	*mmol/liter*	*μmol TG/h/kg*
Control	3	1.8±0.2	2.8±0.2	112.6±19.4
apo E–deficient	3	18.1±1.4*	3.7±0.6	61.1±3.6*
Control Tx	3	1.5±0.2	2.9±0.3	109.8±23.3
apo E–deficient Tx	3	2.5±0.7	3.0±0.1	45.2±14.2*

Total cholesterol (*TC*) and TG levels were measured in the plasma of fasted apo E–deficient and control (C57BL/6J) mice using enzymatic kits (236691 and 701904, respectively; Boehringer Mannheim). Irradiated apo E–deficient and control mice were given transplants (*Tx*) of wild-type bone marrow cells as described in Methods. Hepatic VLDL-TG production rate (*PR*) was measured by injecting mice with Triton WR1339 (500 mg/kg). For the transplanted mice, Triton WR1339 was injected 16–20 wk after bone marrow transplantation. Plasma TG levels were determined before injection (0 min) and at 30, 60, 120, 180, and 240 min after Triton injection. Hepatic VLDL-TG production rate was calculated from the slope of the curve. *$P < 0.05$, indicating significant differences between untreated control and apo E–deficient mice, or between transplanted control and apo E–deficient mice, using Student's *t* test.

Bone marrow transplantation effectively reversed hypercholesterolemia in apo E–deficient mice (Table I), as reported previously by other groups (29, 30). Introduction of wild-type bone marrow into control mice had no effect on plasma lipid concentrations (Table I). In spite of normalized plasma lipid levels, VLDL-TG production rates remained inhibited in transplanted apo E–deficient mice compared with the transplanted control mice (45.2±14.2 vs. 109.8±23.3 μmol TG/h/kg, respectively) (Table I). These results indicate that the reduced hepatic TG production observed in apo E–deficient mice is related to the absence of apo E in the liver.

Secretion of nascent VLDL by isolated perfused mouse livers. To investigate the effects of apo E deficiency on nascent VLDL-TG production by polarized hepatocytes in their physiological environment, we performed studies with isolated perfused livers from apo E–deficient and control mice. To stimulate VLDL-TG production (18), mice were fed the sucrose-containing LFC diet for a period of 3 wk before the liver perfusion experiments.

VLDL-TG secretion by isolated perfused mouse livers was linear during a 3-h period of perfusion (data not shown), indicating that the liver remains functionally viable during this time period. VLDL-TG production by perfused livers from apo E–deficient mice was reduced by 50% compared with perfused control livers (Table II). In addition, the nascent VLDL particles produced by apo E–deficient livers had a lipid composition similar to nascent VLDL secreted by control livers (Table II).

Characteristics of nascent VLDL particles produced by mouse hepatocytes in primary culture. The TG and cholesterol contents of apo E–deficient cells cultured for 24 h in the absence of oleate (0.75 mM) were elevated significantly compared with control cells, whereas no differences in cholesterol ester and phospholipid content were found (Table III). The presence of oleate in the incubation medium resulted in a marked TG accumulation in both apo E–deficient and control cells compared with oleate-free conditions (Table III).

The secretion of nascent VLDL by cultured hepatocytes was quantitated through lipid content analysis of the < 1.006 g/ml fractions obtained by density gradient ultracentrifugation of media collected after 24 h of incubation. As shown in Fig. 1 (*left*), apo E–deficient cells produce slightly but significantly less VLDL-TG compared with control cells in the absence of oleate (77% of control values). The total mass lipid secretion by control cells was stimulated in the presence of oleate (compare *left* and *right panels* in Fig. 1). In contrast, VLDL-TG production by apo E–deficient cells was strongly reduced in the presence of oleate (39% of control values) (Fig. 1, *right*). Furthermore, the relative lipid composition of VLDL secreted by apo E–deficient and control cells appeared to be similar under all conditions (Fig. 1).

Western blot analysis revealed that apo B48 is the major form of apo B secreted by control and apo E–deficient mouse hepatocytes, which is consistent with the high level of apo B mRNA editing activity in mouse liver (31) (results not shown). As expected, apo E could be detected in VLDL particles produced by control cells but not in those from apo E–deficient cells (data not shown).

The size of the particles isolated from the < 1.006 g/ml fractions was determined by electron microscopy. As shown in Fig. 2 (*left*), no differences in size were found between apo E–deficient and control particles when cells were cultured under oleate-free conditions (41.8±0.7 vs. 43.8±2.0 nm, respectively). In contrast, when cells were cultured in the presence of oleate, the average diameter of apo E–deficient VLDL particles was smaller than that of control particles (38.3±3.3 nm vs. 49.5±1.9 nm, respectively) (Fig. 2, *right*). The average size of VLDL particles formed in the presence of oleate was significantly larger for control cells compared with oleate-free conditions (compare *left* and *right panels* in Fig. 2).

Since the size of apo E–deficient VLDL was smaller than control VLDL under oleate-stimulated conditions, it was investigated whether these particles could be recovered in higher density fractions upon ultracentrifugation. Therefore, we performed cell incubation experiments in the presence of 0.75 mM oleate and [^{3}H]glycerol to label the newly synthesized lipids. After 24 h of incubation, the medium was harvested, and VLDL was isolated by ultracentrifugation. Although the total amount of radiolabeled lipids secreted by apo E–deficient cells is decreased compared with control cells, most of the radioac-

Table II. VLDL-TG Production Rate and Relative Lipid Composition of Nascent VLDL Secreted by Perfused Livers from apo E–deficient and Control Mice

Nascent VLDL	VLDL-TG production	TG	FC	CE	PL
	μg TG/g liver	% of total lipid (by wt)			
Control	317±46	80±4	2±1	5±1	13±4
apo E–deficient	158±23*	75±6	2±1	9±5	17±5

Livers of female apo E–deficient and control (C57BL/6J) mice fed a sucrose-based semisynthetic (LFC) diet for 3 wk were perfused in a recirculating fashion as described in Methods. After 3 h of liver perfusion, perfusates were collected, and nascent VLDL was isolated by ultracentrifugation and analyzed for its lipid composition. TG, free cholesterol (*FC*), cholesterol ester (*CE*), and phospholipid (PL) contents of nascent VLDL particles were determined as described in Methods. Values are given as mean±SD of four individual liver perfusion experiments per group. *$P < 0.05$, indicating a significant difference between apo E–deficient and control perfused liver preparations, using Student's *t* test.

Table III. Cellular Lipid Content of apo E–deficient and Control Mouse Hepatocytes in Primary Culture

		TG	FC	CE	PL
		nmol/mg protein			
No oleate	Control	81±9	34±3	4±1	206±25
	apo E–deficient	142±50*	58±8*	5±1	251±44
With oleate	Control	277±79‡	39±6	6±2	255±52
	apo E–deficient	304±71‡	51±4*	9±2	286±46

Cells were cultured for 24 h in the absence or presence of oleate (0.75 mM) and were subsequently washed and harvested for lipid analysis. Cellular TG, free cholesterol (*FC*), cholesterol ester (*CE*), and phospholipid (*PL*) contents were measured as described in Methods. Values are expressed as mean±SD of four individual hepatocyte preparations per group. *$P < 0.05$, indicating a significant difference between apo E–deficient and control preparations under the same culture conditions. ‡$P < 0.05$, indicating a significant difference between hepatocyte preparations in the absence or presence of oleate, using Student's *t* test.

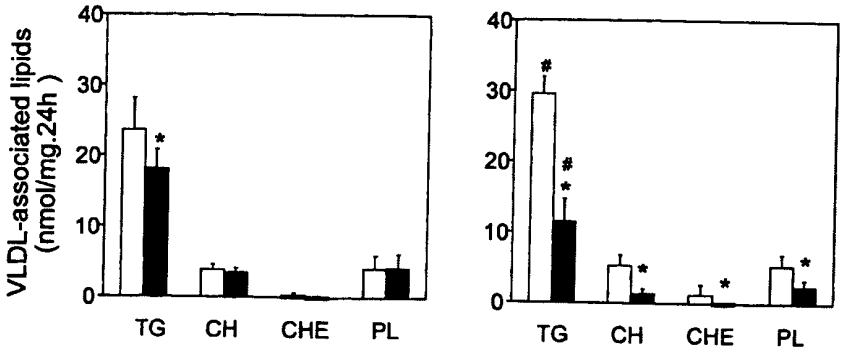

Figure 1. VLDL-associated lipid secretion by apo E–deficient and control mouse hepatocytes. Cells were cultured for 24 h in the absence (*left panel*) or presence (*right panel*) of 0.75 mM oleate as described in Methods. Lipoproteins were isolated from the < 1,006 g/ml fraction after density gradient ultracentrifugation of medium samples, and lipid composition was analyzed, as described in Methods. Values are expressed as mean±SD of four independent experiments in each group. $*P < 0.05$, indicating significant differences between apo E–deficient (*black bars*) and control cells (*white bars*) under the same culture conditions. $*P < 0.05$, indicating significant differences between absence and presence of oleate, using Student's *t* test. *CH*, Cholesterol. *CHE*, Cholesterol ester. *PL*, phospholipid.

tivity is recovered from the < 1.006 g/ml fractions for both control and apo E–deficient cells (Fig. 3). Thus, these results indicate that the decreased recovery of apo E–deficient VLDL in the < 1.006 g/ml fraction is due to an impaired VLDL secretion by apo E–deficient hepatocytes, rather than to a shift in the density of apo E–deficient particles.

Secretion of newly synthesized TG by hepatocytes in primary culture. To compare the cellular synthesis and secretion of newly formed lipids by control and apo E–deficient cells, we performed incubation experiments with either [^{3}H]glycerol or [^{3}H]oleate to label the newly synthesized TG. Fig. 4 shows a similar time-dependent cellular accumulation of [^{3}H]TG formed from radiolabeled glycerol in apo E–deficient and wild-type cells, both in the absence (Fig. 4 *A*) and presence (Fig. 4 *B*) of oleate. Similar results were obtained in three additional independent experiments in which [^{3}H]TG production by apo E–deficient and control cells was compared. On average, the cellular [^{3}H]TG content was 30% (without oleate) and 24% (with oleate) higher in apo E–deficient than in control hepatocytes, after 3 h of incubation. However, these differences were not statistically significant. In contrast, the [^{3}H]TG secretion by apo E–deficient cells was decreased significantly, by 60% in the absence (Fig. 4 *C*) and 73% in the presence of oleate (Fig. 4 *D*) compared with control cells. Similar results were obtained when [^{3}H]oleate was used to label the newly synthesized lipids.

Measurement of the incorporation of [^{14}C]acetate into cellular cholesterol, indicative for cholesterol biosynthesis, did not reveal any significant difference in this respect between apo E–deficient and control cells, either in the absence or presence of oleate in the incubation media (data not shown).

Discussion

Production of VLDL by the liver is an important determinant of plasma lipid levels in humans. It is well-established that apo B is required for the assembly and secretion of these TG-rich lipoproteins by liver cells, and that each particle contains a single apo B molecule (32). Although controversies still exist, most of the available data, as summarized in recent reviews (33–36), indicate that regulation of apo B secretion is primarily a posttranslational event governed by the efficiency of translocation of the protein across the endoplasmic reticulum membrane and its association with lipids. Excess of apo B that does not associate appropriately with lipids inside the endoplasmic reticulum lumen is degraded rapidly. There is a large body of experimental evidence indicating that both the availability of core (TG, cholesterol ester) and surface lipid (phospholipid) can become rate-limiting for VLDL production. Furthermore, several studies have shown that the microsomal triglyceride transfer protein is essential for adequate lipoprotein formation (37–39). In addition, other proteins have been identified that

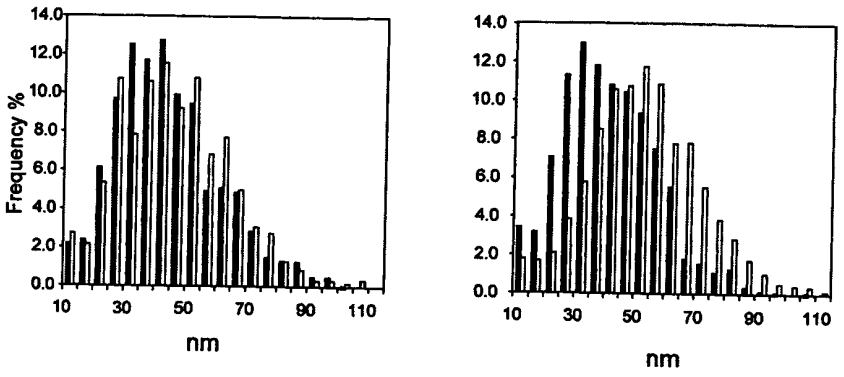

Figure 2. Frequency distribution of particle diameter of VLDL produced by apo E–deficient and control mouse hepatocytes. apo E–deficient (*black bars*) and control (C57BL/6J) mouse (*white bars*) hepatocytes were cultured for 24 h in the absence (*left panel*) or presence (*right panel*) of 0.75 mM oleate, as described in Methods. Lipoproteins ($d < 1.006$ g/ml) were isolated from the media by ultracentrifugation and studied by electron microscopy, as described in Methods. Values are expressed as the mean of four independent VLDL preparations per group. SD bars are not shown for clarity reasons. In each preparation, ~ 500 particles were analyzed.

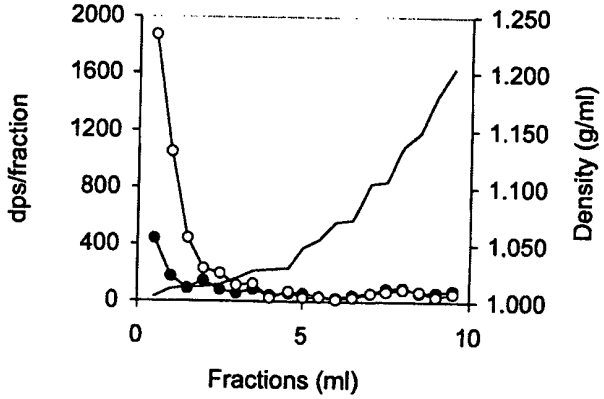

Figure 3. Density gradient ultracentrifugation profiles of radiolabeled lipids accumulated in the culture medium of primary hepatocytes isolated from control (*open symbols*) and apo E–deficient (*closed symbols*) mice. Hepatocytes were incubated in serum-free media containing [^{3}H]glycerol and 0.75 mM oleate complexed with BSA (0.25 mM) for 24 h. After incubation, the media were collected, centrifugated to remove any cell debris, and dialyzed extensively. Immediately before ultracentrifugation, 0.5 ml of normal human plasma was added as a carrier. Fractions were collected, extracted, and assayed for radioactivity as described in Methods. The data represent the mean of three independent experiments per group. *Solid line*, Average density of the collected fractions. *dps*, Desintegrations per second.

may play a role in the assembly of VLDL (for a review, see reference 35).

In this study, data are presented that identify apo E as an additional factor involved in the regulation of VLDL assembly and secretion by hepatocytes. A pronounced reduction in VLDL-TG secretion by apo E–deficient liver cells was observed in three different experimental systems, i.e., in the intact animal, in the isolated perfused liver, and in hepatocytes in primary culture. It could be argued that the decreased VLDL-TG secretion by apo E–deficient hepatocytes is not directly related to the lack of apo E, but rather to aspecific changes in the livers of apo E–deficient mice as induced by profound hypercholesterolemia. To address this possibility, in vivo hepatic TG production studies were performed with apo E–deficient mice in which the hypercholesterolemia was effectively reversed by transplantation of wild-type bone marrow. These studies showed that hepatic TG production is still severely impaired in bone marrow–transplanted apo E–deficient mice (Table I). In addition, no differences were observed between cultured apo E–deficient and control hepatocytes with respect to cell viability, protein synthesis and secretion, and LDH leakage. Altogether, these data indicate strongly that the reduced TG secretion by apo E–deficient liver cells is caused primarily by the absence of apo E.

To gain more insight into the mechanisms underlying reduced TG secretion by apo E–deficient liver cells, nascent VLDL-TG secretion studies were performed using isolated perfused mouse livers and cultured hepatocytes. One of the major advantages of the perfused liver model is that the hepatocytes maintain their secretory polarity, a feature that is obviously lost in cell culture. Secretion of VLDL-TG by livers from apo E–deficient mice was reduced by 50% compared with control mice. In addition, perfused mouse livers of either strain produced nascent VLDL particles with similar lipid composition (Table II), indicating that apo E–deficient mouse livers essentially produce normal TG-rich VLDL.

Much of our knowledge of the VLDL production process is derived from in vitro studies with hepatoma cell lines and primary hepatocyte cultures. Human (HepG2) and rat (McA-RH7777) hepatoma cell lines (15, 16) as well as SV40 large T antigen–immortalized human hepatocytes (40) typically secrete apo B–containing particles in the LDL-density range, probably as a consequence of their dedifferentiated state, in which a number of liver-specific functions are lost (40). In contrast, short-term primary cultures of rat (41), human (28), and

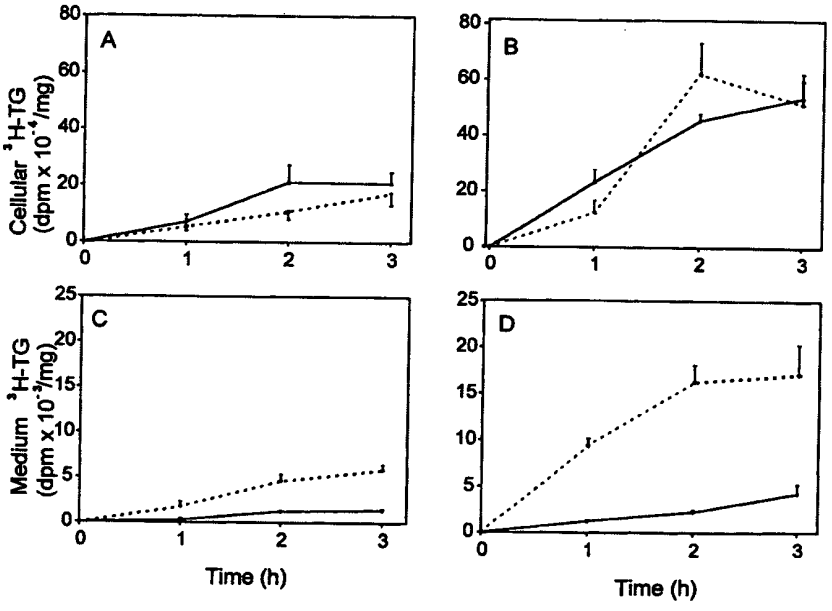

Figure 4. Time-dependent accumulation of [^{3}H]TG in apo E–deficient and control hepatocytes and secretion of [^{3}H]TG-VLDL by these cells. After their isolation, apo E–deficient (*solid line*) and control (C57BL/6J) hepatocytes (*dotted line*) were cultured overnight in FCS and hormone-containing media. Cells were washed thoroughly and incubated for an additional 4 h in FCS and hormone-free medium. Subsequently, cells were incubated with medium containing BSA in the absence (*A* and *C*) or presence (*B* and *D*) of 0.75 mM oleate. [^{3}H]Glycerol was added to label newly synthesized TG, as outlined in Methods. At the indicated time points, cells and media were harvested, and the accumulation of cellular [^{3}H]TG (*A* and *B*) and secretion of [^{3}H]TG-VLDL (*C* and *D*) were determined as described in Methods. A representative experiment is shown in which cells isolated from a single apo E–deficient mouse and a control mouse were studied simultaneously. Values are expressed as the mean±SD of triplicate determinations at each time point.

murine (20) hepatocytes secrete primarily VLDL, reflecting more closely the in vivo situation. The data depicted in Fig. 3 demonstrate that apo E–deficient hepatocytes in primary culture secrete newly synthesized lipids primarily in particles of the VLDL-density range, similar to the situation observed for wild-type control cells.

Experiments with apo E–deficient hepatocytes in culture showed an impaired VLDL-TG secretion, both when mass secretion was determined over a 24-h period (Fig. 1) and when secretion of newly synthesized TG from radiolabeled precursors was measured (Fig. 4, *C* and *D*). This impaired VLDL-TG secretion by apo E–deficient hepatocytes was not likely to be caused by decreased intracellular TG synthesis, since the TG synthesis rate as measured by [^{3}H]glycerol incorporation was similar for apo E–deficient and control cells (Fig. 4, *A* and *B*). In addition, apo E–deficient cells showed significantly higher TG and cholesterol contents compared with cells from wild-type mice (Table III). This is consistent with our previous in vivo observations (17), although the difference in hepatic TG content was larger under in vivo conditions. This may be due to selective isolation of relatively lipid-poor cells from periportal areas (zone 1), since it was found that TG-containing fat droplets are localized predominantly in perivenous (zone 3) hepatocytes in apo E–deficient livers (17). Alternatively, the lipid-laden zone 3 cells may have been lost more easily during isolation and subsequent washing procedures.

In the absence of oleate, cells from apo E–deficient mice secreted less VLDL-TG, whereas the VLDL particles were of similar size and composition as those secreted by cells from control mice (Figs. 1 and 2). These data point to a significant reduction in the number of VLDL particles secreted by apo E–deficient hepatocytes. Since each VLDL particle contains a single molecule of apo B, secretion of this apolipoprotein must also be reduced. However, in the presence of oleate, VLDL particles formed by apo E–deficient cells were significantly smaller than those produced by control cells (Fig. 2). A simple calculation shows that the 10.7-nm difference in diameter between apo E–deficient and control particle size (Fig. 2) results in a 2.2-fold larger particle volume for VLDL produced by control cells. This value relates reasonably well to the 2.6-fold higher production of core lipids by control cells under these conditions (Fig. 1). Thus, under oleate-stimulated conditions, it is suggested that apo E–deficient hepatocytes secrete smaller VLDL particles, but their overall number is not affected. Clearly, further studies are necessary to establish the modulating effect of apo E on VLDL particle size and secretion. Such experiments, including detailed analysis of apo B synthesis and secretion, are currently being performed in our laboratory.

Previous studies have shown that the synthesis rate of cholesterol in the liver may affect VLDL secretion (42). In this study, the incorporation of [^{14}C]acetate into cellular cholesterol was similar in control and apo E–deficient cells both in the absence and presence of oleate in the incubation medium. These results indicate that the impaired VLDL production by apo E–deficient hepatocytes observed in this study is not caused by differences in cholesterol biosynthesis.

How does apo E influence VLDL particle assembly and secretion? As outlined in the Introduction, Fazio et al. (15) have reported an enhanced association of apo E with large, apo B–containing lipoproteins during stimulation of lipogenesis in HepG2 cells, while the total amount of apo E secretion did not change. Similar findings were also reported in a study by Davis et al. (43) using rat hepatocytes in primary culture. Fazio and Yao (16) speculated that this increased association reflects a physical preference of apo E for the larger particles, providing an effective way to enrich these particles with apo E in order to facilitate subsequent carrier-mediated uptake of their remnants from blood. However, our data strongly suggest that apo E actually has a function in the assembly–secretion process at the intracellular level, in particular when lipogenesis is stimulated by the presence of oleate in the culture media. Although the exact mechanism(s) remains to be elucidated, our data seem to indicate that apo E is involved in the incorporation of (newly synthesized) TG into VLDL particles produced by mouse liver cells. At this point, it is tempting to speculate that apo E interferes with the recruitment of newly synthesized TG into the small microsomal secretion-coupled pool of TG that is suggested to be involved in the regulation of apo B secretion (44). Interestingly, Gretch et al. (45) have found recently that the expression of human apo E in insect larvae leads to progressive conversion of the endogenous lipoproteins into more buoyant species. Although there clearly are major differences in lipoprotein assembly between the insect and mammalian systems, this finding demonstrates that apo E can influence the amount of lipid assembled into lipoproteins and thereby affect their size and buoyant density. Thus, in conclusion, we propose that in addition to its well-established function in lipoprotein uptake by the liver, apo E also plays an important physiological role in lipoprotein formation by hepatocytes.

Acknowledgments

The authors thank Dr. Marja van Luyn and Bert Blaauw (Laboratory for Cell Biology and Electron Microscopy, University of Groningen) for excellent technical assistance.

This work was supported by grants 900-716-028, 901-04-092, and 904-39-117 from the Netherlands Foundation of Scientific Research, the Netherlands Heart Foundation, and Nutricia BV, Zoetermeer, The Netherlands. A financial contribution from the specific Research on Cardiovascular Diseases Programme of the European Commission (Biomed-2, BMH-CT96-0898) is gratefully acknowledged. Y. Lin was supported by the Royal Netherlands Academy of Arts and Sciences. F. Kuipers and M.H. Hofker are established investigators of the Netherlands Heart Foundation.

References

1. Mahley, R.W. 1988. Apolipoprotein E: cholesterol transport protein with expanding role in cell biology. *Science.* 240:622–630.

2. Jong, M.C., V.E.H. Dahlmans, P.J.J. van Gorp, M.L. Breuer, M.J.T.M. Mol, A. van der Zee, R.R. Frants, M.H. Hofker, and L.M. Havekes. 1996. Both lipolysis and hepatic uptake of VLDL are impaired in transgenic mice coexpressing human apolipoprotein E*3Leiden and human apolipoprotein C1. *Arterioscler. Thromb. Vasc. Biol.* 16:934–940.

3. Rensen, P.C.N., and T.J.C. van Berkel. 1996. Apolipoprotein E effectively inhibits lipoprotein lipase-mediated lipolysis of chylomicron-like triglyceride-rich lipid emulsions in vitro and in vivo. *J. Biol. Chem.* 271:14791–14799.

4. Ji, Z.-S., S. Fazio, Y.-L. Lee, and R.W. Mahley. 1994. Secretion-capture role for apolipoprotein E in remnant lipoprotein metabolism involving cell surface heparan sulfate proteoglycans. *J. Biol. Chem.* 269:2764–2772.

5. Choi, S.Y., M.C. Komaromy, J. Chen, L.G. Fong, and A.D. Cooper. 1994. Acceleration of uptake of LDL but not chylomicrons or chylomicron remnants by cells that secrete apo E and hepatic lipase. *J. Lipid Res.* 35:848–859.

6. Schwiegelshohn, B., J.F. Presley, M. Gorecki, T. Vogel, Y.A. Carpentier, F.R. Maxfield, and R.J. Deckelbaum. 1995. Effects of apolipoprotein E on intracellular metabolism of model triglyceride-rich particles are distinct from effects on cell particle uptake. *J. Biol. Chem.* 270:1761–1769.

7. Lombardi, P., M. Mulder, H. van der Boom, R.R. Frants, and L.M. Havekes. 1993. Inefficient degradation of triglyceride-rich lipoprotein by HepG2 cells is due to a retarded transport to the lysosomal compartment. *J. Biol. Chem.* 268:26113–26119.

8. Plump, A.S., and J.L. Breslow. 1995. Apolipoprotein E and the apolipoprotein E-deficient mouse. *Annu. Rev. Nutr.* 15:495–518.

9. Breslow, J.L. 1996. Mouse models of atherosclerosis. *Science.* 272:685–688.

10. Plump, A.S., J.D. Smith, T. Hayek, K. Aalto-Setälä, A. Walsh, and J.L. Breslow. 1992. Severe hypercholesterolemia and atherosclerosis in apolipoprotein E-deficient mice created by homologous recombination in ES cells. *Cell.* 71:343–353.

11. Zhang, S.H., R.L. Reddick, J.A. Piedrahita, and N. Maeda. 1992. Spontaneous hypercholesterolemia and arterial lesions in mice lacking apolipoprotein E. *Science.* 258:468–471.

12. Van Ree, J.H., W.J.A.A. van den Broek, V.E.H. Dahlmans, P.H.E. Groot, M. Vidgeon-Hart, R.R. Frants, B. Wierenga, L.M. Havekes, and M.H. Hofker. 1994. Diet-induced hypercholesterolemia and atherosclerosis in heterozygous apolipoprotein E-deficient mice. *Atherosclerosis.* 111:25–37.

13. Strobl, W., N.L. Gorder, G.A. Fienup, Y.C. Lin-Lee, A.M. Gotto, and W. Patsch. 1989. Effect of sucrose diet on apolipoprotein biosynthesis in rat liver. Increase in apolipoprotein E gene transcription. *J. Biol. Chem.* 264:1190–1194.

14. Hamilton, R.L., J.S. Wong, L.S.S. Guo, S. Krisans, and R.J. Havel. 1990. Apolipoprotein E localization in rat hepatocytes by immunogold labeling of cryothin sections. *J. Lipid Res.* 31:1589–1603.

15. Fazio, S., Z. Yao, B.J. McCarthy, and S.C. Rall, Jr. 1992. Synthesis and secretion of apolipoprotein E occur independently of synthesis and secretion of apolipoprotein B-containing lipoproteins in HepG2 cells. *J. Biol. Chem.* 267: 6941–6945.

16. Fazio, S., and Z. Yao. 1995. The enhanced association of apolipoprotein E with apolipoprotein B-containing lipoproteins in serum-stimulated hepatocytes occurs intracellularly. *Arterioscler. Thromb. Vasc. Biol.* 15:593–600.

17. Kuipers, F., J.M. van Ree, M.H. Hofker, H. Wolters, G. In't Veld, R. Havinga, R.J. Vonk, H.M.G. Princen, and L.M. Havekes. 1996. Altered lipid metabolism in apolipoprotein E-deficient mice does not affect cholesterol balance across the liver. *Hepatology.* 24:241–247.

18. Nishina, P.M., J. Verstuyft, and B. Paigen. 1990. Synthetic low and high fat diets for the study of atherosclerosis in the mouse. *J. Lipid Res.* 31:859–869.

19. Lowry, O.H., N.J. Rosenbrough, A.L. Farr, and R.J. Randall. 1951. Protein measurement with Folin reagent. *J. Biol. Chem.* 193:265–275.

20. Aalto-Setälä, K., E.A. Fisher, X. Chen, T. Chajek-Shaul, T. Hayek, R. Zechner, A. Walsh, R. Ramakrishnan, H.N. Ginsberg, and J.L. Breslow. 1992. Mechanism of hypertriglyceridemia in human apolipoprotein (apo) CIII transgenic mice. Diminished very low density lipoprotein fractional catabolic rate associated with increased apo CIII and reduced apo E on the particles. *J. Clin. Invest.* 90:1889–1900.

21. Klaunig, J.E., P.J. Goldblatt, D.E. Hinton, M.M. Lipsky, J. Chacko, and B.F. Trump. 1981. Mouse liver cell culture. I. Hepatocyte isolation. *In Vitro (Rockville).* 17:913–925.

22. Princen, H.M.G., C.M.G. Huijsmans, F. Kuipers, R.J. Vonk, and H.J.M. Kempen. 1986. Ketoconazole blocks bile acid synthesis in hepatocyte monolayer cultures and in vivo in rat by inhibiting cholesterol 7α-hydroxylase. *J. Clin. Invest.* 78:1064–1071.

23. Smit, M.J., H. Beekhuis, A.M. Duursma, J.M.W. Bouma, and M. Gruber. 1988. Catabolism of circulating enzymes: plasma clearance, endocytosis and breakdown of lactate dehydrogenase. *Clin. Chem.* 34:2475–2480.

24. Davis, R.A., M.M. McNeal, and R.L. Moses. 1982. Intrahepatic assembly of very low density lipoprotein. Competition by cholesterol ester for the hydrophobic core. *J. Biol. Chem.* 257:2634–2640.

25. Gamble, W., M. Vaughan, H.S. Kruth, and J. Avigan. 1978. Procedure for determination of free and total cholesterol in micro- or nanogram amounts suitable for studies with cultured cells. *J. Lipid Res.* 19:1068–1070.

26. Böttcher, C.F.J., C.M. van Gent, and C.A. Pries. 1961. A rapid and sensitive sub-micro phosphorous determination. *Anal. Chim. Acta.* 24:203–204.

27. Vance, D.E., D.B. Weinstein, and D. Steinberg. 1984. Isolation and analysis of lipoproteins secreted by rat liver hepatocytes. *Biochim. Biophys. Acta.* 792:39–47.

28. Lin, Y., R. Havinga, H.J. Verkade, H. Moshage, M.J.H. Slooff, R.J. Vonk, and F. Kuipers. 1996. Bile acids suppress the secretion of very-low-density lipoprotein by human hepatocytes in primary culture. *Hepatology.* 23:218–228.

29. Linton, M.F., J.B. Atkinson, and S. Fazio. 1995. Prevention of atherosclerosis in apolipoprotein E-deficient mice by bone marrow transplantation. *Science.* 267:1034–1037.

30. Boisvert, W.A., J. Spangenberg, and L.K. Curtiss. 1995. Treatment of severe hypercholesterolemia in apolipoprotein E-deficient mice by bone marrow transplantation. *J. Clin. Invest.* 96:1118–1124.

31. Greeve, J., I. Altkemper, J.H. Dieterich, H. Greten, and E. Windler. 1993. Apolipoprotein B mRNA editing in 12 different mammalian species: hepatic expression is reflected in low concentrations of apo B-containing plasma lipoproteins. *J. Lipid Res.* 34:1367–1383.

32. Elovsen, J., J.E. Chatterton, G.T. Bell, V.N. Schumaker, M.A. Reuben, D.L. Puppione, J.R. Reeve, and N.L. Young. 1988. Plasma very low density lipoproteins contain a single molecule of apolipoprotein B. *J. Lipid Res.* 29:1461–1473.

33. Yao, Z., and R.S. McLeod. 1994. Synthesis and secretion of hepatic apolipoprotein B-containing lipoproteins. *Biochim. Biophys. Acta.* 1212:152–166.

34. Gibbons, G.F. 1990. Assembly and secretion of hepatic very low density lipoprotein. *Biochem. J.* 268:1–13.

35. Ginsberg, G.N. 1995. Synthesis and secretion of apolipoprotein B from cultured liver cells. *Curr. Opin. Lipidol.* 6:275–280.

36. Hahn, S.E., and D.M. Goldberg. 1995. Factors affecting the regulation of apo B secretion by liver cells. *J. Clin. Lab. Anal.* 9:431–449.

37. Gordon, D.A., H. Jamil, D. Sharp, D. Mullany, Z. Yao, R.E. Gregg, and J. Wetterau. 1994. Secretion of apolipoprotein B-containing lipoproteins from HeLa cells is dependent on expression of the microsomal triglyceride transfer protein and is regulated by lipid availability. *Proc. Natl. Acad. Sci. USA.* 91: 7628–7632.

38. Sharp, D., L. Blinderman, K.A. Combs, B. Kienzle, B. Ricci, K. Wager-Smith, C.M. Gil, C.W. Turck, M.E. Bouma, D.J. Rader, et al. 1993. Cloning and gene defects in microsomal triglyceride transfer protein associated with abetalipoproteinaemia. *Nature.* 365:65–69.

39. Shoulders, C.C., D.J. Brett, J.D. Bayliss, T.M. Narcisi, A. Jarmuz, T.T. Grantham, P.R. Leoni, S. Bhattacharya, R.J. Pease, and P.M. Cullen. 1993. Abetalipoproteinemia is caused by defects of the gene encoding the 97 kDa subunit of a microsomal triglyceride transfer protein. *Hum. Mol. Genet.* 2:2109–2116.

40. Schippers, I.J., H. Moshage, H. Roelofsen, M. Müller, H.S.A. Heymans, M. Ruiters, and F. Kuipers. 1997. Immortalized human hepatocytes as a tool for the study of hepatocytic (de-)differentiation. *Cell Biol. Toxicol.* 13:375–386.

41. Lin, Y., M.J. Smit, R. Havinga, H.J. Verkade, R.J. Vonk, and F. Kuipers. 1995. Differential effects of eicosapentaenoic acid on glycerolipid and apolipoprotein B metabolism in primary human hepatocytes compared to HepG2 cells and primary rat hepatocytes. *Biochim. Biophys. Acta.* 1256:88–96.

42. Kahn, B., H.G. Wilcox, and M. Heimberg. 1989. Cholesterol is required for secretion of very low density lipoprotein by rat liver. *Biochem. J.* 258:807–816.

43. Davis, R.A., J.R. Boogaerts, R.A. Borchardt, M. Malone-McNeal, and J. Archambault-Shexnayder. 1985. Intrahepatic assembly of very low density lipoproteins: varied synthetic response of individual lipoproteins to fasting. *J. Biol. Chem.* 260: 14137–14144.

44. Wu, X., A. Shang, H. Jiang, and H.N. Ginsberg. 1996. Low rates of apo B secretion from HepG2 cells result from reduced delivery of newly synthesized triglyceride to a "secretion-coupled" pool. *J. Lipid Res.* 37:1198–1206.

45. Gretch, D.G., S.L. Sturley, and A.D. Attie. 1995. Human apolipoprotein E mediates processive buoyant lipoprotein formation in insect larvae. *Biochemistry.* 34:545–552.

Low- and High-Density Lipoprotein Metabolism in HepG2 Cells Expressing Various Levels of Apolipoprotein E†

Daniel Charpentier,‡ Caroline Tremblay,‡ Eric Rassart,‡ David Rhainds,‡ Anick Auger,‡ Ross W. Milne,§ and Louise Brissette*,‡

Département des Sciences Biologiques, Université du Québec à Montréal, C.P. 8888, Succ. Centre-ville, Montréal, Québec, Canada, H3C 3P8, University of Ottawa Heart Institute, 40 Ruskin Street, Ottawa, Ontario, Canada, K1Y 4W7

Received June 23, 2000; Revised Manuscript Received September 26, 2000

ABSTRACT: To determine the importance of hepatic apolipoprotein (apo) E in lipoprotein metabolism, HepG2 cells were transfected with a constitutive expression vector (pRc/CMV) containing either the complete or the first 474 base pairs of the human apoE cDNA inserted in an antisense orientation, for apoE gene inactivation, or the full-length human apoE cDNA inserted in a sense orientation for overexpression of apoE. Stable transformants were obtained that expressed 15, 24, 226, and 287% the apoE level of control HepG2 cells. The metabolism of low-density lipoprotein (LDL) and high-density lipoprotein-3 (HDL_3), two lipoprotein classes following both holoparticle and cholesteryl esters (CE)-selective uptake pathways, was compared between all these cells. LDL-protein degradation, an indicator of the holoparticle uptake, was greater in low apoE expressing cells than in control or high expressing cells, while HDL_3-protein degradation paralleled the apoE levels of the cells ($r^2 = 0.989$). LDL- and HDL_3-protein association was higher in low apoE expressing cells compared to control cells. In opposition, LDL- and HDL_3-CE association was not different from control cells in low apoE expressing cells but rose in high apoE expressing cells. In consequence, the CE-selective uptake (CE/protein association ratio) was positively correlated with the level of apoE expression in all cells for both LDL ($r^2 = 0.977$) and HDL_3 ($r^2 = 0.998$). We also show that, although in normal and low apoE expressor cells, 92% of LDL- and 80% HDL_3-CE hydrolysis is sensitive to chloroquine suggesting a pathway linked to lysosomes for both lipoproteins, cells overexpressing apoE lost 60% of chloroquine-sensitive HDL_3-CE hydrolysis without affecting that of LDL-CE. Thus, the level of apoE expression in HepG2 cells determines the fate of LDL and HDL_3.

Apolipoprotein (apo)[1] E, a 299 amino acid protein (*1*), is a constituent of chylomicrons, very low-density lipoproteins (VLDL), and their remnants. It is also found associated with two subclasses of high-density lipoproteins (HDL) known as HDL_1 and HDL_2 but not with HDL_3. At least 75% of plasma apoE is of hepatic origin (*2*), which is coherent with the role of this organ in lipoprotein synthesis. In HepG2 cell, a human hepatoma cell line considered as a good hepatic model (*3*), 75% of synthesized apoE was found to be secreted in the medium, 20% to be localized in the cell and 5% associated at the cell surface (*4*). Approximately 25% of this HepG2 cell-surface apoE is associated with the extracellular matrix, the remaining apoE being associated with the plasma membrane (*5*). In both cases, apoE is associated with proteoglycans.

ApoE is a ligand for the low-density lipoprotein (LDL)-receptor (LDLr) (*6*) and for the LDLr-related protein (LRP) (*7*), two receptors found on hepatic cells that mediate the endocytosis and complete degradation of lipoproteins (holoparticle uptake pathway). ApoE secreted by hepatic cells is known to play a role in the metabolism of lipoprotein containing apoE such as chylomicron remnants (reviewed in ref *8*). However, very few studies were aimed at elucidating the role of apoE expression on the metabolism of apoE-poor lipoproteins such as LDL and HDL_3, two classes of lipoproteins that follow both holoparticle (*9*, *10*) and CE-selective uptake (*11*, *12*) pathways. The latter pathway does not lead to the uptake and degradation of the entire lipoprotein, but only to the transfer of the lipoprotein-CE to the cell by a poorly understood mechanism. It is recognized that most of HDL-CE enters the cell by a selective uptake pathway linked to the scavenger receptor class B type I (SR-BI) identified in rodents (*13*) and to its human homologue known as CD36- and LIMPII-analogous-1 (CLA-

† The work was supported by grants from the Medical Research Council and the Natural Sciences and Engineering Research Council (NSERC) of Canada attributed to Louise Brissette. David Rhainds was the recipient of a studentship from the NSERC of Canada and Anick Auger from the "Fonds pour la Formation des Chercheurs et l'Aide à la Recherche".

* To whom correspondence should be addressed.
‡ Université du Québec à Montréal.
§ University of Ottawa Heart Institute.

[1] Abbreviations: Apo, apolipoprotein; B_{max}, maximal binding capacity; BSA, bovine serum albumin; CE, cholesteryl ester; CHO, chinese hamster ovary; CLA-1, CD36- and LIMPII-analogous-1; EDTA, ethylenediaminetetraacetate; FBS, fetal bovine serum; HDL_3, high-density lipoprotein-3; K_d, dissociation constant; LDL, low-density lipoprotein; LDLr, LDL receptor; LPDS, lipoprotein depleted serum; LRP, LDLr-related protein; MEM, minimal essential medium; PBS, phosphate-buffered saline; SDS−PAGE, sodium dodecyl sulfate−polyacrylamide gel electrophoresis; SR-BI, scavenger receptor class B type I; TBS, tris-buffered saline; TLC, thin-layer chromatography; VLDL, very low-density lipoprotein.

10.1021/bi001436u CCC: $19.00
Published on Web 11/29/2000

1) (*14*). Degradation of HDL_3, by a holoparticle pathway, also occurs but the hepatic receptor involved is not clearly defined (reviewed in ref *15*). In the hepatic cell system, Ji et al. (*16*) reported that preincubating HDL with human apoE increases HDL holoparticle uptake, but not CE-selective uptake by rat hepatoma McA-RH7777 cells. In HepG2 cells, Fragoso and Skinner (*17*) have compared the ability of apoE-rich and apoE-poor subfractions of HDL to associate to HepG2 cells and came to the conclusion that apoE is not directly involved in the CE-selective uptake process, while using the monoclonal antibody anti-human apoE 1D7, Leblond and Marcel (*18*) came to the conclusion that cell-associated apoE is involved in HDL-CE selective uptake. Thus, the studies on HDL metabolism in regards to apoE lead to conflicting results. Furthermore, none of these studies on HDL addresses directly the effect of various levels of apoE expression by hepatic cells on both the HDL holoparticle and CE-selective uptake pathways and the fate of HDL-CE.

CE-selective uptake from LDL has also been shown in HepG2 cells (*11*), and it was shown that chinese hamster ovary (CHO) cells overexpressing SR-BI can selectively take CE from LDL (*19*). However, it is not yet known if under normal conditions SR-BI/CLA-1 is responsible for this activity in the hepatic cell. Indeed, HDL-CE was shown to be hydrolyzed in a nonlysosomal compartment (*20*), while CE coming by a selective uptake from LDL are metabolized in lysosomes (*11*). This is reviewed in more details in ref *21*. To date, there is no report on the role of hepatic cell-secreted apoE on LDL metabolism. The only available information was derived from other cell systems (*22*, *23*). Our aim was to define the role of HepG2 cell-secreted apoE on both LDL and HDL_3 metabolism by comparing HepG2 cells expressing various apoE levels to normal HepG2 cells. Thus, we created HepG2 cells expressing higher levels of apoE with an expression vector containing the full human apoE cDNA and HepG2 cells expressing lower levels of apoE by a constitutive antisense RNA technology. Up to 85% inactivation and 187% overexpression of apoE expression were achieved compared to normal HepG2 cells. The apoE level was found to be positively correlated with HDL_3 holoparticle uptake and LDL- and HDL_3-CE selective uptake. LDL holoparticle uptake was, however, higher in low expressor cells than in normal cells. Furthermore, our data reveal that overexpressing apoE in HepG2 cells reduces the chloroquine-sensitive hydrolysis of HDL_3-CE without modifying that of LDL-CE. Thus, in HepG2 cells, apoE expression level has a similar, yet not identical, effect on LDL and HDL_3 metabolism.

EXPERIMENTAL PROCEDURES

Materials. Human plasma was obtained from the Royal Victoria Hospital (Montréal, Québec, Canada). The human hepatoma cell line HepG2 was obtained from the American Type Culture Collection (Rockville, MD). Purified human apoE came from Calbiochem (La Jolla, CA). Minimal essential medium (MEM), Geneticin (G418 sulfate), penicillin-streptomycin, and trypsin used for cell culture were from Life Technologies Gibco BRL (Burlington, Ontario, Canada). Fetal bovine serum (FBS) was purchased from HyClone (Logan, UT) while L-glutamine, fatty acid-free or regular bovine serum albumin (BSA) (fraction V), phenylmethanesulfonylfluoride (PMSF), anti-mouse IgG antibody, and ampicillin were obtained from Sigma Chemical Co (St-Louis, MO). [^{125}I] (as sodium iodide, 100 mCi/mL)- and [^{3}H]-cholesteryl oleate (30−60 Ci/mmol) were bought, respectively, from Amersham (Oakville, Ontario, Canada) and ICN Biomedical (Montreal, Quebec, Canada). Restriction enzymes and modification enzymes were obtained from Pharmacia (Montréal, Québec, Canada). pRc/CMV and pBluescript II KS+ plasmids came from Invitrogen (San Diego, CA). The vector pJS382 was a gift from Dr. Jonathan Smith (Rockefeller University, New York), while the vector pTV194 came from Dr. Robert Mahley (Gladstone Foundation, San Francisco).

Preparation of Stable Transformants Expressing Various Levels of ApoE. To obtain HepG2 cells deficient in apoE expression, pTV194 (*24*), a vector containing the human apoE3 cDNA, was digested with *Hin*dIII and *Eco*RI, resulting in the obtention of 1.2, 1.3, and 3 kbp fragments. The 1.3 kbp fragment, which contains the full-length apoE cDNA, was subcloned in the pBluescript KS+ vector and sequenced to confirm its identity. Thereafter, the fragment was excised with *Xba*I and *Hin*dIII while, in parallel, the pRc/CMV expression vector was digested with the same enzymes. Ligation between the fragment and the vector was accomplished at 20 °C with T4 DNA ligase followed by transformation in *Escherichia coli* DH5α. A fraction of the recombinant DNA was digested by *Not*I and *Hin*dIII in order to excise a fragment of 831 bp at the 3′ end of the apoE cDNA and the plasmid was ligated. Thus, two vectors were created, one containing the complete apoE cDNA and another containing the first 474 bp of the cDNA, both inserted in the antisense orientation. To create cells overexpressing apoE, pJS382, a vector containing the full human apoE3 cDNA, was digested with *Xba*I and 1.2 and 2.4 kbp fragments were obtained. The 1.2 kbp fragment was inserted in the pRc/CMV expression vector opened with *Xba*I. The three different constructs and the expression vector without insert were separately transfected in HepG2 cells using the standard calcium phosphate method. G418-resistant cell lines were selected and isolated from the pools with cloning cylinders and then propagated to study the apoE expression level. All stable transformants resemble the native HepG2 cells in appearance and in growth rate.

Cell Culturing. HepG2 cells were grown in 75-cm^2 flasks containing 15 mL of MEM supplemented with 10% (v/v) FBS, penicillin (100 units/mL), streptomycin (100 μg/mL), and glutamine (4 mM), as previously described (*11*). Medium was changed every 2 days, and cells were propagated every 7 days. Three days prior to the binding, association, and degradation studies, 4.5×10^5 cells were seeded in 3.8 cm^2 culture dishes (12 well-dishes) for binding, association and degradation assays. The cells were approximately 90% confluent.

ApoE, LDLr, and SR-BI/CLA-1 Protein Estimation by Immunoblotting. Cell medium was changed and harvested 66 h later to measure apoE secretion. Also, cell proteins were obtained by the method of Yoshimura et al. (*25*). Proteins (200−400 μg) were separated by 10% sodium dodecyl sulfate−polyacrylamide gel electrophoresis (SDS−PAGE) (*26*) followed by Western blotting to nitrocellulose paper according to the method of Burnette (*27*). The nitrocellulose

paper was incubated in Tris-buffered saline (TBS) containing the monoclonal anti-human apoE antibody 6C5 (1:500) (*28*) for 90 min at 37 °C. The nitrocellulose was washed with TBS and then incubated with ^{125}I-labeled anti-mouse IgG (10 μg/mL, 1 × 10^6 cpm) for 90 min at 37 °C. Thereafter, the nitrocellulose paper was extensively washed with TBS and an autoradiogram was obtained by exposing the dried nitrocellulose paper to Kodak XAR film at −80 °C. The intensity of the autoradiogram signal was quantified by densitometry using the Imagequant system of Molecular Dynamics (Sunnyvale, CA). Immunoblotting experiments were also conducted with the cultured medium of control HepG2 cells and 0.5, 1.0, and 2.5 μg of purified human apoE in order to determine the rate of apoE synthesis by control HepG2 cells. LDLr and SR-BI/CLA-1 levels were determined from cellular proteins with a rabbit polyclonal anti-human LDLr antibody (Research Diagnostics) for LDLr receptor estimation and a rabbit polyclonal anti-murine SR-BI antibody (Novus Biologicals) for SR-BI/CLA-1, respectively.

Preparation and Radiolabeling of Lipoproteins. To the plasma was added 0.01% (w/v) of ethylenediamine tetraacetate (EDTA), 0.02% (w/v) of sodium azide and 10 μM of PMSF before the isolation of lipoproteins, which was achieved by ultracentrifugation as described by Hatch and Lees (*29*). Human LDL (density 1.025−1.063 g/mL) and HDL_3 (density 1.125−1.21 g/mL) were prepared as described by Brissette and Noël (*30*). Both lipoproteins contained no detectable amounts of apoE, as assessed by SDS−PAGE. LDL and HDL_3 were iodinated by a modification (*31*) of the iodine monochloride method of McFarlane (*32*). One millicurie of sodium 125-iodide was used to iodinate 2.5 mg of LDL or HDL_3 in the presence of 30 or 10 nmol, respectively of iodine monochloride in 0.5 M glycine-NaOH, pH 10. Free iodine was removed by gel filtration on Sephadex G-25 followed by an overnight dialysis in TBS. The specific radioactivity ranged 115000−200000 cpm/μg of protein. LDL and HDL_3 were radiolabeled in their CE with [^{3}H]cholesteryl oleate as described by Roberts et al. (*33*). Briefly, 25 μCi of [^{3}H]CE was evaporated under nitrogen and resuspended in 250 μL of acetone. This volume of acetone was added dropwise to 3 mL of lipoprotein depleted serum (LPDS) in a glass tube at room temperature and acetone was evaporated under a gentle stream of nitrogen. One milliliter of lipoprotein at a concentration of 1 mg protein/mL was added to the LPDS containing [^{3}H]-CE and the mixture was incubated for 30 min at 4 °C. Thereafter, the labeled lipoproteins were reisolated by ultracentrifugation. The specific activity of lipoproteins labeled in CE ranged from 7500 to 20 000 dpm/μg protein.

Binding Assay. The cells were washed twice with 1 mL of phosphate-buffered saline (PBS) and were then incubated for 2 h at 4 °C with 0−50 μg of protein/mL of [^{125}I]LDL or HDL_3 in 125 μL of MEM containing 4% (w/v) fatty-acid free BSA and 50 mM Hepes, pH 7.4, in a total volume of 250 μL (total binding). Nonspecific binding was determined by the addition of 1 mg of protein/mL of the proper unlabeled lipoprotein. At the end of the incubation, the cell monolayers were washed two times with 1 mL of PBS containing 0.2% (w/v) BSA (PBS−BSA), then twice with 1 mL of PBS. The cells were solubilized in 1.5 mL of 0.1 N NaOH, assayed for protein content and counted for radioactivity in a Cobra II counter (Canberra-Packard). The specific binding was calculated by subtracting the nonspecific binding of ^{125}I-labeled lipoproteins from the total binding. The curves generated by the specific-binding data were transformed into plots of the ratio of cell-bound to free ^{125}I-labeled lipoproteins versus cell-bound ^{125}I-labeled lipoproteins, according to the method of Scatchard (*34*). The dissociation constant (K_d) was calculated from the slopes and the maximum binding capacity (B_{max}) was obtained from the *x*-axis intercept.

Cell Association and Degradation Assays. HepG2 cell association of [^{125}I]lipoprotein and [^{3}H]CE-lipoprotein (15 μg of protein/mL) lasted for 3 h at 37 °C, as for the binding studies but without Hepes. At the end of the incubation, dishes were processed as for the binding studies. Association data were obtained from an estimate of the radioactivity of the washed cells resuspended in 0.1 N NaOH. The results are expressed in [^{125}I]lipoprotein−protein/mg of HepG2 cell protein. Associated [^{3}H]CE was quantitated with a beta-counter (Wallach-Fisher). To compare the association of lipoproteins labeled in protein (^{125}I) or in CE (^{3}H), the association data of [^{3}H]CE-lipoprotein were estimated as protein associated/mg cellular protein. To achieve this, the specific activity of [^{3}H]CE-LDL or [^{3}H]CE-HDL_3 was established in disintegrations per minute per microgram of LDL or HDL_3 protein. Selective uptake is demonstrated when the ratio of [^{3}H]CE-lipoprotein (association)/[^{125}I]lipoprotein (association + degradation) is greater than unity. The degradation of the proteins of [^{125}I]lipoprotein was estimated from the medium. Essentially, trichloroacetic acid (TCA) was used at a final concentration of 12% and degradation was estimated as the TCA-soluble fraction. Proper controls without cells were done to account for free ^{125}iodine. Some experiments were conducted after a preincubation for 2 h with 1.5 units/mL of chondroitinase ABC and 4.5 units/mL of heparinase I.

CE Hydrolysis Assays. Cells were washed twice with 1 mL of PBS and were then preincubated for 1 h at 37 °C in the medium used in the association assay but in the presence or absence of 100 μM of chloroquine. After the preincubation period, 40 μg of protein/mL of [^{3}H]CE-LDL or HDL_3 were added to the wells and cells were incubated for 4 h. Nonspecific CE-hydrolysis was determined by the addition of 1 mg of protein/mL of the proper unlabeled lipoprotein. At the end of the incubation, the cell monolayers were washed as for the binding studies. The lipids were extracted in situ following two 30 min incubations with 1 mL of hexane/isopropylic alcohol (3:2, v/v). Cells were solubilized in 1.5 mL of 0.1 N NaOH and assayed for protein content. The lipid extracts were dried under N_2, resuspended in 50 μL of chloroform and separated by thin-layer chromatography on silica gel G plates run in petroleum ether/diethyl ether/acetic acid (90:10:1, v/v). The plates were dried and the lipid spots were revealed by exposure to iodine vapor. Following complete disappearance of I_2, spots corresponding to the free cholesterol and CE positions were scraped from the plates and quantified by liquid-scintillation counting.

Other Methods. Protein content was determined by the method of Lowry et al. (*35*) with BSA as standard. Two-tailed Student's unpaired and paired *t*-test were used to determine significant differences between assays.

RESULTS

Our primary goal was to create HepG2 cells expressing higher and lower levels of apoE compared to normal HepG2

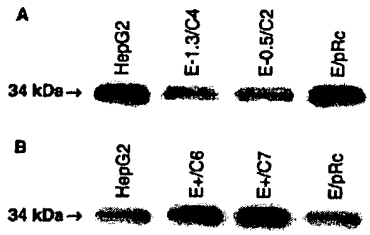

FIGURE 1: Immunoblot analysis of apoE levels in different subtypes of HepG2 cells.Cells were solubilized with 1% Triton X-100 and 400 μg (A) or 200 μg (B) of proteins were separated by 10% SDS–PAGE and transferred onto nitrocellulose membrane. The level of apoE was estimated by immunodetection with 6C5, a monoclonal anti-human apoE antibody, as described in the Experimental Procedures.

cells. We determined by quantitative immunoblotting that normal HepG2 cells secrete 0.25 μg/mg of cell protein/h. To obtain cells expressing high levels of apoE, we constructed an expression vector containing the full-length apoE cDNA in the sense orientation. Low expressor cells were created with a vector producing apoE antisense RNA. Since we could not determine empirically the length of the antisense RNA that would be the most efficient, we used the full-length apoE cDNA or the first 474 bp of the same cDNA. Both were inserted in the antisense orientation in pRc/CMV. Stable transformants were named according to the orientation of their cDNA insert and, in the case of low apoE expressing cells, the length of their cDNA insert. Thus, cells that express the human apoE cDNA were named E+, while cells expressing antisense RNA were named E−1.3 if they received the full length cDNA, or E−0.5 if they received the first 474 base pairs of the cDNA. HepG2 cells were also transfected with the vector pRc/CMV without insert. These cells were named E/pRc. Cellular clones were obtained from each pool of transformants, and their level of apoE was determined by immunoblotting. Figure 1 shows the level of apoE expression in normal HepG2 cells and E/pRc and in our two best overexpressing clones (E+/C6 and E+/C7) and two most deficient clones (E−1.3/C4 and E−0.5/C2). While the level of apoE in E/pRc is not different from the normal HepG2 cells, densitometric analysis of four different experiments taking the HepG2 cell apoE level as 100% revealed that E−1.3/C4 and E−0.5/C2 cells express 15% ± 3 (mean ± SD) and 24% ± 4 of the level of normal HepG2 cells, respectively, while E+/C6 and E+/C7 cells have apoE levels corresponding to 226% ± 6 and 287% ± 8 of the control level, respectively. Thus, there is a 19-fold difference in apoE expression between our most deficient and best overexpressing cells. The measurement in the medium followed the same type of modulation in the level of apoE (data not shown). Expression levels of LDLr and SR-BI/CLA-1 were determined by immunoblotting in E−1.3/C4, E+/C7, and control HepG2 cells. While the LDLr level was the same, a 30% reduction in SR-BI/CLA-1 level was detected in E−1.3/C4 compared to the two other cell types.

Our next goal was to define if the changes of apoE levels in HepG2 cells would affect the ability of HepG2 cells to bind LDL and HDL_3, two lipoprotein classes that can be isolated without detectable amounts of apoE (*30*). Figure 2A shows that the specific binding of [^{125}I]LDL is more important for the cells expressing low levels of apoE than in other cells. The Scatchard plots (panel B) show that the x-intercept is greater in the case of low expressing cells compared to the other cells while the slopes are the same no matter the level of apoE expression by the cells. The binding parameters calculated for each experiment are shown in Table 1. This table reveals that the maximal binding capacity (B_{max}) of [^{125}I]LDL is statistically increased ($p < 0.01$) by 126% and 78% for E−1.3/C4 and E−0.5/C2 cells, respectively, in comparison with the B_{max} of control HepG2 cells. No differences were found between normal and apoE overexpressing cells. Analysis of the dissociation constants (K_d) indicates that a variation in the apoE level has no effect on the affinity of the LDL binding to HepG2 cells. Similar results were obtained for the binding of [^{125}I]HDL_3 to the different subtypes of HepG2 cells as seen in Figure 2, panels C and D. Table 1 shows that the B_{max} of [^{125}I]HDL_3 is statistically increased ($p < 0.001$) by 83 and 53% for E−1.3/C4 and E−0.5/C2 cells, respectively, compared to that of normal cells. In contrast with the observation made with LDL, low apoE expressing cells have a significantly reduced ($p < 0.01$) affinity for HDL_3 as seen by the 39% and 30% increases in the K_d with E−1.3/C4 and E−0.5/C2 cells, respectively. Thus, apoE secreted by HepG2 cells transforms HDL_3, but not LDL, into a higher affinity ligand for cell receptors, while at lower level than normal, apoE favors LDL and HDL_3 binding to HepG2 cells.

Thereafter, we analyzed the metabolism of LDL by these cells, in function of apoE expression. The experiments were conducted at 37 °C, a temperature that allows internalization and degradation of lipoproteins after their binding to cell membranes. Table 2 shows that E−1.3/C4 and E−0.5/C2 cells degrade 51% ($p < 0.05$) and 108% ($p < 0.001$) more [^{125}I]LDL-protein, respectively, than normal HepG2 cells. A parallel effect was observed for LDL-protein association. These results are in agreement with those obtained with the binding studies (Table 1). Association assays were conducted after a preincubation in the absence or presence of heparinase I and chondroitinase ABC in order to evaluate the role of proteoglycans on the cell surface. These enzymes had no effect on [^{125}I]LDL association to our low apoE expressor cells as 101.6 ± 2.7% (mean ± SD, $n = 5$) of the association level of cells preincubated without the enzymes was measured. However, the enzymatic treatment on high apoE expressor cells increased LDL association to 130.4 ± 10.1% ($n = 6$). This statistically significant increase ($p < 0.05$) suggests that apoE on proteoglycans of high expressor cells reduces LDL ability to associate with HepG2 cells.

The association of the lipid moiety of LDL, more precisely CE, was also investigated. For this, LDL were labeled with [^{3}H]CE. Table 3 shows that [^{3}H]CE-LDL cell-association was significantly increased ($p < 0.001$) by 87 and 129% in E+/C6 and E+/C7 cells, respectively, while the association of LDL-CE with cells expressing low levels of apoE was not statistically different from that of normal HepG2 cells. Analysis of the CE/protein association ratio, an indicator of the LDL-CE selective uptake, reveals that the level of apoE expression in HepG2 cells is highly correlated ($r^2 = 0.977$) with this pathway. Indeed, compared to the lowest expressing cells, our highest expressing cells are 3-fold better to selectively take up CE from LDL. Thus, the information gathered on LDL metabolism reveals that subnormal levels of HepG2-apoE favors the holoparticle pathway (LDL-

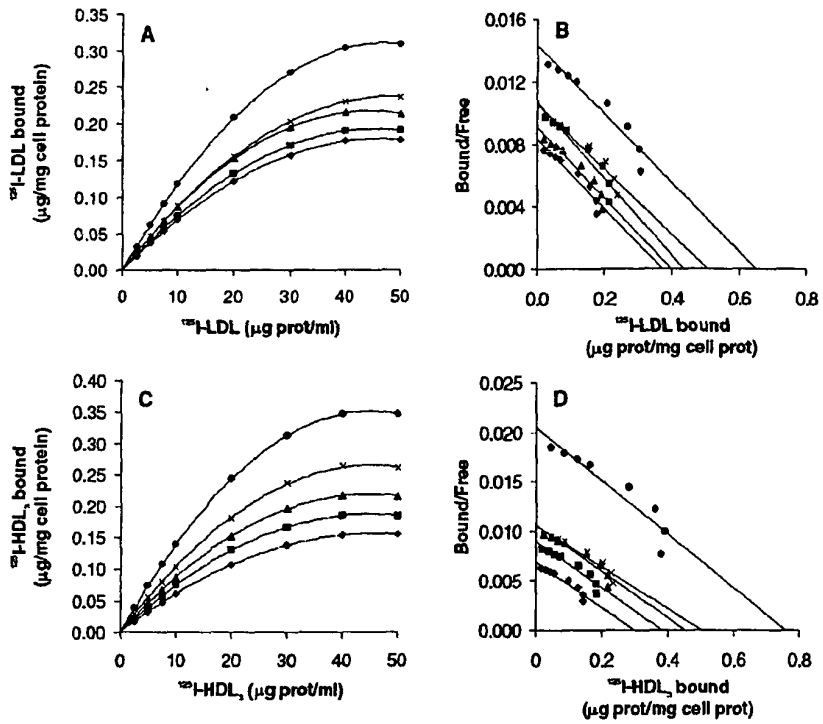

FIGURE 2: Specific binding of [^{125}I]LDL and [^{125}I]HDL$_3$ to different subtypes of HepG2 cells. Saturation curves of the specific binding of [^{125}I]LDL (A) or [^{125}I]HDL$_3$ (C) to either normal HepG2 (◆), E−1.3/C4 (×), E−0.5/C2 (●), E+/C6 (■) or E+/C7 (▲) cells and Scatchard plots of the specific binding of [^{125}I]LDL (B) or [^{125}I]HDL$_3$ (D). To measure the total binding on these cells, [^{125}I]lipoproteins (0−50 μg of protein/mL) were incubated at 4 °C for 2 h with HepG2 cells. The nonspecific binding was measured by adding 1 mg of protein/mL of the proper unlabeled lipoprotein and the specific binding was calculated by subtracting the nonspecific binding from the total binding. These are representative experiments conducted in duplicate.

Table 1: Parameters of LDL and HDL$_3$ Binding to the Different HepG2 Cell Subtypes[a]

lipoprotein	cell	apoE expression level (%)	K_d (μg of protein/mL)	B_{max} (ng of protein/mg of cell protein)
[^{125}I]LDL	E−1.3/C4	15	42.0 ± 3.1	713.0 ± 102.8[b]
	E−0.5/C2	24	45.1 ± 3.7	560.4 ± 71.8[b]
	HepG2	100	43.4 ± 3.5	315.6 ± 22.4
	E+/C6	226	42.3 ± 3.1	380.1 ± 33.4
	E+/C7	287	42.3 ± 1.2	396.1 ± 40.8
[^{125}I]HDL$_3$	E−1.3/C4	15	69.6 ± 6.6[b]	714.9 ± 52.2[c]
	E−0.5/C2	24	65.3 ± 8.0[b]	596.2 ± 43.6[c]
	HepG2	100	50.1 ± 4.1	390.5 ± 20.9
	E+/C6	226	51.2 ± 8.5	402.1 ± 41.2
	E+/C7	287	50.7 ± 9.7	421.9 ± 44.9

[a] Binding assays of ^{125}I-labeled lipoproteins to the different subtypes of HepG2 cells were carried out as described in the Experimental Procedures. Briefly, [^{125}I]lipoproteins (0−50 μg of protein/mL) were incubated with cells at 4 °C for 2 h. Nonspecific binding was measured by adding 1 mg of protein/mL of the proper unlabeled lipoprotein and specific binding was calculated by subtracting the nonspecific from the total binding. K_d and B_{max} were determined from Scatchard plots of the specific binding data. Each value represents the mean ± SD of five experiments conducted each in duplicate. Statistical differences were determined with a paired t-test. [b] Statistically different ($p < 0.01$) from the results obtained with normal HepG2 cells. [c] Statistically different ($p < 0.001$) from the results obtained with the normal HepG2 cells.

protein binding, association and degradation) while higher levels optimize the LDL-CE selective uptake pathway.

Similar experiments were conducted with HDL$_3$. Confirming our previous data (*39*), normal HepG2 cells can degrade (Table 3) and associate HDL$_3$-protein and also selectively take CE from HDL$_3$, but differently from LDL. Indeed, HDL$_3$-protein degradation (Table 2), -protein, and -CE association (Table 3) are 6, 54, and 39% that of LDL, respectively. Table 2 shows that, differently from LDL degradation, HDL$_3$-protein degradation is positively correlated ($r^2 = 0.989$) with the expression of apoE in HepG2 cells. Indeed, the E−1.3/C4 and E−0.5/C2 cells degrade 36% ($p < 0.01$) and 29% ($p < 0.001$) less HDL$_3$-protein, respectively, than normal HepG2 cells while the E+/C6 and E+/C7 cells degrade 49% ($p < 0.01$) and 59% ($p < 0.05$) more HDL$_3$-protein, respectively, than normal HepG2 cells. In agreement with our findings with LDL, there is a significant increase ($p < 0.001$) of 185 and 228% of [^{125}I]-HDL$_3$ cell-association with E−1.3/C4 and E−0.5/C2 cells, respectively, while the association of HDL$_3$ to cells overexpressing apoE was not significantly different from the control cells (Table 2). Again, these results are in agreement with those obtained with the binding studies (Table 1). Table 3 shows a significantly higher [^{3}H]CE-HDL$_3$ association ($p < 0.05$) of 58 and 70% for E+/C6 and E+/C7 cells, respectively, while the same association is measured in low apoE expressing and control cells. As for LDL, CE-selective uptake is highly correlated ($r^2 = 0.998$) with the level of apoE, revealing that the apoE level is also important for HDL$_3$-CE selective uptake by HepG2 cells. As a matter of fact, CE-selective uptake values in E- cells do not differ from unity. Thus, in those cells a reduction of 76% in apoE expression virtually abolished HDL$_3$-CE selective uptake.

The intracellular fate of lipoprotein-CE in conjunction with the apoE expression levels was investigated. For this purpose,

Table 2: Association and Degradation of [^{125}I]Lipoprotein by Different HepG2 Cell Subtypes[a]

lipoprotein	cell	apoE expression level (%)	[^{125}I]lipoprotein degradation (ng of protein/ mg of cell protein)	[^{125}I]lipoprotein association (ng of protein/ mg of cell protein)	degradation/ association ratio
^{125}I-LDL	E−1.3/C4	15	30.0 ± 3.2[c]	94.3 ± 24.2[c]	0.38 ± 0.10
	E−0.5/C2	24	21.8 ± 5.4[c]	60.4 ± 20.6[d]	0.44 ± 0.13
	HepG2	100	14.4 ± 12.6	37.6 ± 14.1	0.42 ± 0.14
	E+/C6	226	13.2 ± 4.0	50.8 ± 20.9	0.29 ± 0.11[d]
	E+/C7	287	13.4 ± 5.7	64.0 ± 29.7	0.23 ± 0.07[d]
^{125}I−HDL$_3$	E−1.3/C4	15	0.52 ± 0.17[d]	69.9 ± 36.9[b]	0.010 ± 0.00[d]
	E−0.5/C2	24	0.58 ± 0.29[d]	60.7 ± 31.0[b]	0.012 ± 0.00[d]
	HepG2	100	0.81 ± 0.26	21.3 ± 6.5	0.046 ± 0.028
	E+/C6	226	1.21 ± 0.24[d]	24.7 ± 7.8	0.062 ± 0.032[c]
	E+/C7	287	1.29 ± 0.40[c]	22.8 ± 7.0	0.061 ± 0.036[c]

[a] Association and degradation assays were conducted as described in the Experimental Procedures with 15 μg of protein/mL of either [^{125}I]LDL or [^{125}I]HDL$_3$. Degradation of LDL- or HDL-protein was measured in the medium. Incubation was conducted in parallel with 1 mg of protein/mL of the proper unlabeled lipoprotein to determine the level of nonspecific association or degradation. Each value represents the mean ± SD of 10 experiments conducted each in triplicate. Statistical differences were determined with a paired t-test. [b] Statistically different ($p < 0.05$) from the results obtained with normal HepG2 cells. [c] Statistically different ($p < 0.01$) from the results obtained with normal HepG2 cells. [c] Statistically different ($p < 0.001$) from the results obtained with normal HepG2 cells.

Table 3: Protein and Cholesteryl Ester Association of LDL and HDL$_3$ with Different HepG2 Cell Subtypes[a]

lipoprotein	cell	apoE expression level (%)	[^{125}I]lipoprotein association (ng of protein/ mg of cell protein)	[^{3}H]CE association (ng of protein/ mg of cell protein)	CE-selective uptake
[^{125}I]LDL	E−1.3/C4	15	100.1 ± 25.6[b]	144.5 ± 73.1	1.68 ± 0.42[b]
	E−0.5/C2	24	69.9 ± 22.5[b]	153.5 ± 65.2	2.21 ± 0.53[c]
	HepG2	100	39.6 ± 12.6	123.6 ± 55.1	3.17 ± 1.11
	E+/C6	226	46.2 ± 18.9	231.1 ± 58.8[b]	4.86 ± 1.04[d]
	E+/C7	287	60.5 ± 24.0	282.7 ± 90.7[b]	5.14 ± 0.68[d]
[^{125}I]HDL$_3$	E−1.3/C4	15	69.9 ± 36.9[c]	42.6 ± 16.9	0.73 ± 0.19[b]
	E−0.5/C2	24	60.7 ± 30.9[c]	42.5 ± 20.0	0.84 ± 0.29[b]
	HepG2	100	21.3 ± 6.5	47.8 ± 14.3	2.37 ± 0.50
	E+/C6	226	24.7 ± 7.8	75.6 ± 22.7[d]	3.47 ± 0.59[c]
	E+/C7	287	22.8 ± 7.0	81.2 ± 25.4[d]	4.02 ± 0.93[c]

[a] Cells were incubated for 3 h at 37 °C with either 15 μg/mL of [^{125}I]lipoprotein or [^{3}H]CE-lipoprotein and cell association was measured as described in the Experimental Procedures. Incubation was conducted in parallel with 1 mg of protein/mL of the proper unlabeled lipoprotein to determine the level of nonspecific association. Each value represents the mean ± SD of 10 experiments conducted each in triplicate. Statistical differences were determined with a paired t-test. [b] Statistically different ($p < 0.001$) from the results obtained with normal HepG2 cells. [c] Statistically different ($p < 0.05$) from the results obtained with normal HepG2 cells. [d] Statistically different ($p < 0.01$) from the results obtained with normal HepG2 cells.

hydrolysis of LDL- and HDL$_3$-CE was analyzed in the presence of chloroquine, an inhibitor of the lysosomal function, in control cells and in our highest and lowest apoE expressing cells. Figure 3 shows that LDL-CE or HDL$_3$-CE hydrolysis is not statistically different between E−1.3/C4, E+/C7, and normal HepG2 cells in the absence of chloroquine. Panel A reveals that chloroquine has a similar effect on the three cell lines, significantly reducing LDL-CE hydrolysis by an average of 92% ($p < 0.001$). Important differences were detectable between sensitivity of LDL- and HDL$_3$-CE hydrolysis in the presence of chloroquine as panel B shows that chloroquine significantly reduces ($p < 0.001$) HDL$_3$-CE hydrolysis by 72 and 86% in E−1.3/C4 and normal HepG2 cells, respectively, while it only decreases HDL$_3$-CE hydrolysis by 35% in cells overexpressing apoE. Thus, an apoE level higher than normal reduces the sensitivity of HDL$_3$-CE hydrolysis to chloroquine without changing that of LDL.

DISCUSSION

Our goal was to define the role that hepatic cell-apoE plays in LDL and HDL$_3$ metabolism. A hepatic-derived cell was chosen since most of the lipoprotein metabolism occurs in the liver. To strengthen our study, we chose to compare HepG2 cells expressing normal, low and high levels of apoE. Thus, we constructed apoE expression vectors in order to obtain HepG2 cells overexpressing apoE and we also created HepG2 cells that constitutively express apoE antisense RNA to reduce apoE expression in HepG2 cells.

The study of LDL binding to the different HepG2 cell subtypes revealed that reducing the apoE level below the control level increases the binding capacity (B_{max}) of LDL, while increasing apoE level has no effect. A parallel effect was demonstrated on LDL-protein association and degradation. This cannot be attributed to higher levels of LDLr in apoE deficient cells since the LDLr expression was the same in all types of cells. Variations of the apoE levels did not modify the affinity (K_d) of LDL for these cell lines. Thus, it has to be concluded that HepG2 cells expressing lower levels of apoE than the control level metabolize more LDL by the endocytosis/degradation pathway. These results were unexpected since there were many reasons to believe that higher levels of apoE would favor the binding/association/degradation pathway by the LDLr following the acquisition of

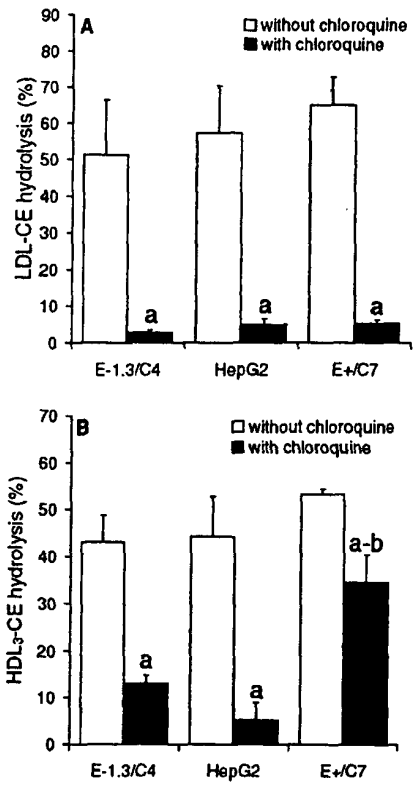

FIGURE 3: Hydrolysis of [H³]CE-LDL and [H³]CE-HDL$_3$ in different subtypes of HepG2 cells. Cells were preincubated for 1 h at 37 °C in the absence or presence of 100 μM of chloroquine. After the preincubation period, 40 μg of protein/mL of [³H]CE-LDL or [³H]CE-HDL$_3$ were added to the wells and CE hydrolysis was measured as described in the Experimental Procedures. Incubation was conducted in parallel with 1 mg of protein/mL of the proper unlabeled lipoprotein to determine the level of nonspecific CE hydrolysis. Each value represents the mean ± SD of four experiments conducted each in duplicate. Statistical differences were determined with unpaired *t*-test. (a) Statistically different ($p < 0.01$) from the results obtained with the same cell line without chloroquine. (b) Statistically different ($p < 0.01$) from the results obtained with normal HepG2 cells.

hepatic apoE by LDL, as suggested by the study of Choi et al. (*22*) with CHO cells overexpressing apoE. The difference can depend either on the different cells used (type or species) or on the levels of apoE expression. Knowing that apoE is found associated with proteoglycans (*5*), we have investigated the role of such molecules on low and high apoE expressor cells. Our results show that heparinase I and chondroitinase ABC do not modify LDL association to HepG2 cells expressing low levels of apoE. Therefore, it appears that proteoglycans do not play a significant role in LDL metabolism in that cell subtype. Interestingly, the same treatment on high apoE expressor cells increases LDL association, suggesting that proteoglycans bearing apoE reduces LDL association to the cell. Other experiments are required to define the mechanism involved.

Study of HDL$_3$ binding/association showed a similar pattern than that observed for LDL suggesting that our conclusion on proteoglycans free of apoE applies also to HDL$_3$. Our degradation experiment is in agreement with the results of Ji et al. (*16*), as a very strong positive correlation was found between HDL$_3$-protein degradation and the various apoE levels of our cells. It can be speculated that the effect observed on HDL$_3$-protein degradation relates to an enrichment of HDL$_3$ in apoE from the medium which would then redirect HDL$_3$ to an apoE receptor such as the LDLr or the LRP for rapid endocytosis and degradation. This is supported by the demonstration of Garcia et al. (*10*) that HDL$_3$ are internalized in HepG2 cells by a classical endocytic pathway. Alternatively, the HDL-receptor responsible for the HDL holoparticle uptake that remains to be clearly identified in the liver (*15*), could see its degradation activity increased with apoE.

Other experiments were conducted to determine the role of hepatic apoE in the selective uptake and processing of CE from LDL and HDL$_3$. For both lipoproteins, the pattern of CE association was the inverse of protein association. In other words, instead of increasing in apoE-deficient cells compared to normal cells, CE association rose in cells overexpressing apoE. Altogether, these effects lead to an almost perfect correlation between apoE expression in HepG2 cells and CE-selective uptake from both lipoproteins. Our immunoblotting experiments reveal that this effect cannot be explained by different levels of SR-BI/CLA-1 in our different cell types. Our findings with LDL are similar to the findings of Swarnakar et al. (*23*) who showed that overexpression of human apoE in murine Y1 adrenocortical cells favors the CE-selective uptake, while the effect that we have detected with HDL$_3$ is in agreement with the results of Leblond and Marcel (*18*). From our results, it can be calculated that in our lowest and highest apoE expressing cells, 60 and 19% of LDL-CE enter the cell by the holoparticle pathway, respectively, the remaining entering by the CE-selective uptake pathway. Results are 100 and 25% for HDL$_3$-CE. In other words, it means that in low apoE expression cells the holoparticle pathway is favored while in high apoE expressor cells the vast majority of lipoprotein-CE is taken by a CE-selective uptake pathway. Our findings are supported by the knowledge that CE-selective uptake is important in cells that are good apoE expressor, such as adrenals and ovary cells. Thus, apoE can be considered as an activator of the CE-selective uptake pathway. Other experiments are needed to define the mechanism by which apoE exerts its effect. Another important issue is that apoE overexpression appears to target HDL$_3$-CE, but not LDL-CE, to a nonlysosomal compartment for hydrolysis as seen by the loss of chloroquine sensitivity. This suggests that even though high levels of apoE favor the CE-selective uptake pathway for both LDL and HDL$_3$, more than one receptor may be involved. It can therefore be proposed that, in normal HepG2 cells, LDL- and HDL$_3$-CE are entering the cells by the same selective uptake pathway that is highly chloroquine sensitive and likely linked to lysosomes, while in high apoE expression cells, HDL$_3$-CE but not LDL-CE are directed to SR-BI/CLA-1 known to lead to extralysosomal hydrolysis. If this is true then clarifying the identity of the receptor different from SR-BI/CLA-1 becomes a priority.

In conclusion, we were successful in reducing and increasing expression of apoE in HepG2 cells. We showed that lower levels of apoE increases binding and protein association of both LDL and HDL$_3$ compared to normal cells, while higher apoE levels increases CE association. ApoE level was found to be positively correlated with HDL$_3$, but not LDL, degradation. Both LDL- and HDL$_3$-CE selective uptake were positively correlated with the level of apoE expressed by

HepG2 cells. However, the selective uptake of CE from LDL and HDL_3, in cell overexpressing apoE, appears to be mediated by distinct receptors as in high apoE expressing cells, the hydrolysis of HDL_3-derived CE is largely chloroquine-insensitive whereas that of LDL-derived CE is predominantly chloroquine-sensitive. Therefore apoE has both similar and different effects on LDL and HDL_3 metabolism.

REFERENCES

1. Rall, S. C., Jr., Weisgraber, K. H., and Mahley, R. W. (1982) *J. Biol. Chem. 257*, 4171−4178.
2. Linton, M. F., Gish, R., Hubl, S. T., Butler, E., Esquivel, C., Boyles, W. I., Wardell, M. R., and Young, S. G. (1991) *J. Clin. Invest. 88*, 270−281.
3. Forte, T., and Nichols, A. V. (1972) *Adv. Lipid. Res. 10*, 1−38.
4. Lilly-Stauderman, M., Brown, T. L., Balasubramaniam, A., and Harmony, J. A. K. (1993) *J. Lipid Res. 34*, 1318−1333.
5. Burgess, J. W., Gould, D. R., and Marcel, Y. L. (1998) *J. Biol. Chem. 273*, 5645−5654.
6. Mahley, R. W., and Innerarity, T. L. (1977) *J. Biol. Chem. 252*, 3980−3986.
7. Herz, J., Haman, U., Rogne S., Myklebost, O., Gausepohl, H., and Stanley, K. K. (1988) *EMBO J. 7*, 4119−4127.
8. Cooper, A. D. (1997) *J. Lipid Res. 38*, 2173−2192.
9. Brown, M. S., and Goldstein, J. L. (1986) *Science 232*, 34−47.
10. Garcia, A., Barbaras, R., Collet, X., Bogyo, A., Chap, H., and Perret, B. (1996) *Biochemistry 35*, 13064−13071.
11. Brissette, L., Charest, M.-C., and Falstrault, L. (1996) *Biochem. J. 318*, 841−847.
12. Johnson, W. J., Mahlberg, F. H., Rothblat, G. H., and Phillips, M. C. (1991) *Biochim. Biophys. Acta 1085*, 273−298.
13. Acton, S., Rigotti, A., Landschulz, K. T., Xu, S., Hobbs, H. H., and Krieger, M. (1996) *Science 271*, 518−520.
14. Murao, K., Terpstra, V., Green, S. R., Kondratenko, N., Steinberg, D., and Quehenberger, O. (1997) *J. Biol. Chem. 272*, 17551−17557.
15. Fidge, N. M. (1999) *J. Lipid Res. 40*, 187−201.
16. Ji, Z. S., Dichek, H. L., Miranda, R. D., and Mahley, R. W. (1997) *J. Biol. Chem. 272*, 31285−31292.
17. Fragoso, Y. D., and Skinner, E. R. (1995) *Biochem. J. 311*, 611−615.
18. Leblond, L., and Marcel, Y. L. (1993) *J. Biol. Chem. 268*, 1670−1673.
19. Swanakar, S., Temel, R. E., Connelly, M. A., Azhar, S., and Williams, D. L. (1999) *J. Biol. Chem. 274*, 29733−29739.
20. Acton, S., Rigotti, A., Landschulz, K. T., Xu, S., Hobbs, H. H., and Krieger, M. (1996) *Science 271*, 518−520.
21. Rhainds, D., and Brissette, L. (1999) *Int. J. Biochem. Cell. Biol. 31*, 915−931.
22. Choi, S. Y., Komaromy, M. C., Chen, J., Fong, L. G., and Cooper, A. D. (1994) *J. Lipid Res. 35*, 848−859.
23. Swarnakar, S., Reyland, M. E., Deng, J., Azhar, S., and Williams, D. L. (1998) *J. Biol. Chem. 273*, 12140−12147.
24. Vogel, T., Weisgraber, K. H., Zeevi, M. I., Ben-Artzi, H., Levanon, A. Z., Rall Jr, S. C., Innerarity, T. L., Hui, D. Y., Taylor, J. M., Kanner, D., Yavin, Z., Amit, B., Aviv, H., Gorecki, M., and Mahley, R. W. (1985) *Proc. Natl. Acad. Sci. U.S.A. 82*, 8696−8700.
25. Yoshimura, A., Yoshida, T., Seguchi, T., Waki, M., Ono, M., and Kuwano, M. (1987) *J. Biol. Chem. 262*, 13299−13308.
26. Laemmli, U. K. (1970) *Nature (London) 227*, 680−685.
27. Burnette, W. N. (1981) *Anal. Biochem. 112*, 195−203.
28. Milne, R. W., Douste-Blazy, P., Marcel, Y. L., and Retegui, L. (1981) *J. Clin. Invest. 68*, 111−117.
29. Hatch, F. T., and Lees, R. S. (1968) *Adv. Lipid Res. 6*, 1−68.
30. Brissette, L., and Noël, S.-P. (1986) *J. Biol. Chem. 261*, 6847−6852.
31. Langer, T., Strober, W., and Levy, R. I. (1972) *J. Clin. Invest. 54*, 1528−1536.
32. McFarlane, A. S. (1958) *Nature 182*, 53−54.
33. Roberts, D. C., Miller, N. E., Price, S. G. L., Crook, D., Cortese, C., La Ville, A., Masana, L., and Lewis, B. (1985) *Biochem. J. 226*, 319−322.
34. Scatchard, G. (1949) *Ann. N. Y. Acad. Sci. 51*, 660−672.
35. Lowry, O. H., Rosebrough, N. J., Farr, A. L., and Randall, R. J. (1951) *J. Biol. Chem. 193*, 265−275.

BI001436U

Review

Antisense therapy in oncology: new hope for an old id a?

Ingo Tamm, Bernd Dörken, Gunther Hartmann

There is a potential role for antisense oligonucleotides in the treatment of disease. The principle of antisense technology is the sequence-specific binding of an antisense oligonucleotide to target mRNA, resulting in the prevention of gene translation. The specificity of hybridisation makes antisense treatment an attractive strategy to selectively modulate the expression of genes involved in the pathogenesis of diseases. One antisense drug has been approved for local treatment of cytomegalovirus-induced retinitis, and several antisense oligonucleotides are in clinical trials, including oligonucleotides that target the mRNA of BCL2, protein-kinase-C alpha, and RAF kinase. Antisense oligonucleotides are well tolerated and might have therapeutic activity. Here, we summarise treatment ideas in this field, summarise clinical trials that are being done, discuss the potential contribution of CpG motif-mediated effects, and look at promising molecular targets to treat human cancer with antisense oligonucleotides.

There is new hope that selective anticancer drugs, with less cytotoxic side-effects than conventional cancer chemotherapy, will be developed. This optimism is based on the identification of new cancer-associated molecular sites, which could allow the selective targeting of cancer cells, while sparing normal cells. Several approaches are available to specifically manipulate gene expression at the DNA or RNA stage of protein synthesis. Gene therapy involves the integration of new genetic material into the genome. This approach can be used to replace defective genes or block the effects of unwanted ones, by the introduction of a counteracting gene. Gene expression can also be altered at the transcriptional stage by use of oligonucleotides that cause the formation of triple helixes. In this method there is no stable integration of genetic material into the genome. An alternative strategy is to use single-stranded oligonucleotides—ie, antisense oligonucleotides—to modify gene expression at the translational step. This approach is not called gene therapy, since the target is messenger RNA (mRNA) rather than a gene.[1]

Antisense oligonucleotides are unmodified or chemically modified single-stranded DNA molecules. They are 13–25 nucleotides long and are specifically designed to hybridise to corresponding RNA by Watson-Crick binding. They inhibit mRNA function in several ways, including modulation of splicing and inhibition of protein translation by disruption of ribosome assembly. However, the most important mechanism seems to be the utilisation of endogenous RNase H enzymes by the antisense oligonucleotides. RNase H recognises the mRNA-oligonucleotide duplex and cleaves the mRNA strand, leaving the antisense oligonucleotides intact. The released oligonucleotides can then bind to other target RNA (figure).[1-5] The specificity of this mechanism has resulted in a new class of drugs with a wide range of potential clinical applications. One approved antisense drug, and results of several clinical antisense drug trials, show the feasibility of this approach, with some evidence for clinical efficiency.[6-11]

Lancet 2001; **358:** 489–97

Department for Haematology and Oncology, Charité, Virchow-Clinic, Humboldt University, Forschungshaus, Room 2.0315, 13353 Berlin, Germany (I Tamm MD, B Dörken MD); **Department of Internal Medicine, Division of Clinical Pharmacology, University of Munich, Munich** (G Hartmann MD)

Correspondence to: Dr Ingo Tamm
(e-mail: ingo.tamm@charite.de)

History

Paterson and colleagues[12] were the first to publish a report saying that gene expression can be modified with exogenous nucleic acids by use of single-stranded DNA to inhibit translation of a complementary RNA in a cell-free system. In 1978, Zamecnik and Stephenson[13] added a synthetic oligonucleotide, complementary to the 3′ end of the Rous sarcoma virus, to the medium of chicken fibroblasts in tissue culture, along with Rous sarcoma virus itself. The antisense construct inhibited the formation of new virus, and also prevented transformation of chicken fibroblasts into sarcoma cells—both surprising results at that time. In a cell-free system, translation of the Rous sarcoma viral message was also greatly impaired.[14,15]

The findings presented in these initial reports showed that antisense oligonucleotides could inhibit gene expression in a sequence specific way. Until 1985, little further progress was made in the field, mainly for three reasons. First, there was doubt that oligonucleotides could enter eukaryotic cells. Second, the synthesis of an oligomer of correct sequence and sufficient length to hybridise well at 37°C was difficult. And finally, there was little information about the sequences of the human genome. In 1983, the existence of naturally occuring antisense RNAs, and their role in the regulation of gene

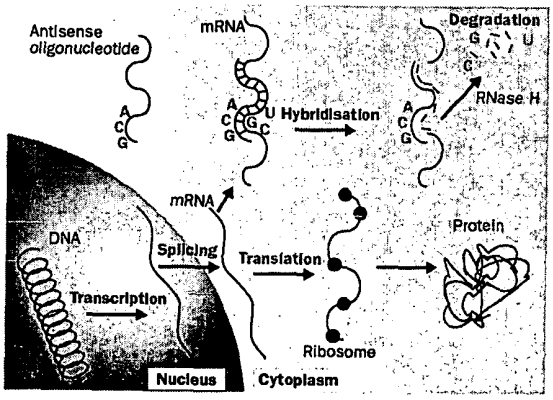

Mechanisms of action of antisense oligonucleotides

Panel 1: **Antisense oligonucleotide targets in oncology tested in vitro and in animals**

Target	Cell type analysed	Biological endpoints
BCL2[19]	B-cell-lymphoma, melanoma, lung tumour	Apoptosis
Survivin[20,21]	Cervical tumour, lung cancer	Apoptosis
MDM2[22]	Multiple tumours	p53 activation
BCLXL[23]	Endothelial cells, lung cancer cells	Apoptosis
RelA[24]	Fibrosarcoma cell line	Cell adhesion, tumorigenicity
RAS[25]	Endothelial cells, bladder cancer	*CAM* expression, proliferation
RAF[26]	Endothelial cells, smooth muscle cells	*CAM* expression, proliferation
BCR-ABL[27]	Primary progenitor bone marrow cells	Adhesion, proliferation
Jun N-terminal kinase 1 and Jun N-terminal kinase 2[28]	Renal epithelial cells	Apoptosis
Telomerase[29]	Prostate cell lines	Cell death
c-MYC[30,31]	Leukaemia cell lines	proliferation, apoptosis
c-MYB[32]	Leukaemia cell lines	Proliferation

expression was proven.[16] These observations were particularly important because they encouraged the notion that antisense oligonucleotides could be used in living cells to manipulate gene expression.[17] The introduction of efficient methods for DNA sequencing and oligonucleotide synthesis led to much activity in the field of antisense research. One of the first published studies to show in-vivo activity of oligonucleotides was done by Whitesell and colleagues.[18] The group infused a phosphodiester oligonucleotide directed toward *N-MYC* in the vicinity of a subcutanously transplanted neuroepithelioma cell line in mice. The investigators showed a loss of N-MYC protein, a change in cellular morphology, and a decrease in tumour mass in response to the antisense oligonucleotide, but not to the control oligonucleotide. Various other targets in the field of oncology have been analysed in vitro and in animals since then with encouraging results (panel 1).[19–32]

Rational drug design

Generally, the essential steps in rational drug design are identification of an appropriate target responsible for a certain disease and development of a drug with specific recognition and affinity to that target. For most drugs the mechanism of action is not well defined. By contrast, the specificity of Watson-Crick hybridisation is the basis for rational drug design of antisense oligonucleotides, leading to a new class of selective protein synthesis inhibitors. At the same time, the elucidation of the pathogenetic role of individual target proteins for certain diseases is rapidly progressing, most notably in cancer research.[33,34]

Since antisense oligonucleotides inhibit gene expression in a sequence specific way, selective alteration of the expression of genes by use of closely related sequences is possible. The antisense strategy allows the detailed analysis of signal transduction pathways, which often comprise groups of highly homologous proteins. Furthermore, research with oligonucleotides might lead to the identification of new therapeutic targets and provide a corresponding drug at the same time. Because most tumour cells have a different pattern of gene expression by comparison with normal cells, antisense oligonucleotides can theoretically be used to specifically target tumour-associated genes, or mutated genes, without altering gene expression of normal cells.[1]

Clinical trials

The number of clinical trials ongoing represents a growing interest in antisense technology (panel 2).[3] Generally, systemic treatment with antisense oligonucleotides is well tolerated and side-effects are dose-dependent. Dose-limiting toxicities include thrombocytopenia, hypotension, fever, and asthenia.[6,35] Furthermore, an increase in concentration of the liver enzymes aspartate aminotransferase and alanine aminotransferase, as well as complement activation and a prolonged partial thromboplastin time, have been reported.[36]

In 1998, the first antisense drug (fomivirsen) was approved by the US Food and Drugs Administration (FDA) for the treatment of cytomegalovirus-induced retinitis in patients with AIDS. The inhibitory constant (IC_{50}) of fomivirsen for cytomegalovirus-replication in vitro is 0·06 μmol/L, for ganciclovir the IC_{50} is 30-fold higher (2 μmol/L). Although fomivirsen is administered locally (intravitreal injection), FDA approval shows the feasibility of antisense oligonucleotides as drugs for the treatment of human diseases.[37]

Most of the proteins involved in the pathogenesis of cancer operate inside the cell, and are thus not accessible to protein-based drugs. To target the genes, which code for those proteins, by use of antisense oligonucleotides, requires a unique target sequence in the gene of interest

Panel 2: **Antisense oligonucleotides in clinical trials or approved in haematology and oncology**

Compound	Company	Protein target	Indication	Development phase
Vitravene (Fomivirsen)	Isis Pharmaceuticals, Carlsbad, USA	CMVIE2	Cytomegalovirus-induced retinitis	Approved
G3139	Genta, Berkeley Heights, USA	BCL2	Malignant melanoma, B-cell lymphoma	Phase III Phase II
ISIS 3521	Isis Pharmaceuticals, Carlsbad, USA	Protein kinase C alpha	Solid cancers	Phase III
ISIS 5132	Isis Pharmaceuticals, Carlsbad, USA	RAF kinase	Solid cancers	Phase II
ISIS 2503	Isis Pharmaceuticals, Carlsbad, USA	HRAS	Cancer	Phase II
GEM 231	Hybridon, Worcester, USA	Protein kinase A	Solid cancers	Phase II
MG 98	MethylGene, Montreal, Canada	DNA methyltransferase	Solid cancers	Phase II

and the design of a complementary oligonucleotide against the target sequence that confers biological activity.[38]

G3139

The BCL2 group of proteins is a promising target for an antisense approach in oncology. *BCL2* is an apoptosis inhibitor, which was discovered as a proto-oncogene located at the breakpoints of t(14;18) chromosomal translocations in low-grade B-cell non-Hodgkin's lymphomas. *BCL2* is overexpressed in most follicular lymphomas, in some diffuse large-cell lymphomas, and in chronic lymphocytic leukaemia.[39] The oncogenic impetus of raised *Bcl2* expression was verified in *Bcl2* transgenic mice. These mice accumulated excess non-cycling mature B lymphocytes.[39] High concentrations of BCL2 are associated with relapse in acute myelogenous leukaemia and in acute lymphocytic leukaemia.[35] The BCL2 group of proteins has been implicated not only in the pathogenesis of cancer but also in resistance to cancer treatment. Anticancer drugs and radiation ultimately destroy cells by induction of apoptosis. BCL2 blocks caspase activation in tumour cells at the mitochondrial stage, which prevents apoptosis induced by radiation and available chemotherapeutic drugs.[40]

In a phase I study,[6] the pharmacokinetics, toxicity, and therapeutic activity of an antisense oligonucleotide targeting the mRNA of BCL2 was assessed. 21 patients with BCL2-positive relapsed non-Hodgkin's lymphoma were given a 14-day subcutaneous infusion of an 18-mer phosphorothioate oligonucleotide complementary to the first six codons of the *BCL2* open reading frame (G3139). Eight cohorts of patients received doses between 4·6 and 195·8 mg/m² daily. No important systemic toxicity was seen at daily doses up to 110·4 mg/m². All patients had skin inflammation at the infusion site. Dose-limiting toxicities in this study were thrombocytopenia, hypotension, fever, and asthenia. The maximum-tolerated dose was 147·2 mg/m² daily. By standard criteria, there was one complete response, two minor responses, nine patients with stable disease, and nine with progressive disease. BCL2 was reduced in seven of 16 assessable patients as measured by fluorescence-activated cell sorting. In two of these seven patients, reduced concentrations of BCL2 were detected in tumour cells derived from lymph nodes, and in the other five, in peripheral blood or bone marrow mononuclear cell populations. Expression of HLA, which was used as a control protein, was not affected by antisense therapy. On the basis of their results the researchers concluded that *BCL2* antisense therapy was feasible, that it showed potential for antitumour activity in non-Hodgkin's lymphoma, and that down-regulation of BCL2 but not HLA suggests a specific antisense mechanism.[6] However, it is noteworthy that BCL2 was diminished in less than half of the treated patients. The mean inhibition of BCL2 expression was moderate (24%) and the biological importance of this relatively small decline is uncertain.[17] A phase II trial is underway with G3139 in combination with standard chemotherapy for patients with relapsed, chemotherapy-resistant non-Hodgkin's lymphoma.

Overexpression of BCL2 is not uncommon in non-B cell malignant tumours. Human melanoma expresses *BCL2* in up to 90% of all cases.[41] Jansen and colleagues[19] showed that G3139 improves the chemosensitivity of human melanoma transplants in severe combined immunodeficient mice. Additionally, in a phase I/II study,[42] Jansen's group tested the combination of G3139 and dacarbazine in patients with advanced malignant melanoma. In a within-patient dose-escalation protocol, G3139 0·6–6·5 mg/kg was given intravenously or subcutanously to 14 patients with advanced malignant melanoma along with standard dacarbazine treatment (total doses up to 1000 mg/m² per cycle). In serial tumour biopsy samples, BCL2 concentrations were measured by immunoblot, and apoptosis of tumour cells was assayed. The combination regimen was well tolerated with no dose-limiting toxicity. Haematological abnormalities were mild to moderate. Lymphopenia was common, but no febrile neutropenia arose. High doses of G3139 were associated with transient fever. Four patients had liver-function abnormalities that resolved within 1 week. Steady-state plasma concentrations of G3139 were obtained within 24 h and increased with the administered dose as assessed by liquid chromatography. By day 5, daily doses of 1·7 mg/kg and higher led to a median decrease of BCL2 expression of 40% in melanoma samples compared with baseline. Reduced *BCL2* expression was associated with increased apoptosis of tumour cells. Apoptosis was further enhanced after dacarbazine treatment. Six of 14 patients showed antitumour responses (one complete, two partial, three minor). The estimated median survival of all patients was more than 12 months, which compares favourably with survival of stage IV malignant melanoma patients (usually 6–9 months with and without treatment). This study is worth mentioning because it was the first antisense trial in which downregulation of the target protein in the target tissue was shown. Based on the promising results of this study, the combination of dacarbazine and G3139 therapy in patients with malignant melanoma received fast-track approval by the FDA, and is in a phase III multicentre trial.

Phase I and II studies[43,44] are also being done to test G3139 in combination with docetaxel in patients with advanced breast cancer, hormone-refractory prostate cancer, and other solid tumours. Another phase I study[45] is analysing the combination of G3139 and mitoxantrone in patients with hormone refractory prostate cancer. In 21 individuals treated so far, toxicities were transient and included neutropenia (grade 3), lymphopenia (grade 2), fatigue, arthralgias, and myalgias (all grade 1). No dose-limiting toxicities were reported for the doses tested, and one patient had a greater than 50% response to prostate specific antigen with symptomatic improvement in bone pain. Another phase I study has been started to test G3139 together with salvage chemotherapy of fludarabine and cytarabine in patients with refractory or relapsed acute myelogenous leukaemia or acute lymphocytic leukaemia. Furthermore, a phase I/II trial of a combination treatment of G3139 and irinotecan has been initiated in patients with metastatic or recurrent colorectal cancer. So far, no results are available for these two trials.

ISIS 3521

Another target of antisense oligonucleotides is protein kinase C-alpha (PKC-alpha). PKC-alpha belongs to a class of serine-threonine kinases whose involvement in oncogenesis is suggested by the fact that they are the major intracellular receptors for tumour-inducing phorbol esters. Results of a phase I study[35] suggested that an antisense oligonucleotide directed against PKC-alpha (ISIS 3521) might be effective in the treatment of low-grade lymphoma. In this trial ISIS 3521 was delivered over 21 days by continuous intravenous infusion followed by a 7-day rest period.[7] Doses were increased from 0·5 to 3·0 mg/kg daily. 21 patients with incurable malignancies were treated in five patient cohorts. The maximum tolerated dose was 2·0 mg/kg daily, equivalent to pharmacologically active doses against human xenografts

in mice. The dose-limiting toxicities were thrombocytopenia and fatigue at a dose of 3·0 mg/kg per day. Evidence of tumour response lasting up to 11 months was seen in three of four patients with ovarian cancer.

Updated results of a phase I/II trial of ISIS 3521 combined with carboplatin and paclitaxel in patients with stage IIIB or IV non-small-cell lung cancer (NSCLC) have been reported.[46,47] In 24 evaluable patients with NSCLC, 46% had a partial response and 33% had a minor response or stable disease. The median time to progression was 6·5 months. The 1 year survival was 78% with a median survival of 18 months. Typical survival of patients receiving standard chemotherapy alone is about 8 months. Toxicity consisted of neutropenia (grade 3 in six patients and grade 4 in eight patients) and thrombocytopenia (grade 3 in six patients and grade 4 in two patients). Thus, the combination of ISIS 3521, carboplatin, and paclitaxel was well tolerated, and showed promising activity in NSCLC. On the basis of these results, a 600-patient, randomised phase III clinical trial of ISIS 3521 in combination with chemotherapy for NSCLC has started.

Alavi and colleagues[48] tested the efficacy, toxicity, and pharmacology of ISIS 3521 delivered as a 21 day continous intravenous infusion in patients with recurrent high grade astrocytomas. Toxicities were mild and reversible. There is no evidence of a clinical benefit so far. Median time to progression was 35 days after entering the protocol and median survival was 93 days.

ISIS 5132

Other attractive targets for antisense therapy in oncology are RAF kinases and RAS. RAF kinases are serine/threonine kinases that regulate mitotic signalling pathways, most notably the mitogen-activated protein kinase pathway that transmits signals from RAS. C-RAF has been reported to bind to BCL2 and to be involved in the regulation of apoptosis. The *RAS* oncogene is deregulated or mutated more frequently than any other oncogene studied in human cancer.[49,50] In several tumours, including breast and NSCLC, the expression of RAS is a prognostic factor.[51] In pancreatic cancer, for which standard therapy is strikingly ineffective, 95% of all cases show *RAS* mutations.[49] This finding suggests that alterations in this pathway play a significant part in the pathogenesis of cancer.[11]

An antisense oligonucleotide directed to the 3′ untranslated region of the c-*RAF* mRNA (ISIS 5132) inhibited the growth of human tumour cell lines in vitro and in vivo in association with specific down-regulation of target message expression. In a phase I trial, changes in c-*RAF1* mRNA expression were analysed in peripheral blood mononuclear cells collected from patients with advanced cancers treated with ISIS 5132. Significant reductions of c-*RAF1* expression from baseline were detected in 13 of 14 patients. Two patients, both of whom had shown tumour progression with previous cytotoxic chemotherapy, exhibited long-term stable disease in response to treatment with antisense oligonucleotides. The researchers suggest that peripheral blood mononuclear cells can be used to confirm antisense-mediated inhibition of the target protein in vivo.[52] However, the decrease in c-*RAF1* expression in total peripheral blood mononuclear cells could represent changes in the proportion of leucocyte populations due to non-antisense-mediated immune stimulation, so this method does not provide proof for an antisense specific effect.

In a phase I trial, 31 patients with advanced malignancies received ISIS 5132 as a 2-h intravenous infusion three times every week for 3 consecutive weeks, with doses ranging from 0·5 to 6·0 mg/kg.[9] Clinical toxicities included fever and fatigue, neither of which were dose limiting. Two patients experienced prolonged disease stabilisation for more than 7 months. In both of these cases, this stabilisation was associated with reduction in c-*RAF1* expression in peripheral blood mononuclear cells.

Cunningham and co-workers[8] reported the results of a trial testing continuous intravenous infusion of ISIS 5132 for 21 days every 4 weeks in 34 patients with various solid tumours refractory to standard therapy. Toxicities up to 4·0 mg/kg were not dose limiting. Doses of 2·0–4·0 mg/kg are comparable to doses in mice at which activity was seen in human xenograft models. Grade 3 fever arose in two of 34 patients treated. One patient treated with 5·0 mg/kg had fever as a dose-limiting toxicity. Three patients developed grade 3 or 4 thrombocytopenia and one had grade 3 leucopenia. Two patients developed sepsis; one of them, while septic, manifested grade 4 thrombocytopenia, grade 4 hyperbilirubinemia, and a grade 3 increase in aspartate aminotransferase, the other developed grade 4 thrombocytopenia. Leucopenia was mild, and no patient had neutropenia. One patient with ovarian cancer refractory to therapy had a large reduction in concentrations of the cancer biomarker CA125 (97%), and two other patients had prolonged disease stabilisation for 9 and 10 months.

Phase II trials of ISIS 5132 have begun. There is no evidence of single agent activity of ISIS 5132 in pretreated patients with recurrent ovarian cancer.[53] In one study, 22 patients were treated at a dose of 4 mg/kg daily by 21-day continous intravenous infusion every 4 weeks. ISIS 5132 was well tolerated with no grade 3 or 4 haematological or biochemical toxicity. There were six documented episodes of grade 3 non-haematological toxicity (two lethargy, one anorexia, two pain, one shortness of breath). No objective clinical response was seen. Three patients had stable disease for a median of 3·8 months, and the other evaluable patients had documented progressive disease. No patient had a decrease in CA125 of 50% or more. The outcome of other phase II clinical studies, including some in prostate and colon cancer, will be available shortly.

ISIS 2503

A 20-base phosphorothioate antisense oligonucleotide (ISIS 2503), which binds to the translation initiation region of human HRAS mRNA, selectively reduced the expression of HRAS mRNA and protein in cell culture. In a phase I trial, ISIS 2503 caused no dose-limiting toxicity at doses up to 10 mg/kg daily by 14-day continous intravenous infusion. A non-toxic dose of 6 mg/kg daily was selected for further study. A phase II trial of ISIS 2503 as first line treatment for patients with untreated stage IV or recurrent colorectal carcinoma is in progress. In an interim analysis, 17 patients had received 38 cycles. Toxicity was limited to grade 1–2 fever and grade 1 thrombocytopenia in three patients. Two patients had stable disease after 3 and 6 cycles of treatment.[54]

C-MYB antisense oligonucleotide

Autologous transplantation has become part of the routine management of many haematological malignancies. However, many patients relapse after the procedure. Results of gene marking studies suggest that contamination of tumour cells, which are inadvertently reinfused with the graft, might contribute to relapse in acute myelogenous leukaemia and chronic myelogenous leukaemia. Antisense oligonucleotides against c-myb have been used to purge haematopoietic cell harvests from patients with chronic myelogenous leukaemia before

autologous transplantation.[1,55] C-MYB is a nuclear binding protein that controls the passage through the G1/S phase of the cell cycle and might play an important part in haematopoiesis. Although expression is not restricted to leukaemic cells, leukaemic progenitors might be more susceptible to inhibition of c-*MYB* than normal progenitors in vitro. In a clinical pilot study, oligonucleotide purging was done for 24 h on CD 34+ marrow cells. Patients received busulfan and cyclophosphamide, followed by reinfusion of previously cryopreserved oligonucleotide purged mononuclear cells. Seven patients with chronic myelogenous leukaemia in chronic phase and one in accelerated phase were treated. Seven of eight patients were engrafted. In four of six assessable patients with chronic myelogenous leukaemia, metaphases were 85–100% normal 3 months after engraftment, suggesting a huge purge in the marrow graft.[1] A phase II study has been initiated to assess the use of a c-*MYB* antisense oligonucleotide to purge bone marrow from clonogenic chronic myelogenous leukaemia cells for subsequent autologous transplantation after treatment with high-dose busulfan or cyclophosphamide.

MG 98

Hypermethylation by the enzyme DNA methyltransferase has been postulated to inactivate tumour suppressor genes, resulting in neoplastic transformation and tumorigenesis. Drugs that prevent or reverse DNA methylation might therefore restore control of growth of cancer cells. MG 98 is a phosphorothioate antisense oligonucleotide, which specifically inhibits translation of the mRNA for human DNA methyltransferase with an IC_{50} of 50–70 nmol/L in tumour cell lines. Delay of tumour growth and tumour regression in response to MG 98 were seen in human lung and colon cancer xenografts. In a phase I study, researchers investigated the effect of MG 98 given as a continuous 21-day intravenous infusion administered at 4-week intervals. In an interim analysis, nine patients with solid cancers received ten courses of therapy at doses up to 240 mg/m² daily. Dose limiting drug-related increases of transaminases (grade 3) were encountered in two of two patients at the 240 mg/m² dose. Other toxicities were minor. Biologically relevant concentrations for the inhibition of human DNA methyltransferase mRNA were achieved with the lowest dose assessed (40 mg/m² daily).[56] MG 98 is in phase II clinical trials.

GEM 231

Several advanced chemical modifications have been used to improve specificity, pharmacokinetics, and safety profiles of phosphorothioate oligonucleotides. Of note, these so-called mixed-backbone oligonucleotides permit oral and colorectal administration as a result of their increased in vivo metabolic stability. One of these compounds, GEM 231, is designed to interfere with the production of the RI-alpha regulatory subunit of protein kinase A (PKA), a cellular growth-promoter whose concentration is increased in a wide variety of cancer cells. PKA is overexpressed in most human cancers, correlating with worse clinicopathological features and prognosis in ovarian and breast cancer patients. After oral or intraperitoneal administration, GEM 231 had dose-dependent in-vivo antitumour activity in severe combined immunodeficient and nude mice bearing xenografts of human cancers of the colon, breast, and lung.[57] In a phase I clinical study, preliminary data show that escalating doses of GEM 231 are well tolerated when given twice every week by intravenous injection. Repeated doses of up to 360 mg/m² (equivalent to a 7–9 mg/kg range) were administered over periods of up to 10 weeks. There are phase I studies ongoing, which are testing the safety of GEM 231 in combination with docetaxel or paclitaxel in patients with advanced cancers. Preliminary results suggest that GEM 231 produces only mild and reversible side-effects and does not increase the side-effects produced by the taxanes.

Non-antisense action of oligonucleotides

Like other new technologies, antisense faces several methodological limitatitons, including oligonucleotide stability versus binding affinity, delivery of oligonucleotides to the target cells, and non-antisense effects of oligonucleotides. There has been good progress in antisense technology over the past years, and most of these issues have been addressed in reviews.[1-3,17,35,55] Here, we will summarise information that has improved our understanding of non-antisense-mediated biological effects of oligonucleotides.

Immune stimulation is widely recognised as an undesirable side-effect of certain antisense oligonucleotides, which can interfere with therapeutic activity. With respect to the clinical application of oligonucleotides, in this review we concentrate on their stimulatory effects in the human immune system. The immunostimulatory activity of unmodified phosphodiester oligonucleotides is strongly dependent on the presence of unmethylated CG dinucleotides in certain base contexts, so-called CpG motifs (GTCGTT in human beings, GACGTT in mice).[58] Of note, the phosphorothioate backbone, which is generally used in antisense oligonucleotides to provide stability against nucleases, has immunostimulating properties itself, which are independent of the sequence.[59] The immunostimulatory activity of a phosphorothioate-modified oligonucleotide is largely unpredictable, and has to be ascertained experimentally. Strong immunostimulatory activity is likely if the sequence starts with a TC at the 5′ end, and if the sequence contains CG dinucleotides (eg, CpG ODU206, prototype to stimulate human immune cells).[60,61] Immune stimulation might be avoided in antisense oligonucleotides by the selection of CG-free target sequences, by the use of oligonucleotide backbones that do not support immune stimulation, or by selective methylation of the cytosine in any CG dinucleotide.

CpG-dependent immune stimulation of a DNA molecule represents a highly evolved immune defense mechanism whose actual goal is the detection of microbial nucleic acids.[62] By contrast with vertebrate DNA, in which CpG dinucleotides are suppressed and highly methylated, microbial genomes do not generally feature CpG suppression or methylation. Immune effector cells, such as B cells and dendritic cells, seem to have evolved pattern recognition receptors that, by binding the microbe-restricted structure of CpG motifs, trigger protective immune responses.[63] CpG oligonucleotides, which are designed to provide optimum immune stimulation, are promising anticancer drugs. They are being tested in several clinical trials including ones for non-Hodgkin lymphoma, melanoma, basal cell carcinoma, and kidney cancer.[64] Although specific immune activation by an oligonucleotide seems to have various potential therapeutic applications, it is generally undesirable in antisense oligonucleotides.

Several of the most advanced antisense oligonucleotides in clinical trials against cancer contain CG dinucleotides.[65] An antisense oligonucleotide directed against the mRNA of BCL2 (G3139) and used in some of the clinical trials

described above contains two CG dinucleotides and a TC at the 5′ end. It is noteworthy that this sequence was successfully used as an immunostimulatory CpG oligonucleotide in animal tumour models.[66] Klasa and colleagues[67] showed that G3139 has reduced but still considerable therapeutic activity in a human lymphoma xenograft in severe combined immune deficient mice, which lack T cells and natural killer cells. From their results the authors concluded that the therapeutic activity of this oligonucleotide is largely due to an antisense mechanism. However, macrophages, which are still present in these immunodeficient mice, might contribute to the antitumour activity of this antisense oligonucleotide. Furthermore, an oligonucleotide with the same sequence as G3139 directly induced activation and differentiation of primary human non-Hodgkin lymphoma cells by a CpG-dependent mechanism.[68] Even if a tumour (ie, melanoma) is not sensitive to direct CpG-mediated activation, CpG-induced stimulation of the immune system might still be involved in eliminating the tumour in vivo. Thus, the relative contribution of a specific antisense mechanism versus immune stimulation, particularly of G3139, is still controversial.

New targets

There are several new potential targets for specific antisense treatment of human cancer. The inhibitor of apoptosis (IAP) family of proteins constitute a group of apoptosis suppressors (XIAP, c-IAP1, c-IAP2, NAIP, survivin, apollon, livin), which are conserved throughout animal evolution, with homologues in flies, worms, mice, and people.[69,70] These proteins function as direct inhibitors of certain caspases.[71,72] Since caspases are central for most apoptotic pathways, the fact that IAPs protect cells from several anticancer drugs and other inducers of apoptosis is not surprising.

c-*IAP2* at 11q21, and a newly discovered gene, *MLT* at 18q21, are involved in t(11;18)(q21;q21) associated with mucosa-associated lymphoid tissue (MALT) lymphoma.[73] The translocation suggests a role for c-*IAP2* in the pathogenesis of MALT-lymphoma, since this rearrangement occurs in about 50% of low-grade MALT-lymphomas.[74] Antisense oligonucleotides that target either the *c-IAP2/MLT* breakpoint or one of the two partners involved in the fusion protein in MALT-lymphoma cells, could potentially alter the antiapoptotic function of c-IAP2 and induce cell death in MALT-lymphoma cells.

Another antiapoptosis molecular target is survivin. Survivin is overexpressed in a large proportion of human cancers, providing evidence that altered expression of these proteins occurs during tumorigenesis.[75,76] In colorectal, gastric, breast, bladder, and lung cancers, as well as in diffuse large B-cell lymphoma, survivin expression is associated with shorter survival.[77–84] In neuroblastoma, survivin expression correlates with a high stage of disease.[85] Interestingly, survivin is expressed in a cell cycle dependent manner, with highest concentrations in G2/M and rapid downregulation after cell cycle arrest.[86] At the beginning of mitosis, survivin associates with the mitotic spindle. Disruption of this interaction results in a loss of its antiapoptotic function.[86] Some researchers have suggested that survivin frees cyclin dependent kinase 4 (CDK4) from the cyclin dependent kinase inhibitor, p16 CDK4 then translocates into the nucleus where it initiates the S-phase of the cell cycle.[87] The overexpression of survivin in cancer might thus overcome cell cycle checkpoints and favour aberrant progression of transformed cells through mitosis. Survivin, therefore, bridges apoptosis and cell cycle. Mutation of a conserved cysteine in the survivin baculovirus-inhibitory repeat (BIR) domain abolishes the cytoprotective abilities of survivin. However, the BIR mutant retains the ability to associate with microtubules similar to wild-type survivin, and interferes with the function of endogenous survivin by competing for microtubule binding.[86] Thus, in contrast to p53, which links DNA replication in the S phase of the cell cycle to apoptosis, survivin seems to couple the cell-suicide response to the checkpoint machinery involved in later cell-cycle steps (G2/M).[88,20] An antisense oligonucleotide, targeting nucleotides 232–251 of human survivin mRNA, has been shown to induce apoptosis in lung cancer cell lines, and to sensitise cells to chemotherapy.[89] Moreover, blockade of survivin expression induces apoptosis in myeloma cell lines.[90]

Other potentially interesting targets are proteins collectively known as heat shock proteins (HSP). HSPs are among the most conserved proteins known and include a number of different families.[91] Among the best analysed HSPs are HSP70 and HSP27. These two proteins possess cytoprotective activity and are frequently overexpressed in human cancer. Results of gene transfer experiments have shown that HSP70 and HSP27 not only confer resistance against heat stress,[92,93] but also against most apoptotic stimuli such as tumour necrosis factor, ceramide, ultraviolet radiation, caspase-3 overexpression, and several chemotherapeutic drugs.[91] HSP expression in certain cancer types correlates with poor prognosis and resistance to treatment. In breast cancer, HSP70 expression is a useful prognostic marker for much shorter disease-free survival, increased cell proliferation, and poor differentiation, as well as lymph node metastases. Furthermore, HSP70 inversely correlates with the response of breast cancer to combination chemotherapy. In ovarian cancer, HSP27 expression increases with advanced stage, and high HSP27 content in tumour cells is associated with greatly reduced survival.[94] Similarly, HSP27 is a marker of poor prognosis in osteosarcoma.[91,95] The data suggest that HSP27 and HSP70 are interesting new targets for a specific antisense-based tumour treatment.

Certain chromosome abnormalities, especially translocations, are associated with particular subtypes of leukaemia, lymphoma, and sarcoma. Among these are the translocations involving *AML1* on 21q22, *MLL* on 11q23, and *TEL* on 12p13. Abnormalities of these genes account for a large proportion of patients with acute lymphocytic leukaemia and acute myelogenous leukaemia.[96] Cloning of translocation breakpoints results in unique diagnostic tools for fluorescence in situ hybridisation and molecular analysis of leukaemic cells. Advances in understanding the alterations in the function of the fusion genes compared with normal genes provide insights with respect to new therapeutic strategies, including antisense therapy.[96]

Virtually all of the translocations in myeloid leukaemias result in a unique fusion or chimeric gene. In the case of the t(8;21) translocation, the 5′ section of *AML1* on chromosome 21, including the DNA-binding domain, is fused to virtually all of the *ETO* gene on chromosome 8. *AML1* is also called *CBF2*, because it codes for the DNA-binding component of core-binding factor. *AML1* is an essential gene, which regulates the expression of several other genes important in haematopoietic cell development, function, and differentiation, such as myeloperoxidase, interleukin-3, granulocyte-macrophage colony-stimulating factor, colony-stimulating factor-1 receptor, and the T-cell receptor.[96] The t(8;21) is among the most common rearrangements in acute myelogenous leukaemia, accounting for about 9% of all patients with the disease.

Thus, to target one causal gene with antisense oligonucleotides in leukaemia patients might be advantageous. The list of fusion proteins that might act as targets for antisense therapy in leukaemias and lymphomas is long and includes, for example, the translocation 4;11 in acute lymphocytic leukaemia, which is associated with a bad prognosis, and t(11;14) in mantle cell lymphoma.[96,97]

Other new targets for antisense therapy are involved in tumour cell proliferation, angiogenesis, and metastasis—eg, growth factor receptor tyrosine kinases such as the epidermal growth factor receptor; transcription factors such as NF-kB, HER-2/neu, cyclin-dependent kinases, and telomerase (proliferation); the vascular endothelial growth factor receptor and the basic fibroblast growth factor receptor (angiogenesis); and matrix metalloproteinases, angiogenin and integrins (angiogenesis and metastasis).[34,98]

Future perspectives

New hope for the idea of antisense is provided by the results of a study done by Jansen and colleagues,[42] which show that, besides the clinical benefit for patients with advanced melanoma, systemic treatment with antisense oligonucleotides results in the downregulation of the target protein within the target tissue. This study is a milestone in the field of antisense, since the results suggest that the principle of antisense works, not only with local treatment, as shown with fomivirsen,[37] but also with systemic treatment with antisense oligonucleotides. If this study is seen as proof of principle, it might now pave the way for development of antisense oligonucleotides for various new potential targets for the treatment of cancer. Once the mechanism for one antisense oligonucleotide is established, the door is open for combination treatment with several oligonucleotides, targeting various oncogenes, to overcome tumour escape and to improve therapeutic activity of this approach.

However, careful assessment of future controlled studies is needed to confirm antisense-mediated downregulation of the target protein in a larger number of patients and for other antisense oligonucleotides. In the end, we might find that a sound proof of principle is virtually impossible in a clinical trial, because of limitations imposed by the lack of adequate controls. In addition to the possibility of specific antisense-mediated inhibition of the target oncogene, decreased concentrations of the oncogene would also be expected as a consequence of oligonucleotide-induced antitumour effects other than antisense.

Besides antisense-mediated inhibition of the target protein, one of the effects likely to be involved in antitumour action of certain antisense oligonucleotides is their immunostimulatory effect based on the presence of CG dinucleotides within the sequence. Of note, the BCL2 antisense oligonucleotide, the most promising oligonucleotide to date, and the only one for which downregulation of the target protein within the target tissue has been shown, is a CpG oligonucleotide as well.[66] CpG oligonucleotides with optimised immunostimulatory activity but no antisense sequence are in clinical development for the immunotherapy of cancer, and could become established as a second pathway of oligonucleotides-based therapy in oncology.

However, there is clear evidence for antisense-mediated target protein inhibition by antisense oligonucleotides. When directed against VEGF, oligonucleotides lack CG dinucleotides, but still show potent in vivo effects. Oligonucleotides with new backbone modifications other than phosphorothioate (ie, 2'-O-methoxy-ethoxy, morpholino) or with methylated cytosines are non-immunostimulatory but are potent inhibitors of target protein expression.[3,99] The future of antisense is likely to be based on these new generation compounds.

Proof of clinical efficacy, of any of the antisense oligonucleotides in the field of oncology, is still missing. Large controlled trials are needed to show that antisense oligonucleotides are better than other treatment approaches. However, if this goal is achieved without a clear proof of principle, the major dilemma of antisense is still unresolved. The beauty and future potential of antisense depends on the design of multiple drugs based on our increasing knowledge of genes and their functions. Only if the therapeutic activity of an antisense oligonucleotide is defined by the antisense sequence, and thus is to some extent predictable, will the future for antisense-based drugs become bright. Otherwise, even if particular antisense oligonucleotides become established for systemic treatment of cancer, antisense will not be better than other drug development strategies, most of which depend on an empirical approach.

This work was supported by grants from the European Haematology Association, José Carreras Leukämie-Stiftung eV, the Dr Mildred Scheel-Stiftung (10-1309-En2), and the German-Israeli Foundation (I-021-203.05/96).

References

1 Clark RE. Antisense therapeutics in chronic myeloid leukaemia: the promise, the progress and the problems. *Leukemia* 2000; 14: 347–55.
2 Gewirtz AM, Sikol DL, Ratajczak MZ. Nucleic acid therapeutics: state of the art and future prospects. *Blood* 1998; 92: 712–36.
3 Koller E, Gaarde WA, Monia BP. Elucidating cell signaling mechanisms using antisense technology. *Trends Pharmacol Sci* 2000; 21: 142–48.
4 Crooke ST. Molecular mechanisms of action of antisense drugs. *Biochim Biophys Acta* 1999; 1489: 31–44.
5 Baker BF, Monia BP. Novel mechanisms for antisense-mediated regulation of gene expression. *Biochim Biophys Acta* 1999; 1489: 3–18.
6 Waters JS, Webb A, Cunningham D, et al. Phase I clinical and pharmacokinetic study of bcl-2 antisense oligonucleotide therapy in patients with non-hodgkin's lymphoma. *J Clin Oncol* 2000; 18: 1812–23.
7 Yuen AR, Halsey J, Fisher GA, et al. Phase I study of an antisense oligonucleotide to protein kinase C-alpha (ISIS 3521/CGP 64128A) in patients with cancer. *Clin Cancer Res* 1999; 5: 3357–63.
8 Cunningham CC, Holmlund JT, Schiller JH, et al. A phase I trial of c-Raf kinase antisense oligonucleotide ISIS 5132 administered as a continous intravenous infusion in patients with advanced cancer. *Clin Canc Res* 2000; 6: 1626–31.
9 Stevenson JP, Yao KS, Gallagher M, et al. Phase I clinical/pharmacokinetic and pharmacodynamic trial of the c-raf-1 antisense oligonucleotide ISIS 5132 (CGP 69846A). *J Clin Oncol* 1999; 17: 2227–36.
10 Nemunaitis J, Holmlund JT, Kraynak M, et al. Phase I evaluation of ISIS 3521, an antisense oligodeoxynucleotide to protein kinase C-alpha, in patients with advanced cancer. *J Clin Oncol* 1999; 17: 3568–95.
11 Khuri FR, Kurie JM. Antisense approaches enter the clinic. *Clin Canc Res* 2000; 6: 1607–10.
12 Paterson BM, Roberts BE, Kuff EL. Structural gene identification and mapping by DNA-mRNA hybrid-arrested cell-free translation. *Proc Natl Acad Sci USA* 1977; 74: 4370–74.
13 Zamecnik PC, Stephenson ML. Inhibition of Rous sarcoma virus replication and transformation by a specific oligodeoxynucleotide. *Proc Natl Acad Sci USA* 1978; 75: 280–84.
14 Stephenson ML, Zamecnik PC. Inhibition of rous sarcoma viral RNA translation by a specific oligodeoxynucleotide. *Proc Natl Acad Sci USA* 1987; 75: 285–88.
15 Zamecnik PC. History of antisense oligonucleotides. In: Agrawal S, ed. Antisense therapy. Totowa: Humana Press, 1996: 5–15.
16 Simons RW, Kleckner N. Translational control of IS10 transposition. *Cell* 1983; 34: 683–91.
17 Gewirtz AM. Oligonucleotide therapeutics: a step forward. *J Clin Oncol* 2000; 18: 1809–11.
18 Whitesell L, Rosolen A, Neckers LM. In vivo modulation of N-myc expression by continous perfusion with an antisense oligonucleotide. *Antisense Res Dev* 1991; 1: 343–50.
19 Jansen B, Schlagbauer-Wadl H, Brown BD, et al. Bcl-2 antisense

therapy chemosensitizes human melanoma in SCID mice. *Nat Med* 1998; **4**: 232–34.

20 Li F, Ackermann EJ, Bennett CF, et al. Pleiotropic cell-division defects and apoptosis induced by interference with survivin function. *Nature Cell Biology* 1999; **1**: 461–66.

21 Olie RA, Simoes-Wüst AP, Baumann B, et al. A novel antisense oligonucleotide targeting survivin expression induces apoptosis and sensitizes lung cancer cells to chemotherapy. *Cancer Res* 2000; **6**: 2805–09.

22 Wang H, Zeng X, Oliver P, et al. MDM2 oncogene as a target for cancer therapy: an antisense approach. *Intl J Oncol* 1999; **15**: 653–60.

23 Leech SH, Olie RA, Simoes-Wüst AP, et al. Induction of apoptosis in lung cancer cells following bcl-xL antisense treatment. *Int J Cancer* 2000; **87**: 582–90.

24 Sharma HW, Narayanan R. The NF-kappaB transcription factor in oncogenesis. *Anticancer Res* 1996; **16**: 589–96.

25 Chen G, Oh S, Monia BP, Stacey DW. Antisense oligonucleotides demonstrate a dominant role of c-Ki-RAS proteins in regulating the proliferation of diploid human fibroblasts. *J Biol Chem* 1996; **271**: 28259–65.

26 Cioffi CL, Garay M, Johnston JF, et al. Selective inhibition of A-Raf and C-Raf mRNA expression by antisense oligodeoxynucleotides in rat vascular smooth muscle cells: role of A-Raf and C-Raf in serum-induced proliferation. *Mol Pharmacol* 1997; **51**: 383–89.

27 Mahon FX, Ripoche J, Pigeonnier V, et al. Inhibition of chronic myelogenous leukaemia cells harboring a BCR-ABL B3A2 junction by antisense oligonucleotides targeted at the B2A2 junction. *Exp Hematol* 1995; **23**: 1606–11.

28 Cioffi CL, Monia BP. Evaluation of biological role of c-Jun N-terminal kinase using an antisense approach. *Methods Enzymol* 2000; **314**: 363–78.

29 Kondo Y, Koga S, Komata T, Kondo S. Treatment of prostate cancer in vitro and in vivo with 2-5A-anti-telomerase RNA component. *Oncogene* 2000; **19**: 2205–11.

30 Wickstrom EL, Bacon TA, Gonzalez A, Freeman DL, Lyman GH, Wickstrom E. Human promyelocytic leukaemia HL60 cell proliferation and c-MYC protein expression are inhibited by an antisense pentadecadeoxynucleotide targeted agaisnt c-MYC mRNA. *Proc Natl Acad Sci USA* 1988; **85**: 1028–32.

31 Holt JT, Redner RL, Nienhuis AW. An oligomer complementary to c-MYC mRNa inhibits proliferation of HL60 promyelocytic cells and induces differentiation. *Mol Cell Biol* 1988; **8**: 963–73.

32 Anfossi G, Gewirtz AM, Calabretta B. An oligomer complementary to c-myb-encoded mRNA inhibits proliferation of human myeloid leukemia cell lines. *Proc Natl Acad Sci USA* 1989; **86**: 3379–83.

33 Brysch W, Rifai A, Tischmeyer W, Schlingensiepen K-H. Antisense-medited inhibition of protein synthesis. In: Agrawal S, ed. Antisense therapeutics. Totowa: Humana Press, 1996: 159–82.

34 Buolamwini JK. Novel anticancer drug discovery. *Curr Opin Chem Biol* 1999; **3**: 500–09.

35 Cotter FE. Antisense therapy of hematologic malignancies. *Semin Hematol* 1999; **36**: 9–14.

36 Levin AA. A review of issues in the pharmacokinetics and toxicology of phophorothioate antisense oligonucleotides. *Biochim Biophys Acta* 1999; **1489**: 69–84.

37 de Smet MD, Meenken CJ, van den Horn GJ. Fomivirsen: a phosphorothioate oligonucleotide for the treatment of CMV retinitis. *Ocul Immunol Inflamm* 1999; **7**: 189–98.

38 Wickstrom E. Antisense tumor therapy. In: Agrawal S, ed. Antisense therapy. Totowa: Humana Press, 1996: 87–108.

39 Adams JM, Cory S. The bcl-2 protein family: arbiters of cell survival. *Science* 1998; **281**: 1322–26.

40 Reed JC. Regulation of apoptosis by bcl-2 family proteins and its role in cancer and chemoresistance. *Curr Opin Oncol* 1995; **7**: 541–46.

41 Cerroni L, Soyer HP, Kerl H. Bcl-2 expression in cutaneous malignant melanoma and benign melanocytic nevi. *Am J Dermatopathol* 1995; **17**: 7–11.

42 Jansen B, Wacheck V, Heere-Reess E, et al. Chemosensitization of malignant melanoma by BCL2 antisense therapy. *Lancet* 2000; **356**: 1728–33.

43 Chen HX, Marshall JL, Trocky N, et al. A phase I study of bcl-2 antisense G3139 (GENTA) and weekly docetaxel in patients with advanced breast cancer and other solid tumors. *Proc Am Soc Clin Oncol* 2000; **19**: 178a (abstr).

44 Tolcher AW, Kuhn J, Basler J, et al. A phase I, pharmacokinetic and biologic correlative study of G3139 (Bcl-2 antisense oligonucleotide) and Docetaxel in patients with hormone-refractory prostate cancer (HRPC). *Clin Canc Res* 2000; **6** (suppl): 4571s (abstr).

45 Chi KN, Gleave ME, Klasa R, Murray N, Bryce C, Tolcher A. A phase I trial of an antisense oligonucleotide to bcl-2 (G3139, Genta) and mitoxantrone in patients with metastatic hormone refractory prostate cancer (HRPC). *Proc Am Soc Clin Oncol* 2000; **19**: 330a (abstr).

46 Yuen A, Advani R, Fisher G, et al. A phase I/II trial of ISIS 3521, an antisense inhibitor of protein kinase C alpha, combined with carboplatin and paclitaxel in patients with non-small cell lung cancer. *Proc Am Soc Clin Oncol* 2000; **19**: 459a (abstr).

47 Yuen A, Halsey J, Lum B, et al. Phase I/II trial of ISIS 3521, an antisense inhibitor of PKC, with carboplatin and paclitaxel in non-small cell lung cancer. *Clin Canc Res* 2000; **6** (suppl): 4572s (abstr).

48 Alavi JB, Grossman SA, Supko J, et al. Efficacy, toxicity, and pharmacology of an antisense oligonucleotide directed against protein kinase C-alpha (ISIS 3521) delivered as a 21 day continous intravenous infusion in patients with recurrent high grade astrocytomas (HGA). *Proc Am Soc Clin Oncol* 2000; **19**: 167a (abstr).

49 Bos JL. Ras oncogenes in human cancer: a review. *Cancer Res* 1989; **49**: 4682–89.

50 Bollag K, McCormick F. Regulators and effectors of ras protein. *Annu Rev Cell Biol* 1991; **7**: 601–32.

51 Eckhardt SG, Rizzo J, Sweeney KR, et al. Phase I and pharmacologic study of the tyrosine kinase inhibitor SU101 in patients with advanced solid tumors. *J Clin Oncol* 1999; **17**: 1095–1104.

52 O'Dwyer PJ, Stevenson JP, Gallagher M, et al. c-raf-1 depletion and tumor responses in patients treated with the c-raf-1 antisense oligonucleotide ISIS 5132 (CGP 69846A). *Clin Canc Res* 1999; **5**: 3977–82.

53 Oza AM, Eisenhauer E, Swenerton K, et al. Phase II study of c-raf kinase antisense oligonucleotide ISIS 5132 in patients with recurrent ovarian cancer. *Clin Canc Res* 2000; **6** (suppl): 4572s (abstr).

54 Saleh M, Posey J, Pleasani L, et al. A phase II trial of ISIS 2503, an antisense inhibitor of H-ras, as first line therapy for advanced colorectal carcinoma. *Proc Am Soc Clin Oncol* 2000; **19**: 320a (abstr).

55 Agarwal N, Gewirtz AM. Oligonucleotide therapeutics for hematologic disorders. *Biochim Biophys Acta* 1999; **1489**: 85–96.

56 Siu LL, Gelmon KA, Moore MJ, et al. A phase I and pharmacokinetik (PK) study of the human DNA methyltransferase (Metase) antisense oligodeoxynucleotide MG98 given as a 21-day continous infusion every 4 weeks. *Proc Am Soc Clin Oncol* 2000; **19**: 250a (abstr).

57 Wang H, Cai Q, Zeng X, Yu D, Agrawal S, Zhang R. Antitumor activity and pharmacokinetics of a mixed-backbone antisense oligonucleotide targeted to the RIalpha subunit of protein kinase A after oral administration. *Proc Natl Acad Sci USA* 1999; **96**: 13989–94.

58 Hartmann G, Krieg AM. Mechanism and function of a newly identified CpG DNA motif in human primary B cells. *J Immunol* 2000; **164**: 944–53.

59 Hartmann G, Krug A, Waller-Fontaine K, Endres S. Oligodeoxynucleotides enhance lipopolysaccharide-stimulated synthesis of tumor necrosis factor: dependence on phophorothioate modifications and reversal by heparin. *Mol Med* 1996; **2**: 429–38.

60 Hartmann G, Weiner G, Krieg AM. CpG DNA as a signal for growth, activation and maturation of human dendritic cells. *Proc Natl Acad Sci USA* 1999; **96**: 9305–09.

61 Hartmann G, Weeratna RD, Ballas ZK, et al. Delineation of a CpG phosphorothioate oligodeoxynucleotide for activating primate immune responses in vitro and in vivo. *J Immunol* 2000; **164**: 1617–24.

62 Krieg AM, Hartmann G, Yi AK. Mechanism of action of CpG DNA. *Curr Top Microbiol Immunol* 2000; **247**: 1–21.

63 Hemmi H, Takeuchi O, Kawai T, et al. A toll-like receptor recognizes bacterial DNA. *Nature* 2000; **408**: 740–45.

64 Krieg AM, Wagner H. Causing a commotion in the blood: immunotherapy progresses from bacteria to bacterial DNA. *Immunol Today* 2000; **21**: 521–26.

65 Smetsers TF, Boezeman JB, Mensink EJ. Bias in nucleotide composition of antisense oligonucleotides. *Antisense Nucleic Acid Drug Dev* 1996; **6**: 63–67.

66 Weiner GJ. CpG DNA in cancer immunotherapy. *Curr Top Microbiol Immunol* 2000; **247**: 157–70.

67 Klasa RJ, Bally MB, Ng R, Goldie JH, Gascoyne RD, Wong FM. Eradication of human non Hodgkin's lymphoma in SCID mice by BCL-2 antisense oligonucleotides combined with low dose cyclophosphamide. *Clin Canc Res* 2000; **6**: 2492–500.

68 Jahrsdörfer B, Hartmann G, Racila E, et al. CpG DNA increases immunogenicity and target-antigen expression of primary B cell non-Hodgkin lymphoma cells. *J Leuk Biol* 2001; **69**: 81–88.

69 Deveraux Q, Reed JC. IAP family proteins: suppressors of apoptosis. *Genes Dev* 1998; **13**: 239–52.

70 Tamm I, Kornblau SM, Segall H, et al. Expression and prognostic significance of IAP-family genes in human cancers and myeloid leukemias. *Clin Cancer Res* 2000; **6**: 1796–1803.

71 Deveraux Q, Takahashi R, Salvesen GS, Reed JC. X-linked IAP is a direct inhibitor of cell death proteases. *Nature* 1997; **388**: 300–03.

72 Takahashi R, Deveraux Q, Tamm I, et al. A single BIR domain of XIAP sufficient for inhibiting caspases. *J Biol Chem* 1998; **273**: 7787–90.

73 Dierlamm J, Baens M, Wlodarska I, et al. The apoptosis inhibitor gene

API2 and a novel 18q gene, MLT, are recurrently rearranged in the t(11;18)(q21;q21) associated with mucosa-associated lymphoid tissue lymphomas. *Blood* 1999; **93**: 3601–09.

74 Baens M, Maes B, Steyls A, Geboes K, De Wolf-Peeters C, Marynen P. Fusion between the apoptosis inhibitor gene API2 and a novel 18q gene MLT, rearranged in the t(11;18)(q21;q21), marks half of the gastro-intestinal MALT-type lymphomas without large cell proliferation. *Blood* 1999; **94**: 384a (abstr).

75 Ambrosini G, Adida C, Altieri DC. A novel anti-apoptosis gene, survivin, expressed in cancer and lymphoma. *Nat Med* 1997; **3**: 917–21.

76 Tamm I, Wang Y, Sausville E, et al. IAP-family protein survivin inhibits caspase activity and apoptosis induced by Fas (CD95), Bax, caspases, and anticancer drugs. *Cancer Res* 1998; **58**: 5315–20.

77 Lu CD, Altieri DC, Tanigawa N. Expression of a novel antiapoptosis gene, survivin, correlated with tumor cell apoptosis and p53 accumulation in gastric carcinomas. *Cancer Res* 1998; **58**: 1808–12.

78 Kawasaki H, Altieri DC, Lu CD, Toyoda M, Tenjo T, Tanigawa N. Inhibition of apoptosis by survivin predicts shorter survival rates in colorectal cancer. *Cancer Res* 1998; **58**: 5071–74.

79 Monzo M, Rosell R, Felip E, et al. A novel anti-apoptosis gene: Re-expression of survivin messenger RNA as a prognosis marker in non-small-cell lung cancers. *J Clin Oncol* 1999; **17**: 2100–04.

80 Sarela AI, Macadam RC, Farmery SM, Markham AF, Guillou PJ. Expression of the antiapoptosis gene, survivin, predicts death from recurrent colorectal carcinoma. *Gut* 2000; **46**: 645–50.

81 Islam A, Kageyama H, Takada N, et al. High expression of Survivin, mapped to 17q25, is significantly associated with poor prognostic factors and promotes cell survival in human neuroblastoma. *Oncogene* 2000; **19**: 617–23.

82 Tanaka K, Iwamoto S, Gon G, Nohara T, Iwamoto M, Tanigawa N. Expression of survivin and its relationship to loss of apoptosis in breast carcinomas. *Clin Cancer Res* 2000; **6**: 127–34.

83 Swana HS, Grossman D, Anthony JN, Weiss RM, Altieri DC. Tumor content of the antiapoptosis molecule survivin and recurrence of bladder cancer. *N Engl J Med* 1999; **341**: 452–53.

84 Kasof GM, Gomes BC. Livin, a novel inhibitor-of-apoptosis (IAP) family member. *J Biol Chem* 2000; **276**: 3238–46.

85 Adida C, Berrebi D, Peuchmaur M, Reyes-Mugica M, Altieri DC. Anti-apoptosis gene, survivin, and prognosis of neuroblastoma. *Lancet* 1998; **351**: 882–83.

86 Li F, Ambrosini G, Chu EY, et al. Control of apoptosis and mitotic spindle checkpoint by survivin. *Nature* 1998; **396**: 580–84.

87 Suzuki A, Hayashida M, Ito T, et al. Survivin initiates cell cycle entry by the competitive interaction with Cdk-4/p16INK4a and Cdk2/Cyclin E complex activation. *Oncogene* 2000; **19**: 3225–34.

88 Reed JC. Survivin' cell-separation anxiety. *Nat Cell Biol* 1999; **1**: 199–200.

89 Olie RA, Simoes-Wüst AP, Baumann B, et al. A novel antisense oligonucleotide targeting survivin expression induces apoptosis and sensitizes lung cancer cells to chemotherapy. *Cancer Res* 2000; **6**: 2805–09.

90 Tamm I, Höhnemann D, Dörken B. Down-regulation of survivin by antisense oligonucleotides in plasmocytoma cells leads to increased apoptosis and sensitivity to chemotherapeutic drugs. *Blood* 2000; **96**: 462a (abstr).

91 Jaattela M. Escaping cell death: survival proteins in cancer. *Exp Cell Res* 1999; **248**: 30–43.

92 Li GC, Li L, Liu Y-K, Mak JY, Chen L, Lee WMF. Thermal response of rat fibroblasts stably transfected with the human 70-kDa heat shock protein-encoding gene. *Proc Natl Acad Sci USA* 1991; **88**: 1681–85.

93 Landry J, Cretien P, Lambert H, Hickey E. Heat shock resistance conferred by expression of the human HSP27 gene in rodent cells. *J Cell Biol* 1989; **109**: 7–15.

94 Langdon SP, Rabiasz GJ, Hirst GL, et al. Expression of the heat shock protein HSP27 in human ovarian cancer. *Clin Canc Res* 1995; **1**: 1603–09.

95 Uozaki H, Horiuchi H, Ishida T, Iijima T, Imamura T, Machinami R. Overexpression of resistance-related proteins (metallothioneins, glutathione-S-transferase pi, heat shock protein 27, and lung resistance-related protein) in osteosarcoma: relationship with poor prognosis. *Cancer* 1997; **79**: 2336–44.

96 Rowley JD. The role of chromosome translocations in leukemogenesis. *Semin Hematol* 1999; **36** (suppl): 59–72.

97 Harris NL, Jaffe ES, Stein H, et al. A revised european-american classification of lymphoid neoplasms: a proposal from the international study group. *Blood* 1994; **84**: 1361–92.

98 Sharma HW, Hsiao R, Narayanan R. Telomerase as a potential molecular target to study G-quartet phosphorothioates. *Antisense Nucleic Acid Drug Dev* 1996; **6**: 3–7.

99 Summerton J. Morpholino antisense oligomers: the case for an RNase H-independent structural type. *Biochim Biophys Acta* 1999; **1489**: 141–58.

Antisense therapeutics. is it as simple as complementary base recognition?

Sudhir Agrawal and Ekambar R. Kandimalla

Antisense oligonucleotides provide a simple and efficient approach for developing target-selective drugs because they can modulate gene expression sequence-specifically. Antisense oligonucleotides have also become efficient molecular biological tools to investigate the function of any protein in the cell. As the application of antisense oligonucleotides has expanded, multiple mechanisms of oligonucleotides have been characterized that impede their routine use. Here, we discuss different mechanisms of action of oligonucleotides and the possible ways of minimizing antisense-related effects to improve their specificity.

SINCE the first report of the use of antisense oligodeoxynucleotides to inhibit *Rous sarcoma* virus gene expression[1], there has been tremendous progress in the understanding and application of antisense oligodeoxynucleotides. Simplicity, rational design, the inexpensive availability of synthetic oligodeoxynucleotides and developments in human genome sequencing have contributed to this progress. In addition, antisense technology has become an essential laboratory tool to study and understand the function of any newly discovered genes in recent years. In principle, the antisense approach should allow the design of drugs that specifically intervene with the expression of any gene whose sequence is known.

Chemical modification of the natural phosphodiester backbone is necessary to prevent its rapid degradation by ubiquitous nucleases. Of all the chemical modifications developed, **phosphorothioate oligodeoxynucleotides (PS-oligonucleotides)** are the most extensively studied analogs of the phosphodiester oligonucleotides and several are currently under evaluation for their therapeutic potential in human clinical trials. In **PS-oligonucleotides**, one of the non-bridging oxygens of the phosphate is replaced with a sulfur in order to prevent rapid degradation by nucleases (Fig. 1). In addition to nuclease resistance, **PS-oligonucleotides** possess important properties such as binding affinity to the target (mRNA), cellular uptake, aqueous solubility and the ability to activate **RNase H**, which is required for antisense activity[2,3]. As a result of these inherent favorable properties, **PS-oligonucleotides** have become the choice as the first generation of antisense molecules in hundreds of studies in cell cultures and animal models[2,3]. Recently, a **PS-oligonucleotide** targeted to human cytomegalovirus (CMV) has been approved for the treatment of CMV-induced retinitis[4]. Many other **antisense oligonucleotides** are at various stages of clinical development (Table 1).

As the number of reports of the use of **PS-oligonucleotides** in the literature increased, it became evident that the use of **PS-oligonucleotides** as antisense agents might not be as simple as initially expected[2,3,5]. The effects observed in many studies could be attributed to the antisense mechanism, but the effects observed in others could not[6,7]. These non-antisense effects could be the result of the presence of certain sequence motifs and/or secondary structures (due to self-complementarity) in the **PS-oligonucleotides** or they could be related to their polyanionic nature. These other modes of action of **PS-oligonucleotides** often overlapped with the mechanism of action and specificity of **antisense oligonucleotides**. It is now becoming evident that such defined factors can directly or indirectly influence the specificity and mechanism of action of **antisense oligonucleotides**.

In this article, the different mechanisms of action of **PS-oligonucleotides** that confuse the understanding of antisense effects are discussed. In addition, methods for the reduction or minimization of these complications by implementation and adherence to certain guidelines for the design and study of **antisense oligonucleotides** *in vitro* and *in vivo* are described. These descriptions cover not only the development of therapeutics, but also functional genomics applications, such as elucidating the biological function of any newly discovered gene by inhibiting its translation.

Sudhir Agrawal DPhil*
Senior Vice President of Discovery and Chief Scientific Officer

Ekambar R. Kandimalla PhD
Senior Research Scientist

Hybridon, 155 Fortune Boulevard, Milford, MA 01757, USA.
Tel: +1 508 482 7530
Fax: +1 508 482 7692
***e-mail: sagrawal@hybridon.com**

1357-4310/00/$ - see front matter PII: S1357-4310(99)01638-X

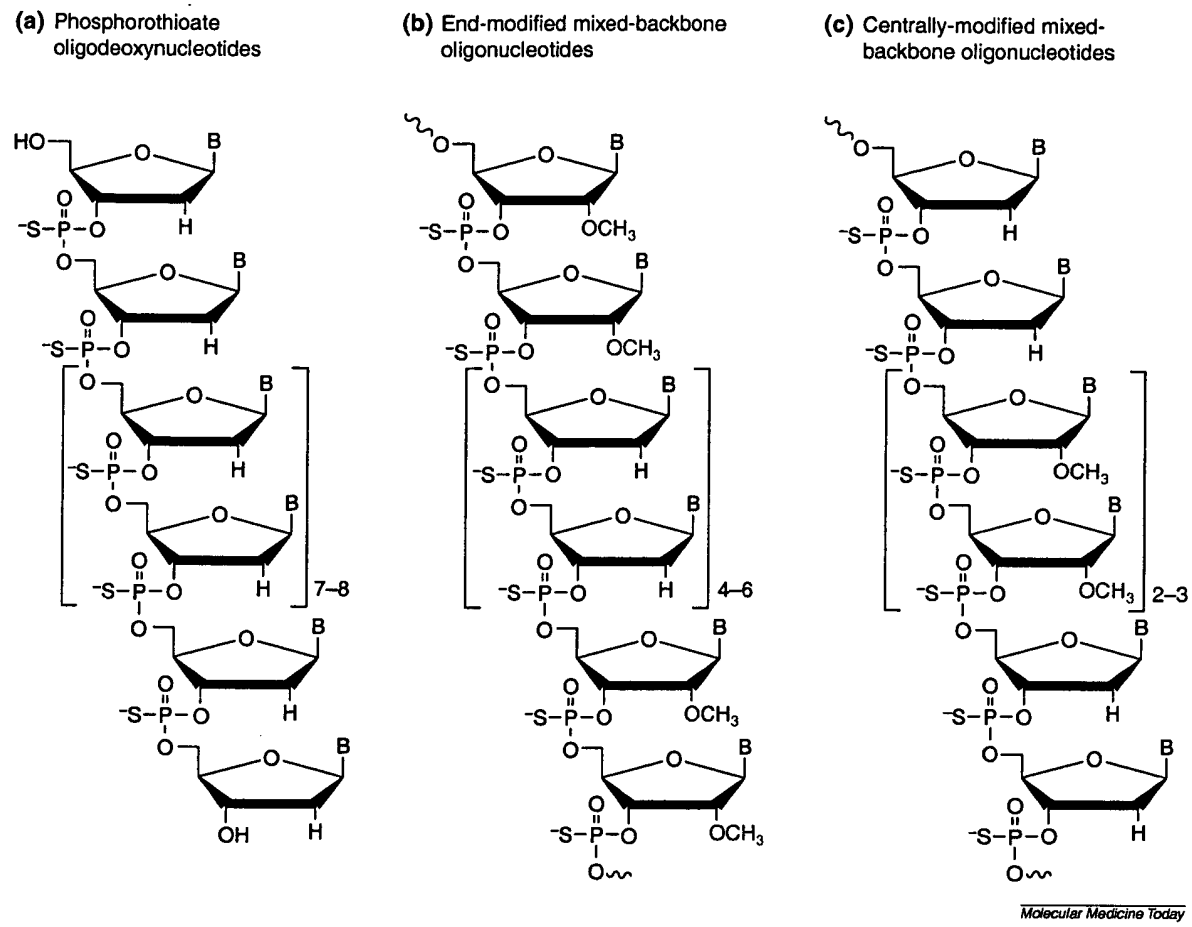

Figure 1. Structures of phosphorothioate (**a**), end-modified mixed-backbone (**b**), and centrally-modified mixed-backbone oligonucleotides (**c**). In (**b**) and (**c**) only 2′-O-methylribonucleotide modification is shown in **MBOs**. Any chemical modification that reduces polyanion-related side effects and increases antisense specificity can be used in both the end- and centrally-modified **MBOs**. The advantage of **MBOs** is that, although they retain the advantage of **PS-oligonucleotides** (**RNase H** activation), the inherent side effects can be minimized. The placement of methylphosphonate linkages (not shown in figure) at the ends reduces the overall polyanionic-related side effects, and increases the *in vivo* stability by protecting both the ends of the **PS-oligonucleotide** from digestion by nucleases. Similarly, placement of 2′-O-methylribonucleotide segments provides increased affinity to the target mRNA and *in vivo* stability. Placement of modified segments in the center provides a handle on modulating the rate of degradation, the nature of metabolites being generated *in vivo* and the elimination of those metabolites. The modification that confers higher stability against nuclease digestion provides two advantages: longer duration of action to enable less frequent dosing and the presence of fewer degradation metabolites to decrease the possible side effects from such metabolites.

Mechanisms of action of PS-oligonucleotides

Theoretically, it is very simple to design oligonucleotides to inhibit the translation of encoded proteins by the antisense mechanism. In principle, an **antisense oligonucleotide** is designed to inhibit expression of specific unwanted protein by hybridizing to the target mRNA through Watson–Crick complementary base recognition, thereby physically blocking the ribosomal machinery and/or activating endogenous **RNase H** that cleaves the mRNA at the duplex site. There are numerous examples in which **PS-oligonucleotides** of varying lengths and base compositions have been employed to inhibit the translation of cellular or foreign genes by an antisense mechanism[7–11].

A major question that remains to be answered, however, is whether the inhibition of expressed protein or the subsequent biological effects observed are the result of a *bona fide* antisense mechanism. Detailed studies of the impact of **PS-oligonucleotide** sequence on their mechanism of action and specificity clearly suggest that sequence is a critical factor for many **PS-oligonucleotides**.

CpG motifs and immunostimulation

PS-oligonucleotides containing CpG motifs have immunostimulatory activity[12–15]: they induce many cytokines, including IL-12, IL-6, IFN-γ, TNF-α and chemokines[16,17]. Their immunostimulatory properties

Table 1. Oligonucleotides in clinical trials[a]

Molecular target	Sequence[b]	Disease target	Route of delivery	Status
Oncological and hematological diseases				
bcl-2	5′-TCTCCCAGCGTGCGCCAT-3′	Prostate; non-Hodgkin's lymphoma	Systemic, sc	Phase I/IIa
bcr-abl	5′-CGCTGAAGGGCTTCTTCCTTATTGAT-3′	CML, advanced phase	*Ex vivo* purging	Pilot
	5′-CGCTGAAGGGCTTTTGAACTGTGCTT-3′	CML, blast crisis	Systemic, iv	Pilot
c-myb	5′-TATGCTGTGCCGGGGTCTTCGGGC-3′	CML, blast crisis, refractory leukemia	Systemic, iv	Phase I
		CML, chronic/accelerated phase	*Ex vivo* purging	Pilot
c-myc	5′-GCTAACGTTGAGGGGCAT-3′	Restenosis	Systemic, iv	Withdrawn
c-raf	5′-TCCCGCCTGTGACATGCATT-3′	Prostate, breast, ovarian, pancreas, colon, lung	Systemic, iv	Phase II
DNA metase	Not known	Solid tumors	Systemic, iv	Phase I
Ha-ras	5′-GGGACTCCTCGCTACTGCCT-3′	Solid tumors	Systemic, iv	Phase I
ICAM-I	5′-GCCCAAGCTGGCATCCGTCA-3′	Crohn's disease, psoriasis, rheumatoid arthritis, ulcerative colitis, tissue rejection after organ transplantation	Systemic, iv	Phase II
p53	5′-CCCTGCTCCCCCCTGGCTCC-3′	AML and myelodysplastic syndrome, refractory or relapsed	Systemic, iv	Phase I
		AML and myelodysplastic syndrome.	*Ex vivo* purging	Pilot
PKA-RIα	5′-**GCGU**GCCTCCTCAC**UGGC**-3′	Solid tumors	Systemic, iv	Phase II
PKC-α	5′-GTTCTCGCTGGTGAGTTTCA-3′	Ovarian, prostate, breast, brain, lung, colon, melanoma	Systemic, iv	Phase II
Viral diseases				
CMV	5′-GCGTTTGCTCTTCTTCTTGCG-3′	CMV-induced retinitis	Local, intravitreal	Approved
CMV	5′-**UG**GGGCTTACCTTGC**GAACA**-3′	CMV-induced retinitis	Systemic, iv	Phase II
HIV-1	5′-CTCTCGCACCCATCTCTCTCCTTCT-3′	HIV-1–AIDS	Systemic, iv	Withdrawn
HPV	5′-TTGCTTCCATCTTCCTCGTC-3′	Genital warts	Local, id	Withdrawn

[a]Abbreviations: AML, acute myeloid leukemia; CML, chronic myeloid leukemia; CMV, cytomegalovirus; HPV, human papilloma virus; ICAM, intercellular adhesion molecule; id, intradermal; iv, intravenous; metase, methyl transferase; PKA, protein kinase A; PKC, protein kinase C; RIα, regulatory subunit Iα; sc, subcutaneous.

[b]All the sequences contain phosphorothioate internucleotide linkages; plain and bold letters indicate deoxy- and 2′-O-methyl-ribonucleosides, respectively.

depend on the sequence, base composition and the position of the CpG motif in the sequence. **PS-oligonucleotides** containing CpG motifs might therefore have immunostimulatory properties in addition to the antisense function that they were designed for. For example, two 29-mers of the same base composition, except that one has a CG-motif and the other has a GC-motif, showed sequence-specific non-antisense mediated antiviral activity (Fig. 2a). Currently, **PS-oligonucleotides** containing CpG motifs are being explored as immunomodulators in antiviral, antibacterial, anticancer and anti-inflammatory therapies[18].

Is it possible that the nucleotide sequence of **PS-oligonucleotides** also has an impact on the observed side effects *in vivo*? For example, two **PS-oligonucleotides** of the same base composition but with different nucleotide motifs caused similar side effects in three different mouse models, but the severity of the side effects was sequence dependent (Fig. 2b–e). This example further indicates that two **PS-oligonucleotides** of the same length and base composition can behave differently *in vivo*. In addition, sequence independent side effects, such as complement activation and prolongation of **activated partial thromboplastin time (aPTT)**, were also observed with the **PS-oligonucleotides**. From these two examples and from other studies reported in the literature, it is clear that if a selected **antisense oligonucleotide** sequence has a CpG motif, extreme care must be taken in establishing its specificity of antisense activity.

Secondary structures interfere with the antisense mechanism

The presence of secondary structures can also interfere with antisense activity by allowing the oligonucleotides to bind to unintended protein targets. Double-stranded **PS-oligonucleotides** that contain a *cis*-transcription recognition sequence bind sequence-specifically to transcription factors competitively and interfere with transcription. This is

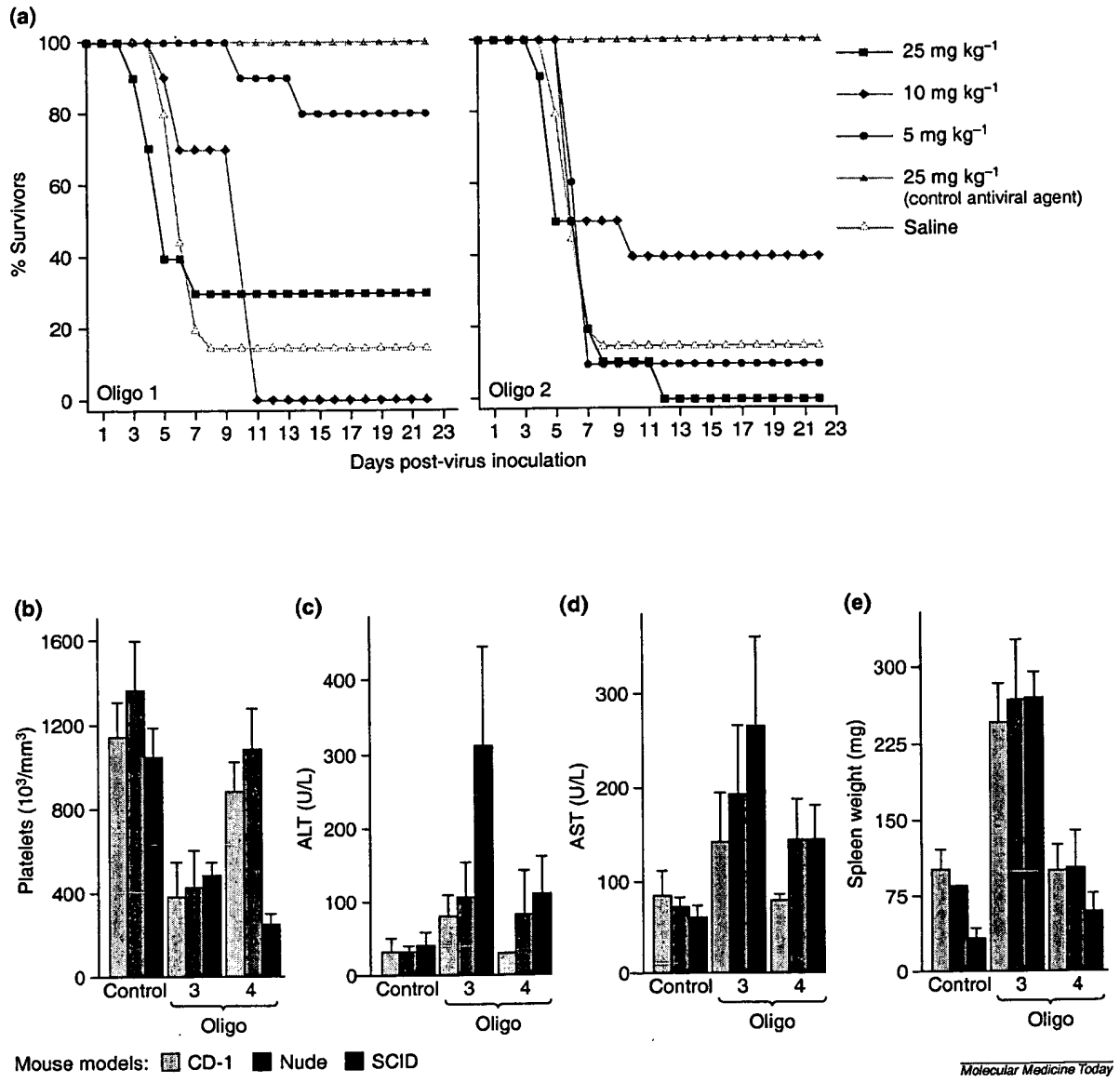

Figure 2. (a) The effect of **PS-oligonucleotides** 1 (oligo 1) (5′-CCATGACGTTCCTGATGCTTTTTGGGGG-3′) and oligo 2 (5′-TCCATGAGCTTCCTGATGCTTTTTGGGGG-3′) at 5, 10 and 25 mg kg^{-1} doses on CMV replication. A control antiviral agent, 3,5-dihydroxyphenylglycine (DHPG), was also used. Neither oligo 1 nor oligo 2 is complementary to murine-CMV RNA. The inhibition of CMV observed in this study was the result of immune stimulation rather than an antisense mechanism. At lower doses, protection of CMV-infected mice was observed with oligo 1. At higher doses, no protection was observed, probably because of hyper-stimulation of the immune system, which also resulted in increased toxicity. Analysis of serum showed an increase in IL-12 levels with oligo 1 compared to control (saline) or oligo 2 treated mice. (**b–e**) Side effects of oligo 3 (5′-TCGTCGCTGTCTCCGCTTCTTCTTGCC-3′) and oligo 4 (5′-TGCTGCCTGTCTGCCCTTCTTCTTGCC-3′) in CD-1, nude and SCID mouse models. Oligo 3 is complementary to the *rev* gene of HIV-1[13]. Oligo 3 caused significant changes in platelet count (**b**) and levels of transaminases, alanine aminotransferase (ALT) (**c**) and aspartate aminotransferase (AST) (**d**) in all three mouse models. Oligo 3 caused a greater increase in spleen enlargement (**e**) in all three mouse models than did oligo 4. In general, oligo 4 had less severe effects on the parameters studied. Examination of kidney, liver and spleen of the three mouse models for histopathology showed more pronounced reticuloendothelial cell hyperplasia with oligo 3 than oligo 4. In addition, hematopoetic cell proliferation was more pronounced in spleens of the three mouse models with oligo 3 than those with oligo 4. The side effects observed could be the result of immune-stimulatory properties of **PS-oligonucleotides** and might involve different pathways in these mouse models. Further studies are needed to characterize the mechanisms involved in inducing these side effects. It is important to note that, in several studies, nude and SCID mice are used as models to evaluate anti-tumor, antiviral or antibacterial activity. Factors responsible for side effects, directly or indirectly, might interfere with the mechanism of action of antisense or control **PS-oligonucleotides**.

generally called the '**decoy**' mechanism of inhibition and it is different from antisense action. There have been several examples of the use of oligonucleotide-derived sequences as **decoys**[19–21].

Single-stranded oligonucleotides called **aptamers** are used to inhibit specific proteins in a sequence-specific manner. Examples of **aptamer** oligonucleotides include inhibitors of thrombin and HIV-1 integrase[22,23]. It is important to note that although the sequence of a **PS-oligonucleotide** is important in exerting non-specific activity, its internucleotide linkages, due to its polyanionic nature, also show sequence-independent side effects[24,25].

Optimal design of antisense oligonucleotides

It is clear that **PS-oligonucleotides** of varying sequences, lengths and base compositions could exert biological activities by many mechanisms. It is always possible that, although a unique structure or motif is required for non-antisense mechanism, the presence of these motifs in an **antisense oligonucleotide** or its control **PS-oligonucleotides** could interfere with the mechanism of action and specificity.

Therefore, **antisense oligonucleotide** design is not as simple as probe design and several points must be considered in the design and study of **antisense oligonucleotides**. A number of lessons have been learned from the **antisense oligonucleotide** studies in the past few years, and several chemical strategies (Fig. 3) have been developed to minimize non-antisense related effects of **PS-oligonucleotides**[2,3].

If proper design precautions, suitable chemical modifications and appropriate control sequences are not selected, **PS-oligonucleotides** with specific sequence motifs or secondary structures could influence the outcome of the experimental results through non-antisense mechanisms. Adoption and application of these modifications for **antisense oligonucleotide** design would be of particular interest to those who use antisense technology for elucidating the functions of newly discovered genes.

Target site selection

The initial step in selecting an **antisense oligonucleotide** is to choose an appropriate target sequence on the mRNA molecule. Antisense

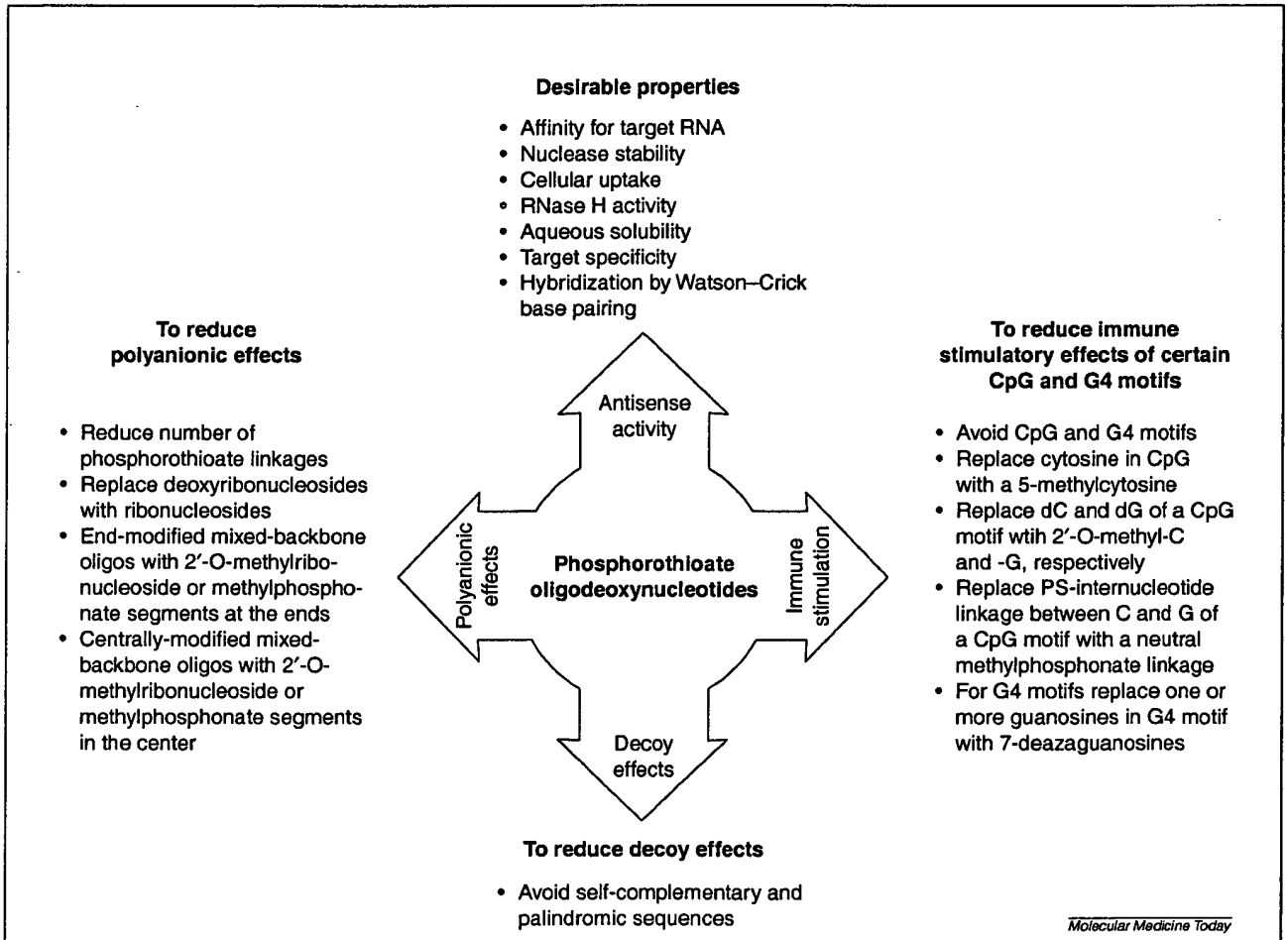

Figure 3. Factors that affect the specificity of antisense oligonucleotides and the chemical strategies that have been developed to reduce these non-antisense-related effects in order to improve specificity, pharmacokinetic and safety profiles.

Glossary

Activated partial thromboplastin time (aPTT) – An *in vitro* measurement to determine the prolongation of blood coagulation by coagulation inhibitors.

Antisense oligonucleotide – A synthetic oligonucleotide that is complementary to a portion of the targeted mRNA. It binds to the mRNA and arrests translation by physical blockade of ribosomal machinery and/or by activation of endogenous **RNase H**.

Aptamer – A single-stranded oligonucleotide that binds sequence-specifically to a protein and inhibits its function. An **aptamer** might adopt a specific structure in order to bind to the protein.

Decoy – A linear or hairpin duplex oligonucleotide that captures a transcription factor by competitive sequence-specific binding and inhibits transcription of a specific gene.

Hyper-structure-forming sequences – The G-rich sequences (containing three or more guanosines in a row) that form Hoogsteen hydrogen bonded structures involving guanines in four or more strands.

Mixed-backbone oligonucleotides (MBOs) – Oligonucleotides that are synthesized with more than one modification in order to improve biophysical, biochemical, pharmacokinetic or safety profiles.

Phosphorothioate oligodeoxynucleotides (PS-oligonucleotides) – Oligodeoxynucleotides in which one of the non-bridging oxygens on the phosphate of the natural phosphodiester backbone is replaced with a **sulfur to make them nuclease resistant.**

RNase H – A ribonuclease that specifically recognizes an RNA–DNA heteroduplex and cleaves the RNA strand of the heteroduplex.

5′- and 3′-untranslated regions (UTRs) – The nucleotide sequences that are present before a start codon and after a termination codon, respectively, in an mRNA and are not translated into protein.

technology has been hampered to some extent by limited knowledge as to the base-pairing accessibility of mRNA target sites *in vivo*. Although a number of models that predict RNA folding are available, their usefulness for predicting the most plausible *in vivo* RNA structure is limited[26]. Alternatively, *in vitro* methods can be used to test the acces--sibility of mRNA sites by oligonucleotides, but this has also met with limited success[27]. It is considered preferable, therefore, to screen a number of oligonucleotides that encompass different regions on RNA to identify a set of optimal target sites, including the **5′- and 3′-untranslated regions (UTRs)**, initiation codon site, coding region and intron–exon junctions. Oligonucleotides that have been targeted to the translation initiation codon region of mRNA are generally believed to be more potent than those targeted to other regions. Our experience, however, shows that it is difficult to find a 20-nucleotide site that includes the initiation codon and satisfies all the criteria discussed in this review for optimal **antisense oligonucleotide** design.

It has recently been shown that sites containing GGGA sequence motifs on mRNA are more accessible to **antisense oligonucleotides** than are other sites[28]. Although it is interesting, it is not possible to generalize this concept for targets other than those examined until further evidence emerges with a number of other targets.

Choice of oligonucleotide sequences

The affinity of an oligonucleotide for its target RNA varies significantly depending on base composition and sequence[29,30]. Therefore, the antisense activity of a selected oligonucleotide is influenced both by its base composition and by its sequence. Oligonucleotides that contain certain sequence motifs, such as CpG (Refs 12,14,15) and GGGG (**hyper-structure-forming sequences**)[31,32], induce cell proliferation and immune responses. G-rich oligonucleotides also have different cellular uptake, tissue distribution, pharmacokinetics and *in vivo* disposition from those oligonucleotides that do not contain four or more adjacent guanosines[31]. Antisense **PS-oligonucleotides** containing CpG and G-rich motifs increase the possibility of exhibiting activities by non-antisense mechanisms. Hence, it is appropriate to avoid sequences containing these motifs for antisense uses.

If an **antisense oligonucleotide** possesses self-complementarity or a palindromic sequence, it can form stable secondary structures, such as short linear duplexes or hairpins (Fig. 4). In such cases, secondary structure formation competes for binding to the target mRNA. In addition, these secondary structures can serve as **decoys** by binding to cellular factors, thereby inhibiting or inducing the functions of non-targeted genes, which could directly or indirectly alter the function of the gene being studied. A number of software packages are currently available for screening oligonucleotides for the formation of secondary structures involving traditional Watson–Crick base pairing rules. However, these packages are not designed to predict non-traditional structures, such as quadruplexes involving G-rich motifs, GA base pairs, parallel-stranded structures and the possible structures formed by chemically modified nucleotides. In these cases, non-denaturing gel electrophoresis or UV thermal denaturation methods can be used to examine the possible secondary structure formation by **antisense oligonucleotides** alone (Fig. 4).

Choice of chemical modification

The sequence-unrelated side effects associated with **PS-oligonucleotides**[32,33] have led to attempts to improve specificity and thereby reduce side effects. The PS-backbone, in association with deoxyribonucleotides, is responsible for polyanion-related effects, such as prolongation of **aPTT** and complement activation[34]. PS-oligoribonucleotides, PS-2′-O-methyl-oligoribonucleotides and PS-2′-5′-linked-oligoribonucleotides (see Fig. 5 for chemical structures) have lower or negligible effects on prolongation of **aPTT** and complement activation[34].

Methylphosphonate oligonucleotides show less severe polyanion-related effects because they have reduced negative charge[15,33,35]. Unfortunately, methylphosphonates and PS-oligoribonucleotides do not activate **RNase H** upon binding to the RNA target, an important property critical for the antisense mechanism. In addition, aqueous solubility of methylphosphonate oligonucleotides containing more than 12 nucleotides becomes a limiting factor. We have therefore attempted to use a combination of these modifications with **PS-oligonucleotides** to develop **antisense oligonucleotides** that have all the required properties for antisense activity while minimizing the polyanion-related effects[3]. These oligonucleotides are referred to as **mixed-backbone oligonucleotides (MBOs)** (Fig. 1).

MBOs containing segments of **PS-oligonucleotide** and other modified oligonucleotide segments have emerged as second-generation **antisense oligonucleotides**[2,3,36–38]. A number of modifications, combined with the **PS-oligonucleotide** backbone, have been studied[3], but two modifications – PS-2′-O-methyl(alkyl)ribonucleotides and methylphosphonate oligonucleotides – stand out because they reduce

several polyanion- and non-antisense-related side effects of **PS-oligonucleotides**[2,3]. Both modifications reduce protein binding and non-antisense effects related to the polyanionic nature of the **PS-oligonucleotides**[33,37–39]. These modifications can be incorporated at the 3′-end or at both the 3′- and the 5′-ends of a **PS-oligonucleotide** to produce 'end-modified **MBOs**', or incorporated in the center of the **PS-oligonucleotide** to produce 'centrally modified **MBOs**'.

End-modified **MBOs** have shown improved specificity, biological activity, *in vivo* stability, pharmacokinetic and safety profiles over **PS-oligonucleotides**[35–42]. Importantly, end-modified **MBOs** permit oral and colorectal administration of **antisense oligonucleotides** as a result of their increased *in vivo* metabolic stability[43]. In addition, end-modified **MBOs** have lower polyanion-related effects, such as complement activation and prolongation of **aPTT**, than do **PS-oligonucleotides**[33].

Centrally-modified **MBOs** contain a modified oligonucleotide segment placed in the center of a **PS-oligonucleotide**[38]. These **MBOs** show increased binding affinity to the target, increased **RNase H** activation, and consequently rapid degradation of RNA compared with end-modified **MBOs**. Centrally modified **MBOs** permit reduction of contiguous **PS-oligonucleotide** length, thereby determining their length-dependent polyanionic effects. These **MBOs** show improved pharmacokinetic and safety profiles and maintain biological activity similar to that of **PS-oligonucleotides**[38].

The purity of **PS-oligonucleotides** also affects their biological activity[44]. As a result of recent developments in synthetic, purification and analytical methodologies, it is now possible to obtain consistently pure **PS-oligonucleotides**. However, it is important for the laboratories that obtain oligonucleotides from commercial suppliers to check purity levels constantly as these vary from vendor to vendor and from batch to batch.

Avoiding CpG motifs in an antisense sequence reduces non-antisense-related activity considerably. However, if a CpG motif is absolutely necessary for antisense activity, the non-antisense-related effects of CpG motifs can be reduced by several chemical modifications (Fig. 3). These modifications include: (1) replacement of the cytosine base in the CpG motif with a 5-methylcytosine base; (2) replacement of the phosphorothioate linkage between C and G of the CpG motif with a methylphosphonate linkage; and (3) replacement of the d(CpG) motif with 2′-O-methylribonucleosides. We have studied a number of **PS-oligonucleotides** that contain CpG motifs with and without the above modifications in mice and rats and have found them to have significantly reduced side effects[15,40,41].

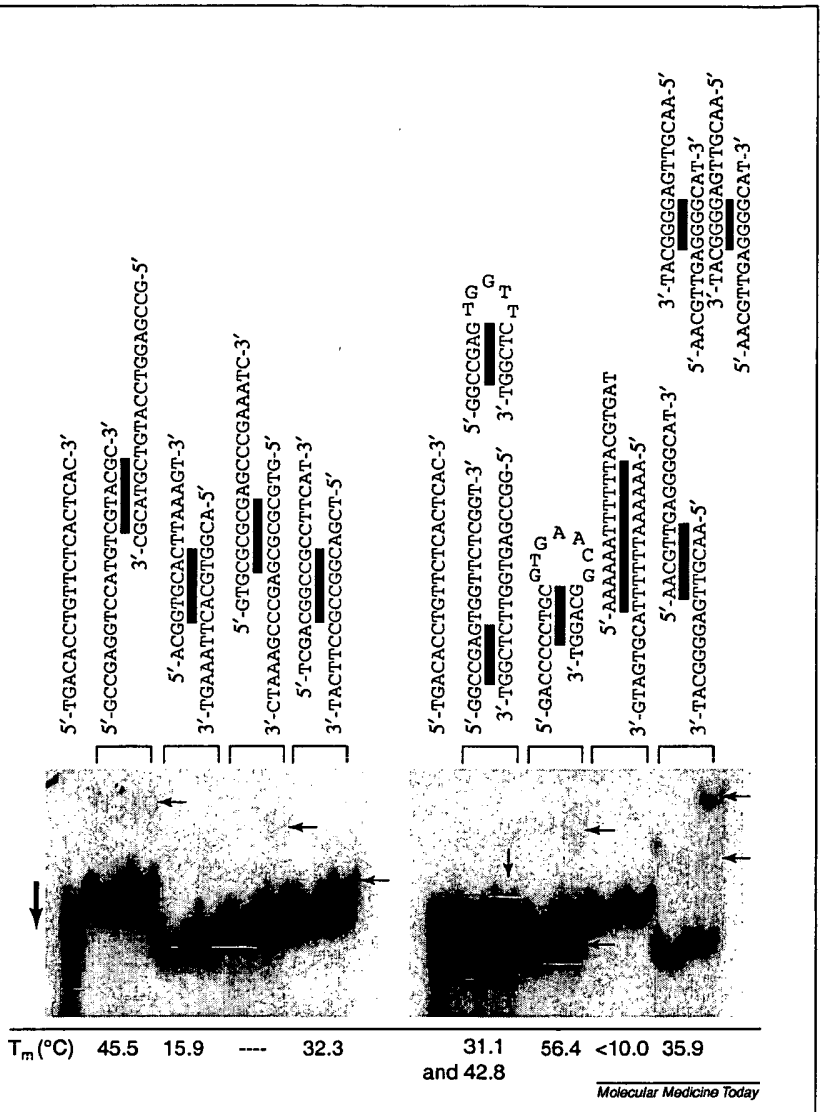

Figure 4. An autoradiogram showing structures formed by a number of **PS-oligonucleotide** sequences that have been reported in the recent literature. Sequences and possible structures formed by these oligonucleotides are shown on top of the gel. For each oligonucleotide there are two lanes except for the oligonucleotide shown as single strand (first lane in both the gels). These left and right lanes represent samples loaded with formamide after heating to 95°C and snap-cooling or loaded with glycerol buffer without heating, respectively. Bands indicated with an arrow are the result of secondary structure formation by these **PS-oligonucleotides**. The thick arrow beside the gel photograph indicates the direction of gel mobility. The UV thermal melting temperature (T_m) of each **PS-oligonucleotide** (measured in 100 mM NaCl, 10 mM sodium phosphate buffer pH 7.4 at a strand concentration of 4 μM in 1 ml) is shown below the autoradiogram. The observation of two T_m values for one oligonucleotide revealed the presence of more than one structure (although this was not distinguishable on the gel). An oligonucleotide that revealed no T_m value indicated the absence of secondary structure formation.

As for G-rich motifs, no known chemical modification (except replacement of Gs in the G-rich site with 7-deazaguanines) prevents hyperstructure formation. It is appropriate, therefore, to avoid sequences that

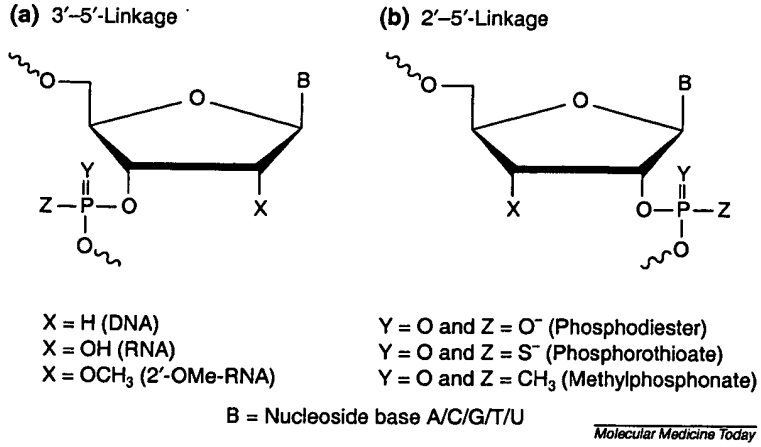

Figure 5. Structures elucidating (a) 3′–5′- and (b) 2′–5′-linkages and some of the chemical modifications discussed in this review.

contain four or more Gs (sometimes three) in a stretch. Hyper-structure formation by oligonucleotides that contain three or four adjacent Gs can be ascertained by examining them on non-denaturing polyacrylamide gels under physiological conditions because hyper-structure formation is also dependent on the flanking sequences (Fig. 4). In addition, synthesis and purification of G-rich oligonucleotides is complex and is not reproducible[45].

Minimization of protein binding and other competing factors

PS-oligonucleotides bind to proteins through sequence-specific, structure-specific and non-specific interactions. As a result of the polyanionic nature of the internucleotide phosphorothioate backbone, **PS-oligonucleotides** interact non-specifically with a number of proteins and enzymes *in vitro* in a sequence-independent, but length-dependent, manner[39,46–48]. **PS-oligonucleotides** inhibit the activities of several enzymes, including DNA polymerases, growth factors, protein kinase C, HIV-gp120, recombinant soluble CD4, reverse transcriptase, **RNase H** and RNase L in a dose-dependent fashion in *in vitro* studies, but at much higher concentrations than those required for antisense activity[39,46,47]. However, the *in vivo* biological relevance of inhibition of these enzymes has not yet been established. Note that these effects are mechanistically distinct from **decoy** and **aptamer** effects.

In addition, **PS-oligonucleotides** bind to a number of plasma/serum-proteins, notably albumin[33,39,48]. The binding affinity of **PS-oligonucleotides** for plasma/serum proteins has been shown to be in the order fibrinogen>γ-globulins>albumin[33,34,39]. As shown previously, **PS-oligonucleotides** demonstrate prolongation of **aPTT** and complement activation in a dose- and length-dependent, but sequence-independent, manner *in vivo* and *in vitro*[32–34,37,38,45,49]. It has recently been shown that **PS-oligonucleotides** inhibit the intrinsic tenase complex (factor IXa_β, factor VIIIa, phospholipid and calcium) in the blood coagulation system[50]. *In vivo* and *in vitro* studies have demonstrated that small molecules, such as aspirin, compete effectively for serum-protein binding and alter pharmacokinetic and tissue distribution profiles of **PS-oligonucleotides**[39,48]. These polyanion-related and protein binding-related side effects can be significantly minimized by maintaining low plasma concentrations by slow intravenous infusion as currently employed in clinical trials[32], by using formulations[33], or by incorporating 2′-O-alkyl(methyl)ribonucleosides or methylphosphonate linkages into **PS-oligonucleotides** as in the case of **MBOs** (Refs 33–35,37,38) (Fig. 3).

Control sequences

Although the antisense field has progressed to clinical trials, there is no consensus on what kind of controls to include in antisense experiments, mainly because of the limited knowledge of the biological effects of possible nucleotide motifs. So far, only the biological consequences of certain motifs, such as CpG and G4s, are known. The use of a variety of control oligonucleotides has been reported in different studies ranging from oligonucleotides containing 1–7 mismatches, to scrambled, sense or random sequences. When control oligonucleotides are designed, some of the motifs that cause adverse or different biological effects can be unknowingly deleted or introduced, resulting in equal or higher activity than the **antisense oligonucleotide**, which can lead to confusing results. Therefore, it might be appropriate to use more than one control oligonucleotide to establish the antisense activity depending on the sequence.

Cellular uptake facilitators for in vitro *studies*

Discussion of cellular uptake facilitators might not be relevant for *in vivo* studies, as no such agents are currently used *in vivo*, but it is certainly important in the initial screening of antisense **PS-oligonucleotides** in cell cultures and their application for functional genomics. The cellular uptake of negatively charged oligonucleotides is one of

The outstanding questions

- What is the impact of the nucleotide base composition of oligonucleotides on their antisense activity and their mechanism of action?
- What are the biological roles of various nucleotide motifs present in oligonucleotides?
- Is it possible to conclusively rule out the possibility that no mechanism other than a *bona fide* antisense mechanism is responsible for the observed biological effects of **antisense oligonucleotides** *in vivo*?

How are oligonucleotides taken up by cells, transported and processed by various tissues?

What is the mechanism of intestinal absorption of oligonucleotides and how can the oral bioavailability of oligonucleotides be improved?

the important factors in determining the efficacy of **antisense oligonucleotides**; the mechanism of their uptake is not yet understood in detail. *In vitro*, cellular uptake of **antisense oligonucleotides** depends on many factors, including cell type, kinetics of uptake, tissue culture conditions, and chemical nature, length and sequence of the oligonucleotide. Any one of these factors can influence the biological activity of an **antisense oligonucleotide**. It is therefore appropriate to study each **antisense oligonucleotide** in its own context, and relevant cell line, without generalizing the results for every oligonucleotide.

Cationic macromolecules such as lipofectin are used to enhance the uptake of **antisense oligonucleotides** *in vitro*. These polycations form complexes with negatively charged oligonucleotides and facilitate their internalization. Complex formation between oligonucleotides and cationic lipid agents might also provide stability against nucleases in cell cultures. The use of cell uptake facilitators could influence the outcome of the biological activity depending on the nature of the polycation used.

Concluding remarks

Many questions about the effects of **antisense oligonucleotide** sequence, secondary structures, cellular uptake, metabolism, excretion, tissue distribution, side effects and mechanism of action have been answered to a large extent, if not completely, in the past few years. As the antisense field progresses and the critical chemical and mechanistic issues of antisense effects are distinguished from those of non-antisense effects, it is becoming clear that **antisense oligonucleotide** therapeutics can in fact be as simple as complementary base recognition, but only if proper design precautions and controls are used. A number of chemical modifications have been developed and tested for antisense activity. Although a first generation **PS-oligonucleotide** has been approved for treating CMV-induced retinitis, a combination of modifications is clearly needed to fine-tune the physicochemical and biochemical properties of **antisense oligonucleotides** to make them effective drugs for multiple applications. **MBOs** have become the choice for second-generation **antisense oligonucleotides**, and several are now being tested for their potential in human clinical trials. In addition, the oral bioavailability of **MBOs** might allow these drugs to be administered in pill form in the near future[43]. The knowledge gained about the effects of antisense **PS-oligonucleotides** and their chemical modifications in the past few years is valuable for the development of antisense drugs in the future. Nonetheless, as is always the case, caution must be exerted in experimental design and interpretation of antisense results until all the critical aspects of **antisense oligonucleotides** are explored beyond reasonable doubt.

Acknowledgments. The authors thank Mrs Allyson Roskey for excellent technical assistance in contributing Figure 4, Dr Robert Sidwell (Utah State University) for performing CMV studies, and Dr David Serota (Southern Research Institute) for performing toxicology studies.

References

1 Zamecnik, P.C. and Stephenson, M. (1978) Inhibition of *Rous sarcoma* virus replication and cell transformation by a specific oligodeoxynucleotide. *Proc. Natl. Acad. Sci. U. S. A.* 75, 280–284

2 Agrawal, S. and Zhao, Q. (1998) Antisense therapeutics. *Curr. Opin. Chem. Biol.* 2, 519–528

3 Agrawal, S. and Kandimalla, E.R. (1999) Medicinal chemistry of antisense oligonucleotides. In *Antisense Technology in the Central Nervous System* (Leslie, R. *et al.*, eds), pp. 108–136, Oxford University Press

4 Crooke, S.T. (1998) Vitravene – another piece in the mosaic. *Antisense Nucleic Acid Drug Dev.* 8, vii–viii

5 Stein, C.A. (1999) Keeping the biotechnology of antisense in context. *Nat. Biotechnol.* 17, 209

6 McIntyre, K.W. *et al.* (1993) A sense phosphorothioate oligonucleotide directed to the initiation codon of transcription factor NF-κB p65 causes sequence specific immune stimulation. *Antisense Res. Dev.* 3, 309–322

7 Chen, L. *et al.* (1998) Synergistic activation of p53 by inhibition of *MDM2* expression and DNA damage. *Proc. Natl. Acad. Sci. U. S. A.* 95, 195–200

8 Chen, L. *et al.* (1999) Ubiquitous induction of p53 in tumor cells by antisense inhibition of *MDM2* expression. *Mol. Med.* 5, 21–34

9 McKay, R.A. *et al.* (1999) Characterization of a potent and specific class of antisense oligonucleotide inhibitor of human protein kinase C-alpha expression. *J. Biol. Chem.* 274, 1715–1722

10 Kita, K. *et al.* (1999) Growth inhibition of human pancreatic cancer cell lines by anti-sense oligonucleotides specific to mutated K-ras genes. *Int. J. Cancer* 80, 553–558

11 Minkoff, R. *et al.* (1999) Antisense oligonucleotide blockade of connexin expression during embryonic bone formation: evidence of functional compensation within a multigene family. *Dev. Genet.* 24, 43–56

12 Kuramoto, E. *et al.* (1992) Oligonucleotide sequences required for natural killer cell activation. *Jpn. J. Cancer Res.* 83, 1128–1131

13 Branda, R.F. *et al.* (1993) Immune stimulation by an antisense oligomer complementary to the *rev* gene of HIV-1. *Biochem. Pharmacol.* 45, 2037–2043

14 Kreig, A.M. *et al.* (1995) CpG motifs in bacterial DNA trigger direct B-cell activation. *Nature* 374, 546–549

15 Zhao, Q. *et al.* (1996) Effect of different chemically modified oligodeoxynucleotides on immune stimulation. *Biochem. Pharmacol.* 51, 173–182

16 Klinman, D.M. *et al.* (1996) CpG motifs present in bacteria DNA rapidly induce lymphocytes to secrete interleukin 6, interleukin 12, and interferon gamma. *Proc. Natl. Acad. Sci. U. S. A.* 93, 2879–2883

17 Zhao, Q. *et al.* (1997) Pattern and kinetics of cytokine production following administration of phosphorothioate oligonucleotides in mice. *Antisense Nucleic Acid Drug Dev.* 79, 495–502

18 Krieg, A.M. (1998) Leukocyte stimulation by oligodeoxynucleotides. In *Applied Antisense Oligonucleotide Technology* (Stein, C.A. and Krieg, A.M., eds), pp. 431–448, Wiley–Liss, New York

19 Park, Y.G. *et al.* (1999) Dual blockade of cyclic AMP response element- (CRE) and AP-1-directed transcription by CRE-transcription factor decoy oligonucleotide. Gene-specific inhibition of tumor growth. *J. Biol. Chem.* 274, 1573–1580

20 Sharma, N.W. *et al.* (1996) Transcription factor decoy approach to decipher the role of NF-kappa B in oncogenesis. *Anticancer Res.* 16, 61–69

21 Morishita, R. *et al.* (1998) Application of transcription factor 'decoy' strategy as means of gene therapy and study of gene expression in cardiovascular disease. *Circ. Res.* 82, 1023–1028

22 Bock, L.C. *et al.* (1992) Selection of single-stranded DNA molecules that bind and inhibit human thrombin. *Nature* 355, 564–566

23 Rando, R.F. and Hogan, M.E. (1998) Biological activity of guanosine quartet-forming oligonucleotides. In *Applied Antisense Oligonucleotide Technology* (Stein, C.A. and Krieg, A.M., eds), pp. 335–352, Wiley–Liss, New York

24 Kanagaratnam, R. *et al.* (1998) Malaria merozoite surface protein antisense oligodeoxynucleotides lack antisense activity but function as polyanions to inhibit red cell invasion. *Int. J. Biochem. Cell Biol.* 30, 979–985

25 Hartmann, G. *et al.* (1996) Oligodeoxynucleotides enhance lipopolysaccharide-stimulated synthesis of tumor necrosis factor: dependence on phosphorothioate modification and reversal by heparin. *Mol. Med.* 2, 429–438

26 Patzel, V. and Sczakiel, G. (1998) Theoretical design of antisense RNA structures substantially improves annealing kinetics and efficacy in human cells. *Nat. Biotechnol.* 16, 64–68

27 Matveeva, O. *et al.* (1998) Prediction of antisense oligonucleotide efficacy by *in vitro* methods. *Nat. Biotechnol.* 16, 1374–1375

28 Tu, G-C. *et al.* (1998) Tetranucleotide GGGA motif in primary RNA transcripts. Novel target site for antisense design. *J. Biol. Chem.* 273, 25125–25131

29 Kandimalla, E.R. *et al.* (1997) Single-stranded DNA and RNA targeted triplex-formation: UV, CD and molecular modeling studies of foldback triplexes containing different RNA, 2′-OMe-RNA and DNA strand combinations. *J. Biomol. Struct. Dyn.* 14, 715–726

30 Freier, S.M. and Altmann, K.H. (1997) The ups and downs of nucleic acid duplex stability: structure-stability studies on chemically-modified DNA:RNA duplexes. *Nucleic Acids Res.* 25, 4429–4443

31 Agrawal, S. *et al.* (1997) *In vivo* pharmacokinetics of phosphorothioate oligonucleotides containing contiguous guanosines. *Antisense Nucleic Acid Drug Dev.* 7, 245–249

32 Galbraith, W.M. *et al.* (1994) Complement activation and hemodynamic changes following intravenous administration of phosphorothioate oligonucleotides in the monkey. *Antisense Res. Dev.* 3, 201–206

33 Shaw, D.R. *et al.* (1997) Effects of synthetic oligonucleotides on human complement and coagulation. *Biochem. Pharmacol.* 53, 1123–1132

34 Kandimalla, E.R. *et al.* (1998) Effects of phosphorothioate oligodeoxyribonucleotide and oligoribonucleotides on human complement and coagulation. *Bioorg. Med. Chem. Lett.* 18, 2103–2108

35 Agrawal, S. *et al.* (1997) Mixed-backbone oligonucleotides containing phosphorothioate and methylphosphonate linkages as second-generation antisense oligonucleotides. *Nucleosides Nucleotides* 16, 927–936

36 Zhang, R. *et al.* (1995) *In vivo* stability, disposition and metabolism of a 'hybrid' oligonucleotide phosphorothioate in rats. *Biochem. Pharmacol.* 50, 545–556

37 Altmann, K-H. *et al.* (1996) Second generation of antisense oligonucleotides: from nuclease resistance to biological efficacy in animals. *Chimia* 50, 168–176

38 Agrawal, S. *et al.* (1997) Mixed-backbone oligonucleotides as second generation antisense oligonucleotides: *in vitro* and *in vivo* studies. *Proc. Natl. Acad. Sci. U. S. A.* 94, 2620–2625

39 Agrawal, S. *et al.* (1998) Effect of aspirin on protein binding and tissue disposition of oligonucleotide phosphorothioate in rats. *J. Drug Targeting* 5, 303–312

40 Agrawal, S. *et al.* (1997) Toxicological effects of an oligodeoxy-nucleotide phosphorothioate and its analogs following intravenous administration in rats. *Antisense Nucleic Acid Drug Dev.* 7, 575–584

41 Agrawal, S. and Zhao, Q. (1998) Mixed backbone oligonucleotides: improvement in oligonucleotide-induced toxicity *in vivo*. *Antisense Nucleic Acid Drug Dev.* 8, 135–139

42 Zhang, R. *et al.* (1996) Pharmacokinetics and tissue disposition of a chimeric oligodeoxynucleoside phosphorothioate in rats after intravenous administration. *J. Pharmacol. Exp. Ther.* 278, 971–979

43 Agrawal, S. *et al.* (1995) Absorption, tissue distribution and *in vivo* stability in rats of a hybrid antisense oligonucleotide following oral administration. *Biochem. Pharmacol.* 50, 571–576

44 Eckstein, F. *et al.* (1996) On the quality control of antisense oligonucleotides. *Antisense Nucleic Acid Drug Dev.* 6, 149

45 Agrawal, S. *et al.* (1996) Effect of G-rich sequences on the synthesis, purification, binding, cell uptake, and hemolytic activity of oligonucleotides. *Bioorg. Med. Chem. Lett.* 6, 2219–2224

46 Gao, W-Y. *et al.* (1992) Phosphorothioate oligonucleotides are inhibitors of human DNA polymerases and RNase H: implications for antisense technology. *Mol. Pharmacol.* 41, 223–229

47 Guvakova, M.A. *et al.* (1995) Phosphorothioate oligodeoxynucleotides bind to basic fibroblast growth factor, inhibit its binding to cell surface receptors, and remove it from low affinity binding sites on extracellular matrix. *J. Biol. Chem.* 270, 2620–2627

48 Srinivasan, S.K. *et al.* (1995) Characterization of binding sites, extent of binding, and drug interactions of oligonucleotides with albumin. *Antisense Res. Dev.* 5, 131–139

49 Wallace, T.L. *et al.* (1996) Single-dose hemodynamic toxicity and pharmacokinetics of a partial phosphorothioate anti-HIV oligonucleotide (AR177) after intravenous infusion to cynomolgus monkeys. *J. Pharmacol. Exp. Ther.* 278, 1306–1312

50 Sheehan, J.P. and Lan, H-C. (1998) Phosphorothioate oligonucleotides inhibit the intrinsic tenase complex. *Blood* 92, 1617–1625

ELSEVIER

Molecular Brain Research 90 (2001) 17–25

MOLECULAR BRAIN RESEARCH

www.elsevier.com/locate/bres

Research report

In vivo control of NMDA receptor transcript level in motoneurons by viral transduction of a short antisense gene

Alan A. Finegold[1], Federico M. Perez, Michael J. Iadarola*

Pain and Neurosensory Mechanisms Branch, NIH-NIDCR, Bldg 49, Rm 1A11, 49 Convent Dr. MSC 4410, Bethesda, MD 20892, USA

Accepted 13 February 2001

Abstract

Glutamate receptors play critical roles in normal and pathological processes. We developed an antisense gene delivery strategy to modulate the NMDA type of glutamate receptor. Using transient transfection in vitro and viral mediated gene transfer in vitro and in vivo, the effect of expression of an antisense gene fragment (60 bp) of the NR1 subunit was tested. Immunoblot analysis showed an antisense-concentration-dependent reduction in the NR1 subunit upon transient co-transfection of a plasmid expressing a sense NR1 gene and a plasmid expressing the antisense fragment into COS-7 cells. After recombination into an adenoviral vector, this antisense fragment reduced the amount of endogenous NR1 protein in PC12 cells. Finally, direct intraparenchymal injection of the viral vector into rat spinal cord resulted in diminished NR1 in motor neurons. Our results demonstrate the efficacy of this approach, which combines antisense with viral gene delivery to control the expression of specific genes in vivo. This approach may also be useful in reducing excitatory neurotransmission in vivo, with implications for the treatment of spinal disorders such as amyotrophic lateral sclerosis or chronic pain.

Theme: Neurotransmitters, modulators, transporters and receptors

Topic: Excitatory amino acid receptors, structure, function, expression

Keywords: NR1 subunit; Gene therapy; Adenovirus; Motor neuron; Excitotoxicity; Excitatory amino acid; Spinal muscular atrophy; Neurodegenerative disorder

1. Introduction

Glutamate is a major excitatory neurotransmitter in the central nervous system [29] and many attempts have been made to regulate its actions through pharmacological manipulation of its receptors. The NMDA type of glutamate receptor is composed of NR1 and NR2 subunits. The NR1 subunit is essential for ionotropic action [19]. Experiments with gene-targeted mice lacking functional NMDA receptors to reveal the functions of the NR1 subunit are mostly uninformative since they are embryonic lethal events, but experiments with NR2-subunit-null mice implicate these channels in neurotoxicity following ischemia [20], regulation of synaptic plasticity, learning, and memory [25]. The importance of the NMDA receptor in neural activity suggests the NMDA receptor as a target for small molecule therapeutics. However, NMDA receptor antagonists have a wide variety of side effects when delivered systemically [11]. An alternative approach is localized delivery of nucleic acids to alter expression of specific subunits of the receptor. Administration of antisense oligodeoxynucleotides (asODNs) represents one way to modify expression of endogenous genes [18,28]. asODNs directed against NR1 influence seizure threshold [32], motor function, and long-term potentiation. Other experiments using intrathecal administration of asODN directed against another type of glutamate receptor, mGluR1, reported reduced nociceptive sensitivity [31].

A second way to administer antisense nucleic acids is by viral-mediated gene delivery [6], which takes advantage of

*Corresponding author. Tel.: +1-301-496-2758; fax: +1-301-402-0667.

E-mail address: miadarola@dir.nidcr.nih.gov (M.J. Iadarola).

[1]Current address: Receptor Biology Inc., a Perkin Elmer NEN Life Science Company, 10000 Virginia Manor Road, Suite 360, Beltsville, MD 20705, USA. Tel.: +1-301-210-4700 (x14); fax: +1-301-210-6266, alan.finegold@perkinelmer.com

0169-328X/01/$ – see front matter
PII: S0169-328X(01)00062-6

viral cellular targeting to localize the effect by expressing the antisense molecule as an RNA species inside cells of interest. An adenoviral vector expressing a full-length antisense NR1 gene has been reported to reduce the excitability of hippocampal neurons [14]. Shafron et al. [23] showed reduced binding of a NMDA receptor-specific drug (MK801) in cultured neurons after treatment with an adeno-associated virus expressing an antisense NR1 gene. The previous viral studies used antisense transcripts of the full length NR1 message and functional assessments of the protein loss. In the present study, we show that a short antisense gene, together with in vivo viral-directed gene transfer, allows control of native NR1 gene expression, which results in reduced NR1 protein level within virally transduced cells as ascertained by immunocytochemistry. We generated several antibodies that react with different splice variants of the NR1 gene. By using multiple antibodies at various in vitro steps of the experiments we show that the decrease is independent of alternative splicing of the NR1 transcript (reviewed in [33]). The antibody directed against the N1 cassette (exon 5), strongly stains the large perikarya of motor neurons in spinal cord ventral horn. This permitted us to use motor neurons in combination with the adenovirus as an in vivo test of the effectiveness of a short antisense NR1 minigene because previous studies with microinjection of Ad-lacZ into the spinal cord resulted in high levels of expression in motor neurons [17]. Thus, our experimental approach was to define the ability of a virally delivered short antisense gene to reduce NMDA receptors in motor neurons of the spinal cord, with the eventual goal of finding a method for stable, long-term manipulation of excitatory neurotransmission in vivo.

2. Materials and methods

2.1. Construction of antisense NR1 plasmid and adenoviral vectors

Oligodeoxynucleotides antisense 5′aattcggcgcgggcgaaggagcaggaaaaaagcagggcgaatgtcagcaggtgcatggtgctcatggtaccg and sense 5′gatccggtaccatgagcaccatgcacctgctgacattcgccctgcttttttcctgctccttcgcccgcgccg corresponding to the first 60 bp of rat NR1 coding sequence were hybridized in solution and subcloned as an EcoRI-BamHI fragment into the adenovirus shuttle plasmid pACCMV.pLpA [2] between the CMV promoter and the SV40 poly(A) signal, creating the plasmid pAC-asNR1. A recombinant replication-deficient, E1-deleted Ad5 clone [2] containing this antisense expression cassette was purified and concentrated to 5×10^8 pfu/ml (titer by infection of HEK293 cells). Quantum Biotechnologies, (Montreal, Quebec, Canada) supplied Ad-GFP (same titer as Ad-asNR1).

2.2. Anti-NR1 antisera

Three sets of sera were raised in rabbits against peptides derived from different alternatively spliced regions [3,33] of the NR1 mRNA, namely N1 (exon 5^+), *N*-acetyl-SKKRNYENLDQLSYDNKRGPCamide; C1 (exon 21^+), *N*-acetyl-DRKSGRAEPDPKKKATFRACamide; and C2′ (exon 22^-), *N*-acetyl-QYHPTDITGPLNLSDPSCamide. The specificity of each of these antisera was confirmed by peptide competition studies for immunocytochemistry, and by immunoblotting experiments using subunit specific cDNAs expressed in COS-7 cells (data not shown). Furthermore, the localization of the splice variant proteins in the adult spinal cord correlated with the localization of their cognate mRNAs [27]; the localization of individual splice variant NR1 proteins to different cell types in the spinal cord will be addressed more fully in a separate publication.

2.3. Cell culture methods

COS-7 cells (ATCC) grown to sub-confluency in 10 cm^2 dishes were transfected using Lipofectamine (Life Technologies Inc.). The pE4A plasmid (a gift of S. Heineman) contains the NMDAR1-4a splice variant ($NR1_{000}$, $N1^-C1^-C2^-$) (GenBank U08267) in pcDNA1 (Invitrogen). pE4A was co-transfected with various amounts of pAC-AS-NR1, with appropriate amounts of pACCMV-.pLpA (empty adenovirus shuttle plasmid) added to maintain a constant total amount of DNA per transfection. After 24 h, cells were collected by scraping, harvested by centrifugation, and lysed by resuspension in 100 μl SDS-sample buffer followed by sonication and boiling for 5 min. Protein corresponding to one-tenth of each dish was subjected to immunoblot analysis using the C2′ antibody (which recognizes this particular splice variant), diluted 1:2000, followed by horseradish peroxidase-linked secondary antibody and enhanced chemiluminescence detection (ECL, New England Biolabs). Quantitation of NR1-immunoreactive protein was performed by densitometry (NIH Image) of a digitized ECL film.

PC12 cells (which express endogenous NR1 [5,15]) were grown on laminin in the presence of 25 ng/ml NGF, virus was added to the culture medium and incubated for 36 h. Cells were then harvested and processed as above for COS-7 cells. The C1 antibody was diluted 1:5000 and used for immunoblot analysis of the endogenously expressed NMDA receptors in PC12 cells.

2.4. In vivo methods

All animal experiments were performed in accordance with the regulations of the NIDCR Animal Care and Use Committee. Sprague–Dawley rats (200–350 g) were anesthetized for surgery by intraperitoneal injection of 50

mg/kg ketamine and 10 mg/kg xylazine. After laminectomy and removal of the dura and arachnoid layers, a 27 gauge Whitacre needle (which had an opening on the side of the shaft and a solid sharp tip), was inserted through a slit made in the pia mater and into one side of the first cervical spinal segment with the opening facing the ventral horn. Placement of the needle tip in the neck of the dorsal horn was achieved by mounting the catheter on a stereotaxic micromanipulator using the following coordinates: 1 mm lateral to midline and at an angle so that the bottom of the opening of the needle was 0.5 mm below the surface of the spinal cord. This particular injection scheme was followed in order to maintain unilateral transgene expression so that the uninjected side served as an internal control. We found the injections directly into the ventral horn frequently yielded bilateral motoneuron transduction [17], which we attribute to viral particles flowing under the ventral white commisure to the contralateral side. Adenoviral vector (10^7 pfu in 3 ul) was infused through this needle over 10 min, using a syringe pump attached to the Whitacre needle via PE-50 tubing. Two to four days following injection, animals were anesthetized and perfused transcardially with 4% paraformaldehyde.

2.5. Histological methods

Sections of spinal cord (30 μm), fixed in 4% paraformaldehyde, were processed through primary antibody. For visualizing virally expressed β-galactosidase in spinal cord sections, a polyclonal rabbit anti-β-galactosidase antibody (5 Prime-3 Prime, Boulder, CO) was diluted 1:100,000. The NR1 subunit in the spinal cord was detected using the anti-N1 primary antibody (1:1000). Primary antibodies were detected by biotinylated anti-rabbit secondary antibody (Vector Laboratories, 1:2000), avidin–biotin complex (ABC, Vector), and nickel-enhanced diaminobenzidine detection (Vector) or rhodamine tyramide signal amplification (NEN Life Science) for double label studies.

Two techniques were used for the purposes of labeling, in the same cells, either of the two viral-encoded markers (lacZ or GFP) and the level of NR1-immunoreactivity. For the first technique, Ad-lacZ (viral marker) and Ad-asNR1 were co-injected and detection was with a combination of histochemistry for β-galactosidase and immunocytochemistry for the NR1 subunit. Two to six days after injection of the two viruses, animals were perfused with 4% paraformaldehyde (but no post-perfusion fixation). Reaction of 2 mm-thick transverse sections of spinal cord with 1 mg/ml X-gal, pH 7.3, at 37°C demonstrated a blue reaction product within 15 min [24], which was restricted to the region close to the surface of the tissue block. The tissue blocks were post-fixed in 4% paraformaldehyde, and sections from the surface, which exhibited a light blue X-gal histochemical reaction product were selected for immunocytochemistry using the anti-N1 NR1 antibody and nickel-enhanced diaminobenzidine (DAB) staining. This allowed simultaneous visualization of the level of the DAB product in the light blue stained cells (in cells stained darkly blue, the level of DAB was difficult to discern). In the second double-label technique, an adenoviral vector encoding green fluorescent protein (Ad-GFP) (Quantum Biotechnologies) was co-injected into the spinal cord parenchyma with Ad-asNR1. After several days, rats were processed for immunofluorescence microscopy using the N1 antibody (1:10,000) and rhodamine tyramide signal amplification. GFP-expressing cells were visualized using fluorescein optics, while N1 immunofluorescence was assessed by rhodamine optics. Signals were merged by sequential photomicrography on the same piece of film. In order for an equivalent comparison to be made between cells in different sections, the fluorescent sections were examined by confocal microscopy. Only cells in which (a) the entire neuronal perikarya was contained within the section and was represented over a similar number of slices in the confocal stack (~90 out of 115 sections, 0.2 micron each) and contained a similar amount of GFP signal were quantified. Intensity determinations from fragments of cells (arrowhead in Fig. 6) gave variable results (i.e. a variable amount of the cell was in the field of view). The fluorescence signals were quantified from three 8–10,000 pixel squares placed over the cytoplasm from digitized slides (analyzed by densitometry using NIH image) or from confocal images (analyzed by the amount signal in the red or green channels using Adobe Photoshop); both gave equivalent results.

3. Results

A short antisense gene fragment (60 bp) directed against the NR1 transcript was expressed under control of a CMV promoter in a plasmid vector or adenoviral vector (Fig. 1A). The transcript was designed to bind to the conserved 5′ end of the coding sequence of all known rat NR1 mRNAs in order to inhibit translation in cells transduced with the antisense vector (Fig. 1B).

Inhibition of NR1 subunit expression was tested in cells co-transfected with a sense NR1 cDNA plasmid and the short antisense-expressing plasmid. Expression of the NR1 transcript alone (Fig. 2A, lane 7) in COS-7 cells produced a protein of the same molecular mass (~117 kDa) as that detected in extracts of whole brain (Fig. 2A, lane 1) or spinal cord (data not shown). Mock-transfected COS cells did not express NR1 (Fig. 2A, lane 2). Co-transfection with various amounts of the antisense-expressing plasmid pAC-asNR1 produced a concentration-dependent decrease in NR1 protein (Fig. 2A, lanes 3–6). Densitometric quantitation of the signal revealed a logarithmic relationship between the amount of antisense vector administered and the NR1 protein level (Fig. 2B). This analysis

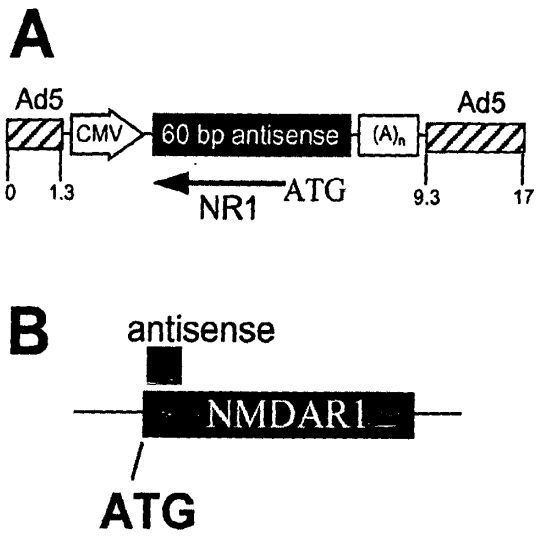

Fig. 1. Strategy for expression of an antisense transcript directed against NR1. (A) Structure of the antisense expression vectors. Both a plasmid and an adenovirus containing the segments indicated were generated. Adenovirus sequences are hatched, with map units indicated. Expression of the antisense was under control of a cytomegalovirus promoter (*CMV*) and contained a 3′ polyadenylation signal ($(A)_n$). (**B**) Expression of a short message (*black box*) complementary to the region encoding the signal sequence was predicted to bind to the endogenous NR1 mRNA and block its translation.

suggested that a half-maximal effect (EC_{50}) was observed when the ratio of antisense to sense plasmids used in the transfection was 1:40.

To test (a) whether production of *endogenous* NR1 protein could be reduced by the antisense construct, and (b) whether the equivalent antisense cassette functioned in the adenoviral vector, we examined NR1 levels in PC12 cells incubated with viral vectors. The amount of NR1 protein in virally transduced cells depended upon the amount of Ad-asNR1 viral vector added to the medium (Fig. 3A, B), and we observed virtually complete elimination of protein at the highest concentration of vector (5×10^7 particles per dish). This effect on NR1 was specific for the antisense gene, since adenoviral expression of a control green fluorescent protein gene, at doses comparable to the highest antisense virus dose, had no discernible effect on NR1 expression. An additional protein species in PC12 cells of unknown identity (~70 kDa) reacted with the antibody. This protein (*open arrow*, Fig. 3) acted as an internal control, since its expression was not altered by transduction with either adenovirus.

Administration of Ad-asNR1 to the ventral horn of the spinal cord in vivo effectively inhibited NR1 protein production in motor neurons. Injection of adenovirus expressing the lacZ marker into the neck of the dorsal horn of the rat spinal cord produced a lateralized expression of β-galactosidase marker protein in motor neurons and in

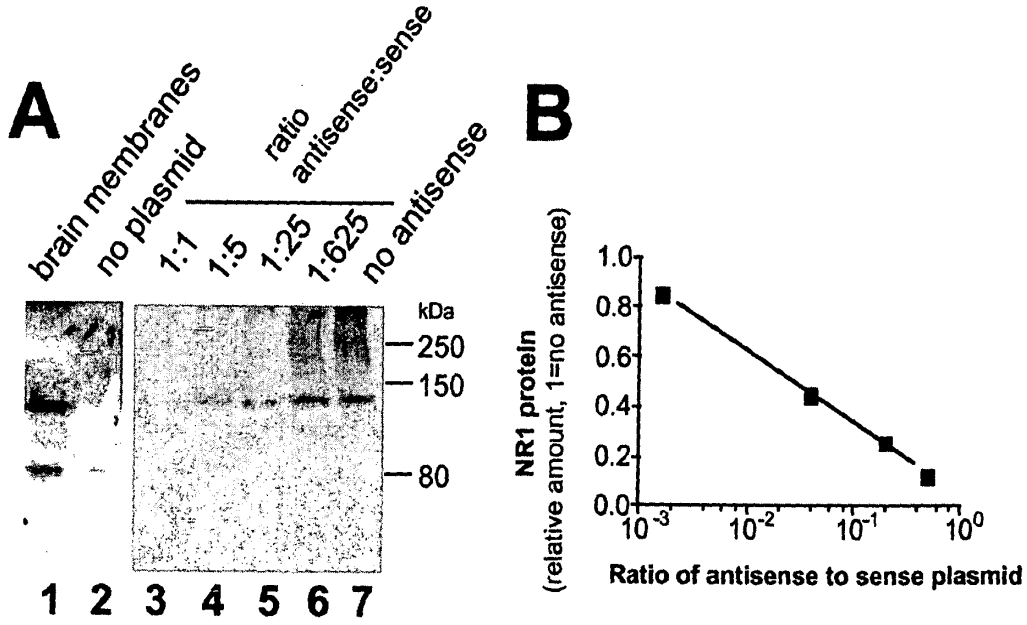

Fig. 2. Blockade of NR1 expression in cells transfected in vitro. (A) Immunoblot of extracts of brain (lane 1), untransfected COS-7 cells (lane 2), or COS-7 cells transfected with 4 ug of pE4A (NR1 expression plasmid) and various amounts of pAC-AS-NR1, resulting in the indicated ratios of antisense to sense plasmid transfected (lanes 3–6). Cells in lane 7 received no antisense. (**B**) The levels of receptor were quantitated by densitometry and normalized to the level in a no-antisense control (lane 7). Note the logarithmic scale of the abscissa.

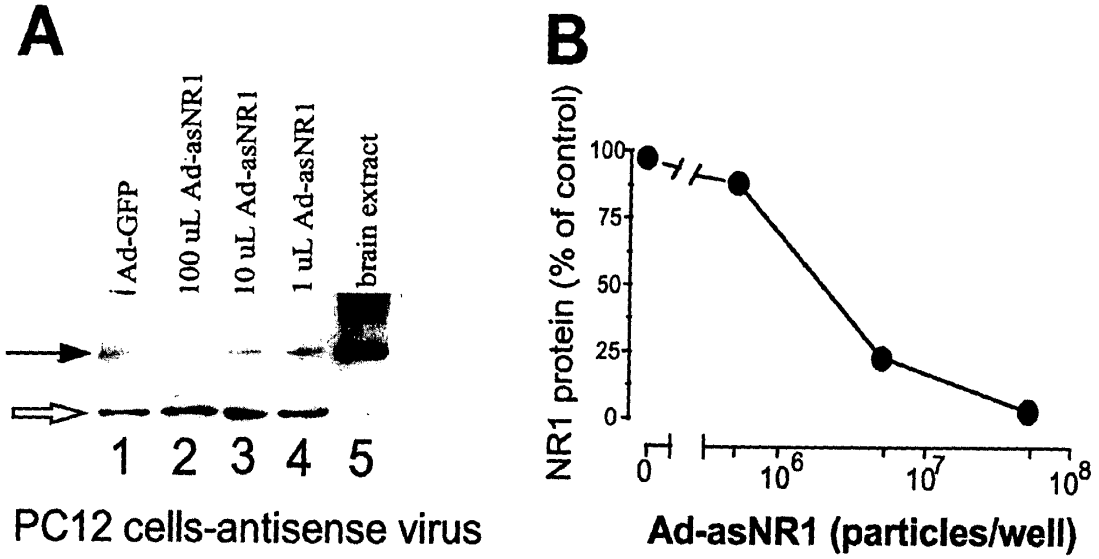

Fig. 3. Ad-asNR1 effect in PC12 cells. (A) A1 antibody was used to probe NR1 levels in extracts of cells incubated for 36 h with the indicated amounts of viral vector. Lanes 1–4, PC12 cells; Lane 5, extracts of whole brain. *Filled arrow* indicates NR1 protein; *empty arrow* indicates a protein of unknown identity in PC12 cells that cross-reacts with the NR1 antibody. (B) The levels of receptor were quantitated and normalized to a no-antisense control. Note the logarithmic scale of the abscissa.

cells of the lateral white matter, as assessed by immunocytochemistry (Fig. 4A). Higher magnification revealed the extensive distribution of transgene product β-galactosidase in cell bodies and processes of motor neurons of the ventral horn (Fig. 4B).

These motor neurons expressed readily detectable levels of the NR1 N1 (exon 5^+) splice variant in the cell soma and proximal dendrites (Fig. 4B). This expression was sensitive to virus-mediated antisense effects. Four days after unilateral co-injection of Ad-lacZ and Ad-asNR1 into the dorsal horn of the spinal cord, the levels of NR1 protein were assessed by immunocytochemistry with the N1-specific antibody. β-galactosidase histochemistry in the same sections served as a marker for the region of the spinal cord infected with virus, and the non-injected contralateral side served as an internal control for NR1 levels. A reduction in NR1 immunoreactivity was observed on the injected side (Fig. 5A), compared to the contralateral side (Fig. 5A,B) or non-injected animals. This effect was especially noticeable in individual cells containing the marker Ad-lacZ (blue cells demonstrated by X-gal histochemistry, Fig. 5C), in which little or no NR1-immunoreactivity is seen in the soma or dendritic shafts. In other animals injected with Ad-asNR1 alone, immunofluorescence analysis demonstrated a similar reduction in intensity of NR1-immunoreactivity in the injected side compared to the contralateral side (data not shown). These effects of Ad-asNR1 were reproduced in several other animals, and were not observed in >10 control animals injected only with Ad-lacZ. With this combined histochemical-immunocytochemical technique it was important to titrate the blue X-gal histochemical reaction prior to immunocytochemistry for the NR1 protein. It was difficult to discriminate between the X-Gal and Ni-DAB reaction products in sections over-reacted for X-Gal histochemical staining. As a gene transfer vector, adenovirus has the advantage of strong expression within 1 day in vivo. Although not systematically examined, we could see effects of the antisense expression as early as 2 days post-surgery, consistent with expression from the CMV promoter in other systems [1,7].

To circumvent the technical problems encountered when the histochemical β-galactosidase staining was over-reacted, as well as provide independent verification of antisense activity, we developed a fluorescent method to visualize both the spinal cord region containing virally transduced motoneurons and the level of NR1-immunoreactivity. In animals co-injected with Ad-GFP as a marker and Ad-asNR1, the expression of NR1 could be followed in adenovirus-transduced cells (which fluoresced green). Six days post-injection, spinal cord sections were stained for NR1 by rhodamine tyramide immunofluorescence. A typical result is shown in Fig. 6. NR1-immunoreactivity was detectable as red fluorescence in large motor neurons (Fig. 6A), which were also marked green by Ad-GFP (Fig. 6B). In contrast, NR1 protein staining was greatly reduced in corresponding neurons of animals co-injected with Ad-asNR1 and Ad-GFP (Fig. 6D). Photographic overlay of the NR1 (red) and GFP (green) images resulted in a yellow signal for animals injected with Ad-GFP only, but little yellow for Ad-GFP+Ad-asNR1 (compare Fig. 6 C and F). The photomicrograph in Fig. 6D shows several immuno-

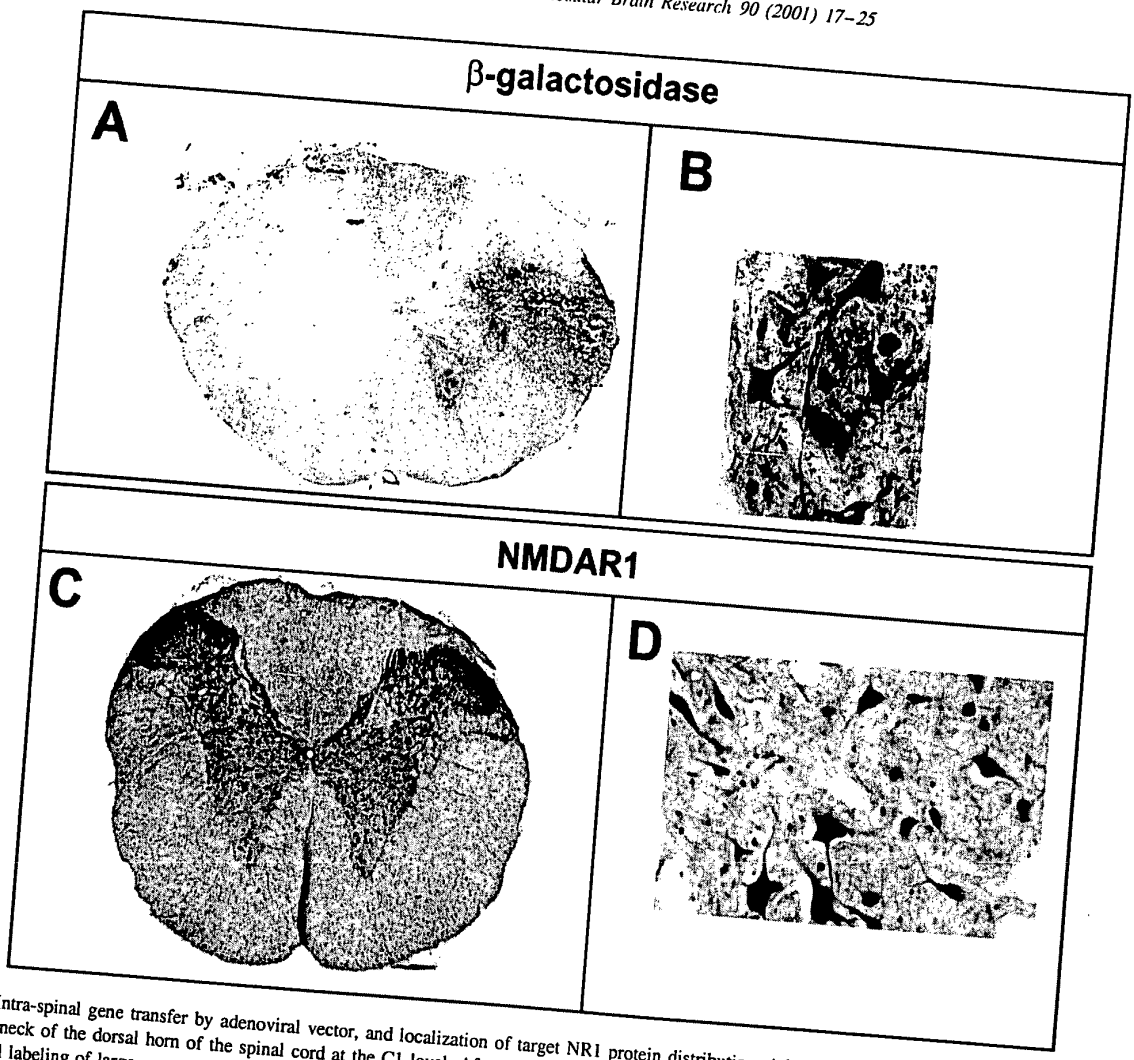

Fig. 4. Intra-spinal gene transfer by adenoviral vector, and localization of target NR1 protein distribution. Ad-lacZ (10^7 pfu in 3 ul) was infused slowly into the neck of the dorsal horn of the spinal cord at the C1 level. After 3 days, immunocytochemistry for β-galactosidase was performed (**A**). Note the unilateral labeling of large motor neurons in ventral horn, lateral white matter, and absence of stain in dorsal horn. (**B**) A high-magnification view of the injected side of the ventral horn shows processes and cell bodies of motor neurons stained by the anti-β-galactosidase antibody. (**C**) NR1 immunocytochemistry of the N1 splice variant protein. Note the readily detectable immunoreactivity in the motor neurons of the ventral horn. (**D**) High-magnification view of NR1-immunoreactivity in motor neurons from one ventral horn. Note reactivity in cell soma and dendritic processes.

reactive cytoplasmic inclusions that serve as markers for the antisense-affected cell, but which have not been further characterized at present. However, the confocal microscopy analysis of these samples indicated that the inclusions were not nuclear (data not shown). Quantitation of the NR1 and GFP fluorescence by densitometry of the digitized slides showed approximately an 85% reduction of NR1 immunoreactivity in the cell (arrow) in Fig. 6 panel D in comparison to the cell in panel A. Quantification of the GFP signal showed approximately the same amount of GFP in both cells. Analysis of this same field by was performed on a 115-section series of confocal images, which showed that the entire parikarya of the arrowed cells were contained within slices 5 through 110 (not shown). Having the entire cell body in the section was essential since the amount of fluorescence in fragments of cells (Fig. 6A, arrowhead) varied according to the how much of the cell was represented in the confocal image stack.

4. Discussion

Using an antisense approach, levels of the NR1 subunit of the NMDA glutamatergic neurotransmitter receptor were reduced in transfected COS-7 cells cultured in vitro. These cells, transiently transfected with an exogenous NR1 gene not normally expressed in this cell type, made a protein of similar molecular size to that observed in brain extracts. The extent of reduction in NR1 depended upon the amount of antisense plasmid introduced, indicating that the inhibition was specifically due to the antisense portion

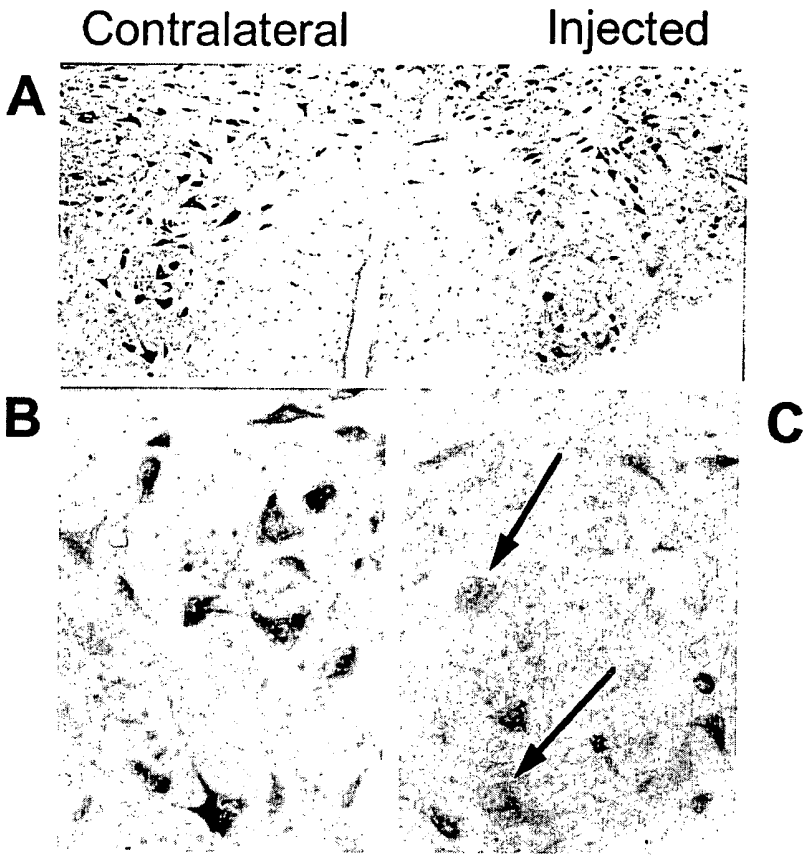

Fig. 5. In vivo reduction of NR1 receptors by antisense. Ad-lacZ was co-injected with Ad-AS-NR1 into one side of the spinal cord, and a double-label histo- and immunocytochemical analysis was performed 3 days later. Co-stain of neurons marked with beta-galactosidase histochemical reaction (blue) and NR1 by ICC with the N1 antibody and DAB (black). The right side was injected with viral vectors. (A), low power view of ventral grey matter demonstrating reduction in NR1-immunoreactivity on the injected side. (B), High power view of control, uninjected side stained with NR1. (C), High power view of injected side, stained blue with X-Gal and also for NR1. Note the reduction in immunoreactivity in the soma and dendrites of motor neurons of the injected side, particularly in cells co-stained with the light blue X-gal reaction product.

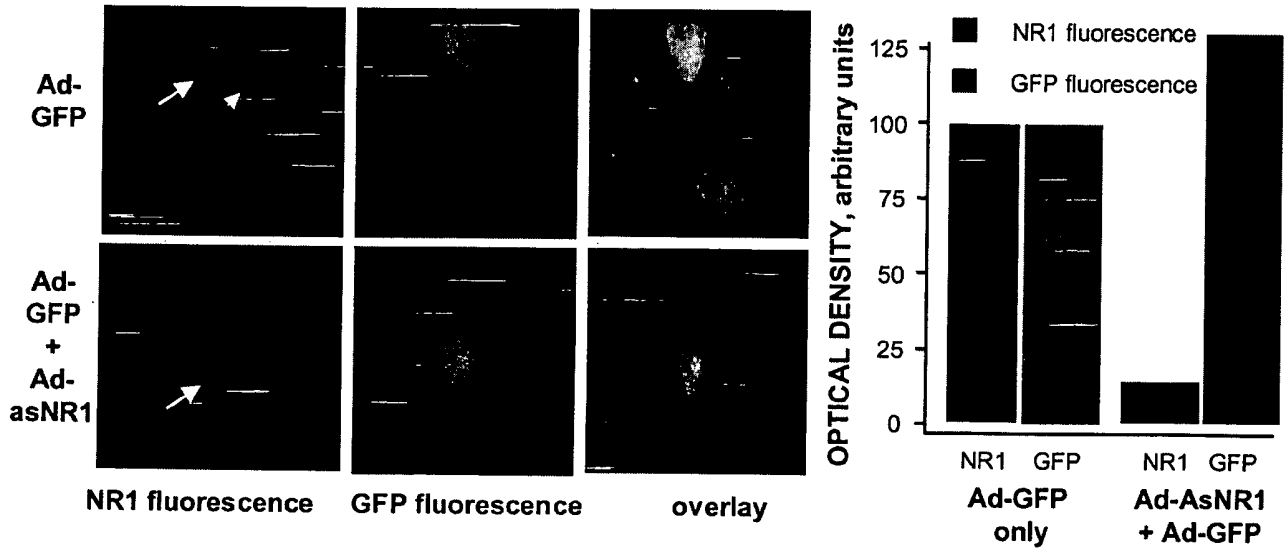

Fig. 6. Immunofluorescence microscopic analysis of NR1-ir in motor neurons of animals injected with antisense virus. Co-expression of NR1 and GFP was evaluated in sections from an animal injected with Ad-GFP alone (A–C) or both Ad-GFP and Ad-asNR1 (D–F). NR1-ir detected by immunofluorescence using rhodamine tyramide (A, D) was photographically combined with the intrinsic GFP signal (B, E) to create an overlay (C, F). Quantitation was by densitometry of the cells using NIH Image. A similar analysis of the same cells (arrows) using confocal microscopy (not shown) showed that the entire perikarya was in the confocal stack and occupied the same number of individual slices. Quantification of the center slice, slices at ±4 microns from the center, or the entire stack, yielded the same results as obtained from the densitometry of the digitized photographic images (shown at right). There was an approximately 85% reduction in NR1 immunoreactivity in the cell shown.

of the plasmid since the total amount of DNA was kept constant by addition of empty shuttle vector. The concentration–response curve suggested that a ratio of one antisense gene to 40 sense genes produced a 50% reduction of protein (Fig. 2). These data demonstrate the efficacy of the short antisense cassette under controlled conditions in a simplified cellular preparation.

Building upon this plasmid result, a logical next step was to test the ability of the antisense gene to reduce NR1 when expressed from the adenoviral vector in vitro. The endogenous NR1 protein in PC12 cells [5,15] was reduced in quantity by an adenovirus expressing the 60-bp antisense, but not a control adenovirus expressing GFP (Fig. 3), suggesting that the effect was due to the antisense gene. Finally, a striking result was obtained when Ad-asNR1 was injected into the parenchyma of one side of the spinal cord by microinfusion into live animals. After several days, the amount of NR1-immunoreactivity was reduced in motoneurons transduced with the viral vectors compared with animals injected with control virus or with non-transduced motor neurons on the contralateral side. In vivo, the extent of this reduction varied but in cells in which the transduction marker was well expressed, the antisense expression nearly eliminated NR1 protein from the cell. Both the in vitro and in vivo data indicated that a short antisense transcript was effective at reducing NR1 protein levels (Fig. 3). In vivo, using a cell-by-cell analysis we did observe variation in antisense effect that are not apparent when analyzing effects on a whole plate of cultured cells. Individual variation may be due several factors: (a) differences in the endogenous level of NR1 (higher levels may be more difficult to decrease), (b) the degree of expression of the antisense transgene (less likely since CMV is a very effective promoter), or (c) the number of viral particles entering the cells (probably the most relevant variable).

The mechanism of antisense-mediated reduction in NR1 expression presumably proceeds through blockade of translation of NR1 mRNA into new NR1 protein by the virus-encoded antisense transcript, followed by degradation of pre-existing NR1. The rate and level of production of the antisense transcript affects the efficacy as well. Little information is available about the time course of these processes. In PC12 cells, we observed that NR1 protein was nearly completely eliminated within 36 h (Fig. 3). Studies on the turnover of NR1 in cultured cerebellar granule cells suggest that NR1 exists in two populations, with half-lives of 2 h and 34 h [13]. This may be consistent with the experiments in Figs. 5–6, where a small amount of intracellular NR1 remained after 4–6 days of antisense expression. Persistent expression of the antisense for longer periods may be required to allow more extensive degradation of protein. This may be difficult to achieve with this first-generation adenoviral vector in vivo, since it has been noted by ourselves [17] and others that transgene expression declines appreciably by 12–14 days.

The choice of particular sequences used for antisense is a difficult one, as predictive methods are unreliable [12] especially for exogenously administered oligodeoxynucleotides. In this report, we describe a short antisense gene, 60 bp, which produced a strong antisense effect. Viral gene delivery allows the possibility of introducing relatively long antisense sequences compared with synthetic oligodeoxynucleotides. However, viruses also impose constraints upon the size of inserted nucleic acid, and our demonstration of functional effects from a short antisense transcript provides a new degree of flexibility not previously recognized. For example, it allows the insertion of multiple antisense genes into a single viral particle, thereby targeting several different genes involved in a particular disorder. Additionally, specific splice variants of NR1 might be targeted through specific antisense sequences. This approach would not be possible with long sequences.

Tests of the efficacy of the antisense in spinal cord neurons depended upon delivery of the antisense gene by the adenoviral vector. This vector appears to have a tropism for motor neurons in the ventral horn, rather than neurons in other spinal laminae [17]. This surprising result may be due to non-uniform distribution of receptors and internalization mechanisms for adenovirus [4,22,30]. Alternatively, viral uptake may occur via non-receptor dependent mechanisms in motor neurons or be influenced by physical parameters such as adenovirus particle size (~90 nm) and its ability (or inability) to spread within the interstitial space [16,17]. Other viral vectors have different sizes (such as adeno-associated virus, ~20 nm) and altered tropism, and thus may allow delivery to the dorsal horn [21]. Regardless of the mechanism of tropism, motor neurons are excellent targets for transduction by adenovirus.

The antisense gene transfer approach described here, where genes expressed in neurons are the target, may be useful for therapy of spinal neurological disorders such as amyotrophic lateral sclerosis, spinal muscular atrophy, or spinal cord injury, where excitotoxic death of motor neurons has been implicated [19,26]. It remains to be determined whether the reduction of NR1 using the antisense approach described herein, would be neuroprotective. Gene therapy vectors have been used to deliver genes encoding secreted factors such as neuroprotective growth factors to degenerating nerve endings in the peripheral musculature, with therapeutic effect in animal models [8–10]. In a complementary approach, gene transfer may also be directed to non-neuronal cells such as glia or even cells of the meninges surrounding the spinal cord. We have used the latter cellular target for secretion of therapeutic biomolecules into the cerebrospinal fluid and into the parenchyma of the spinal cord. Viral expression of β-endorphin by the pia mater secretory or 'paracrine delivery' route alleviates hyperalgesia in a model of chronic pain [7]. The clinical utility of such an approach may be realized through delivery of therapeutic viruses

into the subarachnoid CSF. Thus, gene therapy for neurobiological disorders in practice may well involve the manipulation of multiple genes, through both the addition and subtraction of functional proteins by both paracrine and local intraparenchymal gene transfer.

Acknowledgements

We thank Hector Carrero for excellent technical assistance. The NMDAR1 cDNA expression plasmid pE4A was a gift from Bryce Vissel and S. Heineman, Salk Institute, La Jolla, CA.

References

[1] G. Bajocci, S.H. Feldman, R.G. Crystal, A. Mastrangeli, Direct in vivo gene transfer to ependymal cells in the central nervous system using recombinant adenovirus vectors, Nat. Genet. 3 (1993) 229–234.

[2] T.C. Becker, R.J. Noel, W.S. Coats et al., Use of recombinant adenovirus for metabolic engineering of mammalian cells, Meth. Cell Biol. 43 (1994) 161–189.

[3] R. Benoliel, M. Tanaka, R.M. Caudle, M.J. Iadarola, Co-localization of NMDA receptors and substance P (neurokinin-1) receptors in rat spinal cord, Neurosci. Lett. (2000) in press.

[4] J.M. Bergelson, J.A. Cunningham, G. Droguett et al., Isolation of a common receptor for coxsackie B viruses and adenoviruses 2 and 5, Science 275 (1997) 1320–1323.

[5] M. Casado, A. Lopez-Guajardo, B. Mellstrom, J.R. Naranjo, J. Lerma, Functional *N*-methyl-D-aspartate receptors in clonal rat phaeochromocytoma cells, J. Physiol. (Lond.) 490 (1996) 391–404.

[6] E.A. Chiocca, X.O. Breakefield, Gene Therapy for Neurological Disorders and Brain Tumors, Humana Press, Totowa, N.J, 1998.

[7] A.A. Finegold, A.J. Mannes, M.J. Iadarola, A paracrine paradigm for in vivo gene therapy in the central nervous system: treatment of chronic pain, Hum. Gene Ther. 10 (1999) 1251–1257.

[8] M. Gimenez y Ribotta, F. Revah, L. Pradier, I. Loquet, J. Mallet, A. Privat, Prevention of motoneuron death by adenovirus-mediated neurotrophic factors, J. Neurosci. Res. 48 (1997) 281–285.

[9] G. Haase, P. Kennel, B. Pettmann et al., Gene therapy of murine motor neuron disease using adenoviral vectors for neurotrophic factors, Nat. Med. 3 (1997) 429–436.

[10] G. Haase, B. Pettmann, E. Vigne, L. Castelnau-Ptakhine, H. Schmalbruch, A. Kahn, Adenovirus-mediated transfer of the neurotrophin-3 gene into skeletal muscle of pmn mice: therapeutic effects and mechanisms of action, J. Neurol. Sci. 160 (Suppl 1) (1998) S97–S105.

[11] P.L. Herrling, Excitatory Amino Acids-Clinical Results with Antagonists, Academic Press, San Diego, 1997.

[12] S.P. Ho, D.H. Britton, Y. Bao, M.S. Scully, RNA mapping: selection of potent oligonucleotide sequences for antisense experiments, Methods Enzymol. 314 (2000) 168–183.

[13] K.H. Huh, R.J. Wenthold, Turnover analysis of glutamate receptors identifies a rapidly degraded pool of the *N*-methyl-D-aspartate receptor subunit, NR1, in cultured cerebellar granule cells, J. Biol. Chem. 274 (1999) 151–157.

[14] A. Kammesheidt, K. Kato, K. Ito, K. Sumikawa, Adenovirus-mediated NMDA receptor knockouts in the rat hippocampal CA1 region, Neuroreport 8 (1997) 635–638.

[15] C.L. Leclerc, C.L. Chi, M. Awobuluyi, N.J. Sucher, Expression of *N*-methyl-D-aspartate receptor subunit mRNAs in the rat pheochromocytoma cell line PC12, Neurosci. Lett. 201 (1995) 103–106.

[16] R.R. Lonser, N. Gogate, P.F. Morrison, J.D. Wood, E.H. Oldfield, Direct convective delivery of macromolecules to the spinal cord, J. Neurosurg. 89 (1998) 616–622.

[17] A.J. Mannes, R.M. Caudle, B.C. O'Connell, M.J. Iadarola, Adenoviral gene transfer to spinal-cord neurons: intrathecal vs. intraparenchymal administration, Brain Res. 793 (1998) 1–6.

[18] O. Matveeva, B. Felden, A. Tsodikov et al., Prediction of antisense oligonucleotide efficacy by in vitro methods, Nat. Biotechnol. 16 (1998) 1374–1375.

[19] D.T. Monaghan, R.J. Wenthold, The Ionotropic Glutamate Receptors, Totowa, N.J, Humana Press, 1997.

[20] E. Morikawa, H. Mori, Y. Kiyama, M. Mishina, T. Asano, T. Kirino, Attenuation of focal ischemic brain injury in mice deficient in the epsilon1 (NR2A) subunit of NMDA receptor, J. Neurosci. 18 (1998) 9727–9732.

[21] A.L. Peel, S. Zolotukhin, G.W. Schrimsher, N. Muzyczka, P.J. Reier, Efficient transduction of green fluorescent protein in spinal cord neurons using adeno-associated virus vectors containing cell type-specific promoters, Gene Ther. 4 (1997) 16–24.

[22] P.W. Roelvink, G. Mi Lee, D.A. Einfeld, I. Kovesdi, T.J. Wickham, Identification of a conserved receptor-binding site on the fiber proteins of CAR-recognizing adenoviridae, Science 286 (1999) 1568–1571.

[23] D.R. Shafron, C.E. Simpkins, B. Jebelli, A.L. Day, E.M. Meyer, Reduced MK801 binding in neocortical neurons after AAV-mediated transfections with NMDA-R1 antisense cDNA, Brain Res. 784 (1998) 325–328.

[24] S. Shimohama, M.B. Rosenberg, A.M. Fagan et al., Grafting genetically modified cells into the rat brain: characteristics of *E. coli* beta-galactosidase as a reporter gene, Brain Res. Mol. Brain Res. 5 (1989) 271–278.

[25] R. Sprengel, B. Suchanek, C. Amico et al., Importance of the intracellular domain of NR2 subunits for NMDA receptor function in vivo, Cell 92 (1998) 279–289.

[26] D.L. Tanelian, M.A. Barry, S.A. Johnston, T. Le, G.M. Smith, Semaphorin III can repulse and inhibit adult sensory afferents in vivo, Nat. Med. 3 (1997) 1398–1401.

[27] T.R. Tolle, A. Berthele, D.J. Laurie, P.H. Seeburg, W. Zieglgansberger, Cellular and subcellular distribution of NMDAR1 splice variant mRNA in the rat lumbar spinal cord, Eur. J. Neurosci. 7 (1995) 1235–1244.

[28] B. Weiss, G. Davidkova, S.P. Zhang, Antisense strategies in neurobiology, Neurochem. Int. 31 (1997) 321–348.

[29] H.V. Wheal, A.M. Thomson, Excitatory Amino Acids and Synaptic Transmission, Academic Press, London, 1995.

[30] T.J. Wickham, P. Mathias, D.A. Cheresh, G.R. Nemerow, Integrins alpha v beta3 and alpha v beta5 promote adenovirus internalization but not virus attachment, Cell 73 (1993) 309–319.

[31] M.R. Young, G. Blackburn-Munro, T. Dickinson et al., Antisense ablation of type I metabotropic glutamate receptor mGluR1 inhibits spinal nociceptive transmission, J. Neurosci. 18 (1998) 10180–10188.

[32] A. Zapata, J.L. Capdevila, G. Tarrason et al., Effects of NMDA-R1 antisense oligodeoxynucleotide administration: behavioral and radioligand binding studies, Brain Res. 745 (1997) 114–120.

[33] R.S. Zukin, M.V. Bennett, Alternatively spliced isoforms of the NMDARI receptor subunit, Trends Neurosci. 18 (1995) 306–313.

Original Paper

Cellular Physiology and Biochemistry

Cell Physiol Biochem 1999;9:139–149 Accepted: March 22, 1999

Cell Culture Conditions Determine Apolipoprotein CIII Secretion and Regulation by Fibrates in Human Hepatoma HepG2 Cells

V. Clavey C. Copin M.C. Mariotte E. Baugé G. Chinetti
J. Fruchart J.C. Fruchart J. Dallongeville B. Staels

INSERM U325, Institut Pasteur de Lille et Faculté de Pharmacie, Université Lille 2, Lille, France

Key Words

Apolipoproteins, gene expression · Peroxisome proliferator-activated receptor · Fibrates

Abstract

Fibrates are widely used drugs which lower triglycerides and increase HDL concentrations in serum. Recent findings from our laboratory have shown that fibrates repress apolipoprotein (apo) CIII gene expression, an effect that explains partially the triglyceride-lowering activity of these drugs. The goal of the present study was to compare the effect of various fibrates on apo CIII gene expression in the human hepatoblastoma cell line HepG2. First, we demonstrate that the level of apo CIII secretion by HepG2 cells is controlled by serum factors whereas apo CIII mRNA levels are not and even increase under conditions when apo CIII secretion dramatically decreases. Twelve different fetal calf serum batches were tested during this study and apo CIII secretion in cell medium could only be detected with three of them. The effect of serum on apolipoprotein secretion was more pronounced for apo CIII whereas other apolipoproteins (apo E, apo B, apo AII and apo AI) were affected to a lesser extent. Under serum conditions allowing apo CIII secretion, treatment with the peroxisome-proliferator activated receptor (PPAR)α activators fenofibrate, gemfibrozil and Wy-14643 result in a marked lowering of apo CIII secretion and gene expression, this effect being most pronounced with Wy-14643. Comparison of the activity of a PPARγ-specific ligand, the antidiabetic thiazolidinedione, BRL-49653 and a PPARα ligand Wy-14643 showed a marked decrease of apo CIII secretion and gene expression after activation of PPARα but not PPARγ. In conclusion, fibrates down-regulate apo CIII gene expression in human HepG2 cells, most likely via PPARα but not via PPARγ. However, these effects are only observed in HepG2 cells cultured under appropriate conditions.

KARGER
Fax + 41 61 306 12 34
E-Mail karger@karger.ch
www.karger.com

1015–8987/99/0093–0139$17.50/0

Accessible online at:
http://BioMedNet.com/karger

V. Clavey
INSERM U325, Institut Pasteur de Lille
1, rue du Professeur Calmette, BP 245
F–59019 Lille Cédex (France)
Fax +33 3 20 87 73 60, E-Mail veronique.clavey@pasteur-lille.fr

Introduction

Apolipoprotein (apo) CIII is a component of several classes of plasma lipoproteins such as triglyceride-rich particles (chylomicrons, very low density lipoproteins (VLDL)), intermediate density lipoproteins (IDL) and high density lipoproteins (HDL). Apo CIII is produced predominantly in the liver and to a lesser extent in the intestine [1].

The importance of apo CIII in triglyceride-rich lipoprotein metabolism is demonstrated by the positive correlation between apo CIII levels and triglyceride concentrations in plasma from normal or dyslipemic subjects [2]. Patients deficient in apo CIII exhibit an increased catabolism of VLDL and an unusually efficient conversion of VLDL to IDL and low density lipoproteins (LDL) [3]. In contrast, elevated apo CIII synthetic rates have been observed in hypertriglyceridemic patients [4]. Fat ingestion is associated with increased levels of apo CIII-containing apo B lipoproteins [5]. In human apo CIII transgenic mice, triglyceride levels were found to be proportional to apo CIII gene expression and human apo CIII plasma concentrations [6, 7]. Inversely, transgenic mice with a targeted disruption of the apo CIII gene were shown to be protected from postprandial hypertriglyceridemia [8]. In vitro apo B binding to the LDL receptor was inhibited by apo CIII and this inhibition was dependent of the apo CIII level [9, 10] and in vivo the catabolism of apo B-containing lipoproteins was increased in subjects with apo CIII deficiency [11].

Relatively few factors regulating apo CIII secretion are described, among which are cytokines activating the NFκB transcription pathway [12] and insulin [13]. Furthermore, hypolipidemic drugs such as fibrates and, to a lesser extent, statins reduce apo CIII-containing particles in plasma [14, 15]. Transcriptional regulation of the apo CIII gene by fibrates [16, 17] has been studied in vivo in rodents. The mode of action of these hypolipidemic drugs in suppressing plasma apo CIII levels has been suggested to result from transcriptional suppression of the apo CIII gene mediated via the peroxisome proliferator-activated receptor (PPAR) [18]. The mechanism of apo CIII repression by fibrates may involve competition by PPAR for binding of the strong activator hepatic nuclear factor-4 (HNF-4) to a *cis*-acting sequence on the apo CIII promoter as well as a direct repression of HNF-4 expression. Recently it was demonstrated that in PPARα-deficient mice, serum triglyceride levels and hepatic apo CIII mRNA levels were unaffected by fibrate treatment [18]. In primary cultures of human hepatocytes, fibrates have been shown to down-regulate apo CIII expression in a manner independent of the induction of peroxisomal enzyme activity [19, 20].

However, the low availability of human hepatocytes has led to the use of human cell lines. The human hepatoblastoma-derived cell line, HepG2, expresses many functions of human hepatocytes. This cell line synthesizes and secretes lipoprotein fractions within the density ranges of VLDL, LDL and HDL [21–23]. Much information on the regulation of apo B-containing lipoproteins have been obtained from these cultured liver cells [24, 25]. Passilly et al. [26], comparing human HepG2 and rat Fao cells, found that ciprofibrate treatment influenced cell cycle, palmitoyl-CoA oxidase activity and peroxisome proliferation in rat but not in human cells. HepG2 cells have furthermore been used to study transcriptional regulation of the apo CIII gene [12, 27] and these cells secrete also apo CIII [23, 28, 29]. In this paper we studied the optimal conditions to measure apo CIII secretion by HepG2 cells with an appropriate enzyme immunoassay to quantify apo CIII. Our results indicate that in certain cases, apo CIII

gene expression does not correlate with apo CIII secretion and that both parameters should be taken into account when performing regulation studies. Using this well-defined system, we go on to study the activities of different fibrate PPARα activators and of a PPARγ activator, the antidiabetic thiazolidinedione BRL-49653, on apo CIII secretion and transcription in HepG2 cells.

Materials and Methods

Products

Twelve different fetal calf serum (FCS) batches were tested during this study and apo CIII secretion in cell medium could only be detected with three of them. Two representative batches were used for the experiments described here, Gibco BRL 40Q1443K FCS (FCS1) allowing apo CIII secretion and a Gibco BRL 40G1646J FCS (FCS2) impairing apo CIII secretion. Lipoprotein-deficient FCS (LPDS) was obtained by two successive ultracentrifugations of FCS (KBr density: 1.21 g/ml) for 24 h at 100,000 *g;* the infranate LPDS was dialyzed against 0.01 *M* sodium phosphate buffer pH 7.4, 0.15 *M* NaCl (PBS). LPDS was deactivated on activated charcoal.

BRL-49653 and fenofibric acid were kind gifts of Dr. Berthelon (Merck-Lipha SA, Lyon, France) and Dr. Alan Edgar (Laboratoires Fournier, Daix, France). Pirixinic acid (Wy-14643) was from Chemsyn Science Laboratories, Kans., USA, and gemfibrozil was purchased from Sigma, St. Louis, Mo., USA.

Cells

HepG2 cells (hepatocellular carcinoma, ref. ATCC: HB8065) were grown and maintained in Dulbecco's modified Eagle's medium containing 10% FCS (v/v), 2 m*M* glutamax (Gibco BRL), penicillin (1,000 U/ml), streptomycin (1,000 U/ml) and gentamicin. Cells were grown in 75-cm^2 flasks and before experiments transferred in 28.6-cm^2 plates (3×10^6 cells/plate: 10^5 cells/cm^2) in FCS medium for 24 h. Culture medium was removed and 3 ml of experimental medium was added for 24 h then removed for analysis. In experiments where secretion was studied for 48 h a fresh experimental medium was provided after the first 24 h.

Usually experimental medium was the same as growing medium except that FCS was removed and replaced by 2 g/l bovine serum albumin (BSA). In some experiments indicated apolipoprotein secretion was studied in medium where BSA was replaced by FCS or LPDS (10% v/v). When fibrates were added to experimental medium they were dissolved in DMSO then diluted in the medium. The final DMSO concentration was 0.1% (v/v) and DMSO was also added to control cells without fibrates. Cells were washed with PBS then scraped in 2 ml of 4 *M* guanidine isothiocyanate buffer. Cell proteins were measured by the Coomassie Blue method (BioRad) and mRNA extracted. Each experiment was performed in triplicate and results are expressed as the mean ± SD.

Apolipoprotein Determinations by Enzyme Immunoassay

Human apo CIII was measured by a noncompetitive enzyme-linked immunosorbent assay (sandwich ELISA) as described previously [30] using specific antibodies. Briefly, polystyrene microtiter plates were coated with affinity-purified rabbit polyclonal antibodies to human apo CIII. Cell secretion medium samples diluted with 0.1 *M* sodium phosphate, 0.15 *M* NaCl buffer pH 7.4 containing 1% albumin (phosphate buffer) were added to the wells along with the standards and controls and incubated for 2 h at 37°C. After incubation, the plates were washed 4 times with phosphate buffer and the corresponding rabbit polyclonal peroxidase labeled anti-apolipoprotein antibody was added. The plates were incubated for 2 h at 37°C and then washed. 30 min after the addition of peroxidase substrate (*o*-phenylenediamine dichloride; Sigma Chemical Co., St. Louis, Mo., USA), the coloration was measured at 492 nm using an automated microplate reader model EL340 (Bio-Tek Instruments, Inc., Winooski, Vt., USA). A pool of 400 different plasma samples was used as secondary standard. Intra- and interassay reproducibility was respectively 6.5 and 11.6%.

Human apo E [31], apo AII [32], apo AI [33] and apo B [34] levels were measured by noncompetitive ELISAs adapted from previously described methods.

RNA Extraction and Analysis

RNA extractions, Northern and dot-blot hybridizations, and quantification of apo CIII mRNA levels were performed as described previously [20]. The cDNA clone 36B4 [35] encoding for the human acidic ribosomal phosphoprotein PO [36] was used as control. cDNA probes were labeled by random primed labeling (Boehringer Mannheim). Filters were hybridized to 1.5×10^6 cpm/ml of each probe as described [37]. They were washed once in 0.5 × SSC and 0.1% SDS for 10 min at room temperature and twice for

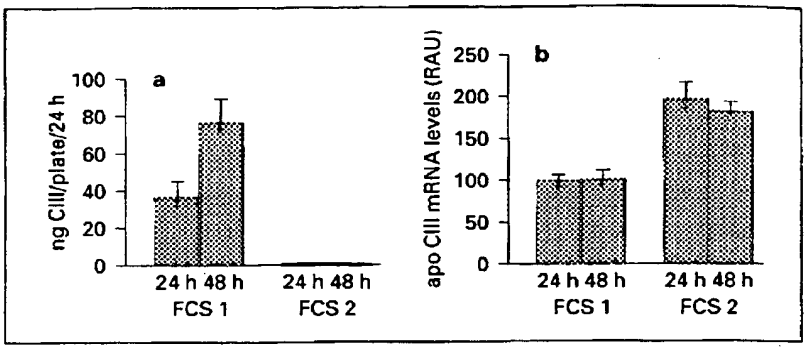

Fig. 1. Influence of different batches of FCS on apo CIII secretion and gene expression in HepG2 cells. Cells were grown for several weeks in medium containing different FCS batches (FCS1, FCS2). The medium was subsequently removed and cells were incubated in 3 ml of the experimental medium (BSA 2 g/l). Results are expressed as ng apo CIII secreted per plate and per 24 h. apo CIII mRNA levels in FCS2 cultured cells were expressed as a percent of the levels in cells cultured in FCS1 for the same period of time.

30 min at 65°C and subsequently exposed to X-ray films (X-OMAT-AR, Kodak). Autoradiograms were analyzed by quantitative scanning densitometry (Bio-rad GS670 Densitometer) and results normalized to 36B4 mRNA levels as described [37].

Western Blot Analysis

Cells were washed twice in ice-cold PBS and harvested in ice-cold lysis buffer containing PBS, 1% Triton X-100, and a freshly prepared protease inhibitor cocktail (ICN, Orsay, France) (10 mg/ml AEBSF, 1 mg/ml leupeptin, 1 mg/ml pepstatin, 5 mg/ml EDTA-Na_2) to which 1 m*M* PMSF was added. Cell homogenates were collected by centrifugation at 13,000 rpm at 4°C. Electrophoresis of 100 µg of protein lysate was performed through a 10% polyacrylamide gel under reducing conditions (sample buffer containing 10 m*M* dithiothreitol (DTT)). Proteins were transferred onto nitrocellulose membranes and nonspecific binding sites were blocked overnight at 4°C with 10% skim milk powder in TBST (20 m*M* Tris, 55 m*M* NaCl, 0.1% Tween 20). Membranes were subsequently incubated for 4 h at room temperature in 5% skim milk-TBST containing specific rabbit polyclonal antibodies raised against N-terminal PPARα [38] or PPARγ peptides [39]. After incubation with a secondary peroxidase conjugation, signals were visualized by chemiluminescence (Amersham, Bucks., UK).

Results

First HepG2 cells were cultured for several weeks in medium constituted with either FCS batch representative of three different batches allowing apo CIII secretion (FCS1) or an FCS batch representative of 9 batches impairing apo CIII secretion (FCS2). apo CIII secretion experimental medium without FCS, but containing BSA 2 g/l, was used to avoid a direct effect of FCS on apo CIII secretion. Figure 1a shows that apo CIII secretion could only be detected in significant amounts from cells cultured in FCS1. apo CIII secretion by cells grown in FCS2 was undetectable (<1 ng/mg cell protein). No differences in cell growth (measured by the cell protein content) were observed after 24 or 48 h of incubation of cells previously grown in FCS1 or in FCS2. An unexpected result was that apo CIII mRNA levels were not decreased but rather increased in cells cultured in FCS2 (fig. 1b), indicating that the effect of FCS2 was not due to a dedifferentiation of the hepatoma cells.

When cells were cultured for several weeks in FCS2 medium and then switched to FCS1 medium, apo CIII secretion could not be restored. Inversely when cells were grown in FCS1 medium and then switched to FCS2 medium, the apo CIII secretion diminished after each passage and was abolished after a few weeks. In order to study the short-term influence of the different batches of FCS on apo CIII secretion, cells cultured in FCS1 were switched to the experimental medium containing either FCS1, FCS2, LPDS prepared from FCS2, or BSA for 48 h. In figure 2, it is shown that after 48 h, apo CIII secretion was similar in BSA and in FCS1 medium, whereas FCS2 inhbited its secretion after 48 h of incubation. The difference in secretion compared to BSA medium suggests the presence of an inhibitor of apo CIII secretion in FCS2, since secretion in BSA and FCS1 medium were nearly identical. Furthermore, secretion of apo CIII by cells cultured in LPDS from FCS2 was also decreased, indicating that the hypothetical inhibitor is not lipophilic.

In order to study whether certain FCS batches abolished protein secretion by the HepG2 cells in general, we investigated their influence on the secretion of other apolipoproteins. No major morphologic change can be observed when FCS2 was used. Our results indicate that the secretion of all other apolipoproteins analyzed was much less affected by the nature of the FCS batches whereas apo CIII secretion was again abolished by long-term culture in FCS2 medium (table 1). Al-

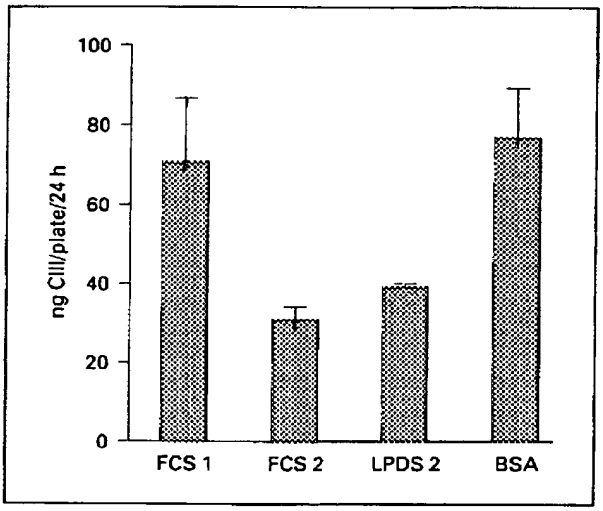

Fig. 2. Short-term effect of different batches of FCS on apo CIII secretion by HepG2 cells. Cells were grown for several weeks in FCS1. Cells were subsequently incubated with 3 ml of experimental medium containing either FCS1, FCS2, LPDS prepared from FCS2 (LPDS2) or BSA (2 g/l). Results are expressed as ng apo CIII secreted per plate and per 24 h.

Table 1. Apolipoprotein secretion by HepG2 cells cultured in medium containing different batches of FCS

Apolipoprotein	Secretion in FCS1 ng/mg/24 h	Secretion in FCS2 ng/mg/24 h	FCS1/FCS2 ratio
AI	3,899±491	1,864±352	2.09
B	2,473±243	1,344±160	1.84
E	610±56	458±58	1.3
AII	181±1	24±2	7.5
CIII	63.9±6	<2	>31.9

Cells were grown for several weeks in medium containing either FCS1 or FCS2. Secretion was measured after 48 h in secretion BSA medium. Results are expressed as ng apolipoprotein secreted per 24 h and per mg of cell protein.

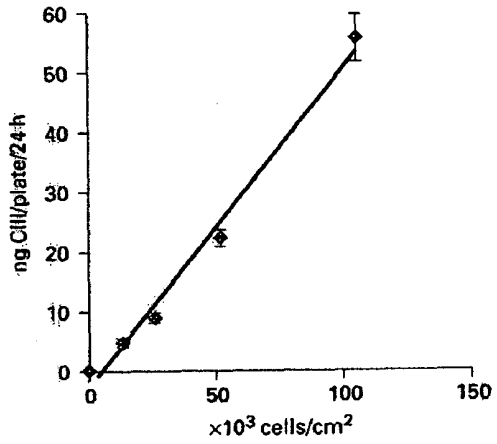

Fig. 3. Influence of cell density on apo CIII secretion by HepG2 cells. Cells were grown in medium with FCS1. Medium was removed and 3 ml of the experimental medium (BSA 2 g/l) was supplied to cells. After 24 h, experimental medium was analyzed for apo CIII concentrations. Values are expressed as ng apo CIII/plate/24 h.

though the secretion of certain other apolipoproteins was also decreased when cultured in FCS2, their decrease was much less pronounced being 1.3-fold for apo E, 1.84-fold for apo B and 2.09-fold for apo AI. apo AII secretion decreased to a much larger extent (by 7.5) but was not abolished. Under the same conditions, apo CIII secretion decreased by a factor which was at least 31.9.

The nature of FCS used to culture the HepG2 cells could therefore limit the use of HepG2 cells to study factors regulating apo CII secretion. However, our results indicate that it is possible to maintain apo CIII secretion depending of the FCS used. To further analyze the effects of cell culture conditions, we studied the influence of cell density on apo CIII secretion. Therefore, cells grown in FCS1 medium were plated at different densities (10^4–10^5 cells/cm^2) and cultured for 24 h in the same medium. The medium was then removed and the experimental BSA medium was added. apo CIII secretion (ng/24 h), measured after 24 h, was directly dependent on the cell density at the beginning of the experiment (fig. 3). Thus when expressed as ng of apo CIII per mg of cell protein in the plate at the end of the experiment (76.88 ± 9.6 ng/mg cell protein), apo CIII secretion was constant. These results demonstrate that, within the limits of the cell density tested in the experiment, apo CIII secretion is proportional to the number of cells and that the measure of the protein content at the end of the experiment is a reflection of the cell density at the beginning. Therefore, the following experiments were performed using cells cultured in FCS1 medium and plated at a cell density of 10^5 cells/cm^2. Results are expressed as ng apo CIII secreted per 24 h and per mg cell protein measured at the end of the experiment. Under these well-defined conditions the intra-assay reproducibility of the apo CIII secretion measurement was tested on 15 plates (10^5 cells/cm^2) and the CV was 18.5%. However, apo CIII secretion can vary between experiments, and factors regulating apo CIII secretion should be tested within the same experiment.

The assay was then used to test the effect of different fibrates on apo CIII secretion. Therfore, cells were grown in FCS1 medium, followed by plating for 24 h in the same medium, and addition of the experimental medium which included different fibrates. As shown in figure 4a, fenofibric acid, gemfibrozil and Wy-14643 inhibited apo CIII secretion. apo CIII mRNA levels decreased in parallel after treatment with the three drugs (fig. 4b), the effect being more pronounced for Wy-14643. The use of fenofibrate instead of fenofibric acid partially impaired the inhibitory effect on apo CIII secretion probably because cells cannot hydrolyze fenofibrate es-

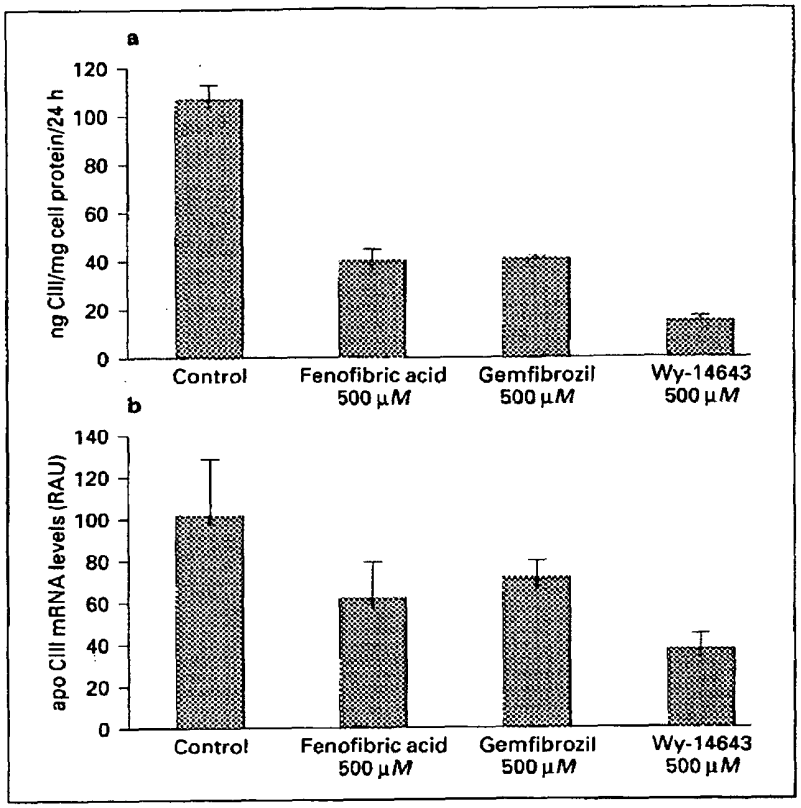

Fig. 4. Apo CIII secretion and mRNA levels after incubation of HepG2 cells with different fibrates. Cells were grown in FCS1 medium. The medium was removed and 3 ml of the experimental medium (BSA 2 g/l with fibrates at the indicated concentrations) was supplied to the cells. After 24 h, the experimental medium was analyzed for apo CIII concentration (**a**). Results are expressed as ng apolipoprotein/mg cell protein. mRNA levels were expressed as a percent of the control vehicle-treated cells (**b**).

ter in its active acid derivative (data not shown).

Since cells grown in FCS2 medium did not secrete apo CIII, the influence of fibrate treatment on apo CIII secretion could not be determined. However, we observed, as shown in figure 1b, that apo CIII mRNA was expressed in cells cultured in FCS2. When these cells were treated for 48 h with fenofibric acid (500 μ*M*) or Wy-14643 (500 μ*M*), apo CIII mRNA levels remained unchanged (respectively 123 ± 6 and 90 ± 6% of the control level in FCS2). By contrast, in the same cells, stimulation of apo AII mRNA by these fibrates was maintained (respectively 150 ± 8 and 171 ± 13% of the control level).

Finally, the influence of a specific PPARγ activator, the thiazolidinedione BRL-49653 [40, 41], was tested on apo CIII secretion and gene expression. Addition of BRL-49653 did not decrease apo CIII gene expression and secretion at concentrations as high as 30 μ*M* (table 2). Higher concentrations (100 μ*M*) had a toxic effect on the cells. To explain the specific effect of PPARα ligands on apo CIII secretion, we determined by Western blot analysis which PPARs are expressed in HepG2 cells (fig. 5). Our results indicate that, under the culture conditions used, only PPARα but not PPARγ protein could be detected. PPARα is also expressed in HepG2 cells cultured in FCS2 medium, indicating that the decrease of apo CIII secretion by these cells was not due to the loss of PPARα expression.

Table 2. Influence of BRL-49653 on apo CIII gene expression and secretion by HepG2 cells cultured in FCS1 medium

	Control	BRL-49653 30 μM	Wy-14643 500 μM
mRNA level, % of control	100±4	118±16	28±11
Secretion, ng/ml cell protein	49±4	49±4	24±3

Cells were grown in medium with FCS1 then incubated for 24 h in 3 ml of the experimental medium (BSA 2 g/l) with or without BRL-49653 or Wy-14643. Results are expressed as ng apolipoprotein/mg cell protein. mRNA was extracted as indicated in Methods and mRNA levels were expressed as a percent of the control vehicle-treated cells.

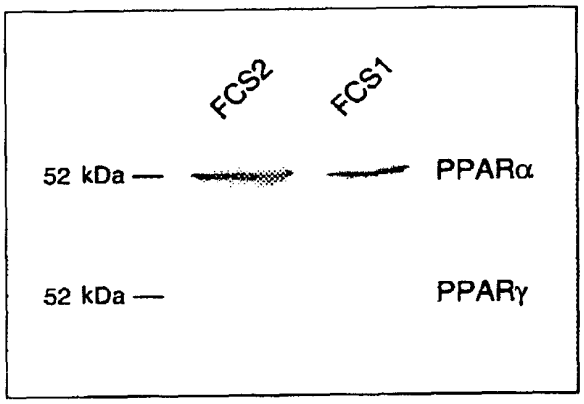

Fig. 5. Immunoblotting of HepG2 cellular extracts with anti-PPAR antibodies. Cellular extracts from HepG2 cells cultured in FCS1 or FCS2 were prepared as indicated in Methods and submitted to SDS-PAGE electrophoresis. After electrotransfer, the nitrocellulose membrane was incubated either with anti-PPARα or with anti-PPARγ antibodies.

Discussion

Regulation of apo CIII secretion plays a major role in the control of triglyceride-rich lipoprotein metabolism. HepG2 cells, a human hepatoma cell line widely used to study hepatic function, are often used to study apolipoprotein gene regulation and in some cases also apolipoprotein secretion. However, in only a few publications apo CIII secretion was also analyzed. In the present study we demonstrate that apo CIII secretion can be measured in culture medium of HepG2 cells, but that its secretion is inhibited by the use of certain commercial calf serum batches. The mechanism by which the fetal calf serum regulates apo CIII secretion is unclear at present. However, it does not appear to result in a general abolition of apolipoprotein secretion. Indeed comparison with other apolipoproteins, such apo AI, B, AII, and E, reveals that the choice of the FCS used to grow the cells can affect the secretion of all these apolipoproteins but that only apo CIII secretion can be abolished. This effect is a long-term and irreversible effect. Therefore, to study apo CIII secretion it is important to carefully select the appropriate FCS. Interestingly these data indicate that apo CIII secretion is under negative control of a nonlipophilic serum factor and that this effect can be dissociated from any effect on apo B secretion. So, if these hypothetical factors play a role in vivo, selective impaired apo CIII secretion may interfere with apolipoprotein composition of VLDL and their catabolism. Therefore, it will be of interest to determine the nature of this factor.

apo CIII is regulated at the transcriptional level by a number of biological and pharma-

cological factors. Gruber et al. [12] demonstrated its regulation in HepG2 cells by cytokines acting via a NFκB element. Chen et al. [13] reported that insulin treatment in diabetic mice and in HepG2 cells induced a dose-dependent down-regulation of apo CIII transcriptional activity and they assumed that apo CIII mRNA levels reflect the synthesis and secretion of the protein. Different authors demonstrated HNF-4 activation of apo CIII transcription [42–45] and a complex interaction between different nuclear receptors modulates apo CIII transcription.

Hypotriglyceridemic drugs such as fibrates are largely used in humans. They have profound effects on triglyceride-rich lipoprotein metabolism. VLDL composition is modified with slight decreases in apo B and apo E content and an important decrease in apo CIII. These modifications in lipoprotein composition have a stimulatory effect on the catabolism of these lipoproteins which become better substrates for LPL [3] and ligands for the LDL receptor [10]. The hypotriglyceridemic action of fibrates has been shown to be partly due to a decrease of plasma apo CIII levels which are the result of apo CIII gene transcription suppression mediated by PPARα [17]. Administration of the fibrate derivative Wy-14643 to wild-type mice resulted in a marked decrease of hepatic apo CIII mRNA levels and serum triglyceride concentrations; in contrast, PPARα-deficient mice were unaffected by Wy-14643 treatment [18]. Although animal models are often used to study the mechanisms of regulation of lipoproteins, their lipid metabolism is very different compared to humans. So gene regulation and secretion of apolipoproteins have to be tested on human cells, before extrapolation of the results obtained in animals can be made to man. Hertz et al. [17] used HepG2 cells to extend the results obtained in rodents to humans but they only studied apo CIII mRNA levels and did not provide any information with respect to apo CIII secretion. Here we demonstrate that apo CIII secretion does not necessarily correlate with mRNA levels when analyzed under inappropriate culture conditions. Previous studies from our laboratory [20] have shown a decrease of apo CIII gene expression and secretion by human primary hepatocytes. However, human hepatocytes cannot be routinely used for screening purposes. Our results indicate that the human HepG2 cell model can be a suitable system to study apo CIII secretion when appropriate culture conditions are used. However, apo CIII secretion should be carefully monitored before these experiments are performed.

In conditions where apo CIII is secreted, inhibition of secretion can be obtained by fenofibric acid and by other fibric acid derivatives, such as Wy-14643. This inhibition is due to a transcriptional inhibition. The lack of effect of the thiazolidinedione (BRL-49653) on HepG2 cells suggests that similar as in rodents, in human hepatic cells, apo CIII secretion is not regulated via PPARγ but via PPARα. This hypothesis is strenghtened by the presence of PPARα protein in HepG2 cell extracts whereas PPARγ could not be detected.

Acknowledgments

We thank O. Vidal and B. Derudas for their excellent technical help.

References

1 Mahley RW: Plasma lipoprotein: Apolipoprotein structure and function. J Lipid Res 1984;25:1277–1294.

2 Luc G, Fievet C, Arveiler D, Evans A, Bard JM, Cambien F, Fruchart JC, Ducimetière P: Apolipoproteins C-III and E in apoB- and non-apoB-containing lipoproteins in two populations at contrasting risk for myocardial infarction: The ECTIM Study. J Lipid Res 1996;37:508–517.

3 Ginsberg HN, Le NA, Goldberg IJ, Gibson JC, Rubinstein A, Wang-Iverson P, Norum R, Brown WV: Apolipoprotein B metabolism in subjects with deficiency of apolipoproteins C-III and A-I. Evidence that apolipoprotein C-III inhibits catabolism of triglyceride-rich lipoproteins by lipoprotein lipase in vivo. J Clin Invest 1986;78:1287–1295.

4 Malmendier CL, Lontie JF, Delcroix C, Dubois DY, Magot T, De Roy L: Apolipoprotein C-II and C-III metabolism in hypertriglyceridemic patients. Effect of a drastic triglyceride reduction by combined diet restriction and fenofibrate administration. Atherosclerosis 1989; 77:139–149.

5 Dallongeville J, Bauge E, Lebel P, Fruchart JC: Fat ingestion is associated with increased levels of apoC-III- and apoE-B-containing lipoprotein particles in humans. Eur J Clin Invest 1997;27:1055–1060.

6 Ito Y, Azrolan N, O'Connell A, Walsh A, Breslow JL: Hypertriglyceridemia as a result of human apolipoprotein CIII gene expression in transgenic mice. Science 1990;249: 790–793.

7 Aalto-Sctälä K, Fisher EA, Chen X, Chajek-Shaul T, Hayek T, Zechner R, Walsh A, Ramakrishnan R, Ginsberg HN, Breslow JL: Mechanism of hypertriglyceridemia in human apo CIII transgenic mice: Diminished VLDL fractional catabolic rate associated with increased apo CIII and reduced apo E on the particles. J Clin Invest 1992;90:1889–1990.

8 Maeda N, Lee D, Oliver P, Quarford SH, Osada J: Targeted disruption of the apolipoprotein C-III gene in mice results in hypertriglyceridemia and protection from postprandial hypertriglyceridemia. J Biol Chem 1994;269:23610–23616.

9 Agnani G, Bard JM, Candelier L, Delattre S, Fruchart JC, Clavey V: Interaction of LpB:E, LpB:C-III and LpB:C-III:E lipoproteins with the low density lipoprotein receptor on HeLa cells. Arteriosclerosis 1991; 11:1021–1029.

10 Clavey V, Lestavel-Delattre S, Copin C, Bard JM, Fruchart JC: Modulation of lipoprotein binding to the LDL receptor by exogenous lipids and apolipoproteins C-I, C-II, C-III and E. Arteriosclerosis 1995;15: 963–971.

11 Ginsberg HN, Le NA, Goldberg IJ, Gibson JC, Rubinstein A, Wang-Iverson D, Norum R, Brown WV: Apolipoprotein B metabolism in subjects with deficiency of apolipoprotein CIII and AI. J Clin Invest 1986;78:1287–1295.

12 Gruber PJ, Torres-Rosaro A, Wolak ML, Leff T: Apolipoprotein CIII gene transcription is regulated by a cytokine-inducible NF-kappa B element. Nucleic Acids Res 1994;22: 2417–2422.

13 Chen M, Breslow JL, Li W, Leff T: Transcriptional regulation of the apoC-III gene by insulin in diabetic mice: Correlation with changes in plasma triglycerides levels. J Lipid Res 1994;35:1918–1924.

14 Bard JM, Parra HJ, Douste-Blazy P, Fruchart JC: Changes in lipoprotein particles defined by their apolipoprotein composition on pravastatin and cholestyramine therapy. J Drug Dev 1990;3:111–115.

15 Bard JM, Luc G, Douste-Blazy P, Drouin P, Ziegler O, Jacotot B, Dachet C, De Gennes JL, Fruchart JC: Effect of simvastatin on plasma lipids, apolipoproteins and lipoprotein particles in patients with primary hypercholesterolemia. Eur J Clin Pharmacol 1989;37:545–550.

16 Haubenwallner S, Essenbourg AD, Barnett BC, Pape ME, Demattos RB, Krause BR, Minton LL, Auerbach BJ, Newton RS, Leff T, Bisgaier CL: Hypolipidemic activity of select fibrates correlates to changes in hepatic apolipoprotein C-III expression: A potential physiologic basis for their mode of action. J Lipid Res 1995;36:2541–2551.

17 Hertz R, Bishara-Shieban J, Bar-Tana J: Mode of action of peroxisome proliferators as hypolipidemic drugs. Suppression of apolipoprotein C-III. J Biol Chem 1995;270: 13470–13475.

18 Peters JM, Hennuyer N, Staels B, Fruchart JC, Fievet C, Gonzalez FJ, Auwerx J: Alterations in lipoprotein metabolism in peroxisome proliferator-activated receptor alpha-deficient mice. J Biol Chem 1997;272: 27307–27312.

19 Hertz R, Arnon J, Hoter A, Shouval D, Bar-Tana J: Clofibrate does not induce peroxisomal proliferation in human hepatoma cell lines PLC/PRF/5 and SK-HEP-1. Cancer Lett 1987;34:263–272.

20 Staels B, Vu Dac N, Kosykh VA, Saladin R, Fruchart JC, Dallongeville J, Auwerx J: Fibrates downregulate apolipoprotein C-III expression independent of induction of peroxisomal acyl coenzyme A oxidase. A potential mechanism for the hypolipidemic action of fibrates. J Clin Invest 1995;95:705–712.

21 Tam PS, Archer TK, Deeley RG: Effects of oestrogen on apolipoprotein secretion by the human hepatocarcinoma cell line, HepG2. J Biol Chem 1985;260:1670–1675.

22 Zannis VI, Brewslow JL, San Giacomo TR, Aden DP, Knowles BB: Characterization of the major apolipoproteins secreted by two human hepatoma cell lines. Biochemistry 1981;20:7089–7096.

23 Dashti N, Wolfbauer G, Secretion of lipids, apolipoproteins, and lipoproteins by human hepatoma cell line, HepG2: Effects of oleic acid and insulin. J Lipid Res 1987;28:423–436.

24 Dixon JL, Ginsberg HN: Regulation of hepatic secretion of apolipoprotein B-containing lipoproteins: Information obtained from cultured liver cells. J Lipid Res 1993;34:167–179.
25 Haghpassand M, Wilder D, Moberly JB: Inhibition of apolipoprotein B and triglyceride secretion in human hepatoma cells (HepG2). J Lipid Res 1996;37:1468–1480.
26 Passilly P, Jannin B, Hassel SJ, Latruffe N: Human HepG2 and rat Fao hepatic-derived cell lines show different responses to ciprofibrate, a peroxisome proliferator: Analysis by flow cytometry. Exp Cell Res 1996; 223:436–442.
27 Ladias JA, Hadzopoulou-Cladaras M, Cardot P, Cheng J, Zannis VI, Cladaras C: Transcriptional regulation of human apolipoprotein genes apoB, apoCIII, and apoAII by members of the steroid hormone receptor superfamily HNF-4, ARP-1, EAR-2, and EAR-3. J Biol Chem 1992; 267:15849–15860.
28 Benoist F, Grand-Perret T: A sensitive method to analyze in vitro secretion of lipoproteins: Distribution of apolipoproteins is modulated by oleic acid in HepG2 cells. J Lipid Res 1995;36:2243–2250.
29 Tam SP: Effect of ethanol on lipoprotein secretion in two human hepatoma cell lines, HepG2 and Hep3B. Alcohol Clin Exp Res 1992; 16:1021–1028.
30 Parsy D, Clavey V, Fievet C, Kora I, Duriez P, Fruchart JC: Quantification of apolipoprotein CIII in serum by noncompetitive immunoenzymometric assay. Clin Chem 1987; 31:1632–1635.
31 Leroy A, Vu Dac N, Koffigan M, Clavey V, Fruchart JC: Characterization of monoclonal antibody that binds to apo E and lipoprotein of human plasma containing apo E. Applications to ELISA quantification of plasma apo E. J Immunoassay 1988;9:309–334.
32 Puchois P, Kandoussi A, Duriez P, Fruchart JC, McConathy WJ, Koren E: Quantitative determination of human plasma apo-AII by a noncompetitive enzyme-linked immunosorbent assay. J Immunoassay 1986;7:285–307.
33 Betard C, Vu-Dac N, Mezdour H, Nestruck AC, Leroy A, Fruchart JC: Standardization of an enzymometric assay for apolipoprotein A-I by using mixtures of monoclonal antibodies. J Clin Chem Clin Biochem 1987;25:893–899.
34 Fievet C, Dedieu A, Kandoussi A, Luyeye I, Fruchart JC: Quantitation of human serum apolipoprotein B by enzyme immunoassay in excess antigen. Clin Chim Acta 1986;159: 269–278.
35 Masiakowski PR, Breathnach R, Bloch J, Gannon F, Krust A, Chambon P: Cloning of cDNA sequences of hormone-regulated genes from MCF-7 human breast cancer cell line. Nucleic Acids Res 1982;10: 7895–7903.
36 Laborda J: 36B4 cDNA used as an estradiol-independent mRNA control is the cDNA for human acidic ribosomal phosphoprotein PO. Nucleic Acids Res 1991;19:3998.
37 Staels B, Auwerx J: Perturbation of developmental gene expression in rat liver by fibric acid derivatives: Lipoprotein lipase and alpha-fetoprotein as models. Development 1992;115:1035–1043.
38 Chinetti G, Griglio S, Antonucci M, Torra IP, Delerive P, Majd Z, Fruchart JC, Chapman J, Najib J, Staels B: Activation of proliferator-activated receptors alpha and gamma induces apoptosis of human monocyte-derived macrophages. J Biol Chem 1998;273:25573–25580.
39 Fajas L, Auboeuf D, Raspe E, Schoonjans K, Lefebvre AM, Saladin R, Najib J, Laville M, Fruchart JC, Deeb S, Vidal-Puig A, Flier J, Briggs MR, Staels B, Vidal H, Auwerx J: The organization, promoter analysis, and expression of the human PPARγ gene. J Biol Chem 1997;272:18779–18789.
40 Lefebvre AM, Peinado-Onsurbe J, Leitersdorf I, Briggs MR, Paterniti JR, Fruchart JC, Fievet C, Auwerx J, Staels B: Regulation of lipoprotein metabolism by thiazolidinediones occurs through a distinct, but complementary mechanism relative to fibrates. Arterioscler Thromb Vasc Biol 1997;17:1756–1764.
41 Lehmann JM, Moore LB, Smith-Oliver TA, Wilkison WO, Willson TM, Kliewer SA: An antidiabetic thiazolidinedione is a high affinity ligand for peroxisome proliferator-activated receptor-gamma (PPARγ). J Biol Chem 1995;270: 12953–12956.
42 Furth EE, Sprecher H, Fisher EA, Fleishman HD, Laposata M: An in vitro model for essential fatty acid deficiency: HepG2 cells permanently maintained in lipid-free medium. J Lipid Res 1992;33:1719–1726.
43 Nishiyama C, Hi R, Osada S, Osumi T: Functional interactions between nuclear receptors recognizing a common sequence element, the direct repeat motif spaced by one nucleotide (DR-1). J Biochem (Tokyo) 1998;123:1174–1179.
44 Fraser JD, Martinez V, Straney R, Briggs MR: DNA binding and transcription activation specificity of hepatocyte nuclear factor 4. Nucleic Acids Res 1998;26:2702–2707.
45 Taylor DG, Haubenwallner S, Leff T: Characterization of a dominant negative mutant form of the HNF-4 orphan receptor. Nucleic Acids Res 1996;24:2930–2935.

1: J Biol Chem 1997 May 16;272(20):13000-5

Lipoprotein lipase reduces secretion of apolipoprotein E from macrophages.

Lucas M, Iverius PH, Strickland DK, Mazzone T.

Department of Medicine, Rush Medical College, Chicago, Illinois 60612, USA.

Macrophages are a significant source of lipoprotein lipase (LPL) and apolipoprotein E (apo E) in the developing arterial wall lesion, and each of these proteins can importantly modulate lipid and lipoprotein metabolism by arterial wall cells. LPL and apo E share a number of cell surface binding sites, including proteoglycans, and we have previously shown that proteoglycans are important for modulating net secretion of apoprotein E from macrophages. We therefore evaluated a potential role for LPL in modulating net secretion of macrophage-derived apo E. In pulse-chase experiments, addition of LPL during the chase period produced a decrease in secretion of apoprotein E from human monocyte-derived macrophages, from the human monocytic THP1 cell line, and from J774 cells transfected to constitutively express a human apo E cDNA. LPL similarly reduced apo E secretion when it was prebound to the macrophage cell surface at 4 degrees C. A native LPL particle was required to modulate apo E secretion; addition of monomers and aggregates did not produce the same effect. Depletion of cell surface proteoglycans by a 72-h incubation in 4-methylumbelliferyl-beta-D-xyloside did not attenuate the ability of LPL to reduce apo E secretion. However, addition of receptor-associated protein attenuated the effect of LPL on apo E secretion. Although LPL could mediate removal of exogenously added apo E from the culture medium, detailed pulse-chase analysis suggested that it primarily prevented release of newly synthesized apo E from the cell layer. Cholesterol loading of cells or antibodies to the low density lipoprotein receptor attenuated LPL effects on apo E secretion. We postulate that LPL sequesters endogenously synthesized apo E at the cell surface by a low density lipoprotein receptor-dependent mechanism. Such post-translational regulation of macrophage apo E secretion by LPL could significantly influence apo E accumulation in arterial vessel wall lesions.

PMID: 9148908 [PubMed - indexed for MEDLINE]

Display Abstract Save Text Order Add to Clipboard

1: Arterioscler Thromb Vasc Biol 1997 Nov;17(11):2707-12

Upregulation of low density lipoprotein receptor by gemfibrozil, a hypolipidemic agent, in human hepatoma cells through stabilization of mRNA transcripts.

Goto D, Okimoto T, Ono M, Shimotsu H, Abe K, Tsujita Y, Kuwano M.

Department of Biochemistry, Kyushu University School of Medicine, Fukuoka, Japan.

Gemfibrozil reduces the plasmal levels of cholesterol and triglyceride in patients with hyperlipidemia by a mechanism that is not well understood. The present study evaluated the effect of gemfibrozil on the LDL receptor in human hepatoma cells compared with that of pravastatin, an inhibitor of 3-hydroxy-3-methylglutaryl coenzyme A reductase. Exposure to gemfibrozil, 40 mumol/L, for 3 days increased the binding of 125I-LDL to the surface of three lines of human hepatoma cell, HepG2, HuH7, and HLE by 1.5- t 2.0-fold. Similar findings were observed with pravastatin. Scatchard analysis with 125I-LDL indicated an increased number of LDL receptors on the cell surface of HepG2 cells when treated with gemfibrozil and pravastatin. However, the gemfibrozil-treated cells exhibited no increase in the binding of 125I-epidermal growth factor (EGF). Gemfibrozil increased the levels of LDL receptor mRNA and protein in HepG2 cells. The increase in LDL receptor activity induced by pravastatin was abolished by concomitant administration of mevalonic acid, 770 mumol/L. This effect was not seen with gemfibrozil, suggesting the mechanism differs for the two lipid-lowering drugs. To determine whether this increase in mRNA was due to transcriptional activation, we prepared HepG2 cells transfected with an LDL receptor promoter-reporter construct that contained a sterol regulatory element. The expression of LDL receptor regulated by the sterol regulatory element was increased by pravastatin, but not by gemfibrozil. We evaluated the stability of the mRNA in the presence of actinomycin D to explain the increase in the LDL receptor mRNA. Gemfibrozil prolonged the half-life of the mRNA for LDL receptor but not that for the EGF receptor. Stabilization of the LDL receptor mRNA is suggested to be the novel mode of action of gemfibrozil.

PMID: 9409246 [PubMed - indexed for MEDLINE]

1: Biochem Mol Biol Int 1997 Dec;43(5):1071-80 Related Articles, Books

Effect of n-3 fatty acids on VLDL production by hepatocytes is mediated through prostaglandins.

Anil K, Jayadeep A, Sudhakaran PR.

Department of Biochemistry, University of Kerala, Kariavattom, Trivandrum, India.

The mechanism of the hypolipidemic effect of n-3 fatty acids was studied using isolated rat hepatocytes maintained in culture. EPA and DHA caused a significant reduction in the incorporation of 3[H]-leucine into apoB associated with the VLDL produced by hepatocytes in culture when compared to that in presence of palmitic acid. Presence of indomethacin, an inhibitor of cyclo-oxygenase reversed the effect of EPA on VLDL synthesis while diethyl carbamazine an inhibitor of lipoxygenase did not show any effect suggesting that the effect of EPA may be mediated through prostaglandins. This was further tested by invivo experiments where animals were fed fish oil containing diet with and without aspirin, which inhibits formation of prostaglandins. The incorporation of 3[H]-leucine into apo B and 14[C]-acetate into cholesterol of VLDL produced by hepatocytes from aspirin treated animals were significantly high. The reversal of the effect of n-3 fatty acids by agents which inhibit the formation of prostaglandin suggests that the n-3 fatty acids may exert their effect on VLDL production by liver cells through prostaglandins.

PMID: 9415816 [PubMed - indexed for MEDLINE]

Display Abstract Sort Save Text Clip Add Order

1: Biochem J 1997 Aug 1;325 (Pt 3):711-9

Related Articles, Books, LinkOut

Biochem J

Decreased secretion of very-low-density lipoprotein triacylglycerol and apolipoprotein B is associated with decreased intracellular triacylglycerol lipolysis in hepatocytes derived from rats fed orotic acid or n-3 fatty acids.

Hebbachi AM, Seelaender MC, Baker BW, Gibbons GF.

Oxford Lipid Metabolism Group, Metabolic Research Laboratory, Nuffield Department of Clinical Medicine, University of Oxford, Radcliffe Infirmary, Oxford OX2 6HE, U.K.

Hepatocytes from rats fed a chow (control) diet or from rats fed a chow diet supplemented with either orotic acid (OA; 1%, w/w) or fish oil (FO; 20%, v/w) were maintained in culture for periods up to 48 h. during the first 24 h period, the low rates of output of very-low-density lipoprotein (VLDL)-associated triacylglycerol (TAG) and apolipoprotein B (apoB) in hepatocytes from the FO- and OA-fed animals were associated with significantly lower rates of intracellular TAG lipolysis and re-esterification. Most of the VLDL TAG secreted was mobilized via lipolysis of the intracellular TAG pool, but the proportion of VLDL TAG secreted via this route in cells from the FO-fed and OA-fed animals was decreased compared with that in the control-fed animals' cells. In the presence of exogenous oleate the inhibitory effect of OA feeding on VLDL apoB and TAG secretion persisted in the derived hepatocytes for up to 48 h following isolation. However, when oleate was absent no inhibitory effect on the secretion of TAG and apoB was observed between 24 and 48 h. Under these conditions the rate of intracellular TAG turnover returned to normal. The initial inhibitory effect of FO feeding on VLDL TAG and apoB secretion did not persist in the derived hepatocytes between 24 h and 48 h of culture in the presence of exogenous oleate. Although intracellular TAG lipolysis and VLDL TAG and apoB secretion rates appear to be positively correlated, a causal relationship has not been conclusively established.

PMID: 9290048 [PubMed - indexed for MEDLINE]

1: J Lipid Res 1989 Jun;30(6):785-807 Related Articles, Books

Fish oils and plasma lipid and lipoprotein metabolism in humans: a critical review.

Harris WS.

Department of Medicine, University of Kansas Medical Center, Kansas City 66103.

Epidemiological studies in Greenland Eskimos led to the hypothesis that marine oils rich in n-3 fatty acids (also referred to as omega (omega)-3 fatty acids) are hypolipidemic and ultimately antiatherogenic. Metabolically controlled trials in which large amounts of fish oil were fed to normal volunteers and hyperlipidemic patients showed that these fatty acids (FAs) are effective at lowering plasma cholesterol and triglyceride levels. Although more recent trials using smaller, more practical doses of fish oil supplements have confirmed the hypotriglyceridemic effect, they have shown little effect on total cholesterol levels; hypertriglyceridemic patients have even experienced increases in low density lipoprotein cholesterol (LDL-C) levels of 10-20% while taking n-3 FA supplements. Discrepancies among fish oil studies regarding the effects of n-3 FAs on LDL-C levels may be understood by noting that, in the majority of studies reporting reductions in LDL-C levels, saturated fat intake was lowered when switching from the control diet to the fish oil diet. When fish oil is fed and saturated fat intake is constant, LDL-C levels either do not change or may increase. Levels of high density lipoprotein cholesterol have been found to increase slightly (about 5-10%) with fish oil intake. Plasma apolipoprotein levels change in concert with their associated lipoprotein cholesterol levels. Although the decrease in triglyceride levels appears to result from an inhibition in hepatic triglyceride synthesis, the mechanisms leading to the increases in LDL and HDL have not been determined. Finally, fatty fish or linolenic acid may serve as alternative sources of long-chain n-3 FAs, but further studies will be needed to document their hypolipidemic and/or antiatherogenic effects.

Publication Types:
- Review
- Review, Academic

PMID: 2677200 [PubMed - indexed for MEDLINE]

Display Abstract Sort Save Text Clip Add Order